Department of Precision and Microsystems Engineering

Design of a multi-purpose research cabin mounted upon a hexapod motion simulator

M. Zhang

Report no   : MSD 2016.022
Coach   : ir. J.W. Spronck
Professor   : prof.dr.ir. J.L. Herder
Specialisation   : Mechatronic System Design
Type of report : MSc Thesis
Date   : 26-09-2016

TUDelft
Delft
University of
Technology

Challenge the future

MSc Graduation Project

Design of a multi-purpose research cabin mounted upon a hexapod motion simulator

by

Mengying Zhang

in partial fulfillment of the requirements for the degree of

Master of Science

at the Delft University of Technology,
to be defended publicly on Monday September 26, 2016 at 10:00 AM.

Student number:	4403436	
Department:	Precision and Microsystems Engineering	
Thesis committee:	Prof. dr. ir. Just.L. Herder,	TU Delft
	Prof. ir. Jo.W. Spronck,	TU Delft
	dr. ir. J.M.J.F. van Campen,	TU Delft
	dr. ir. Joost Venrooij,	MPI for Biological Cybernetics
	ir. Werner van de Sande,	TU Delft

An electronic version of this thesis is available at http://repository.tudelft.nl/.

TUDelft
Delft
University of
Technology

Abstract

Motion simulators have increasingly been applied for research purposes due to their large motion capabilities and short response time. Key applications are including vehicle simulation, experiments on control behavior in virtual environments and studies into human self-motion perception. To maintain a good dynamic capability, the known motion simulator usually has a custom-designed cabin with optimized stiffness and weight to encapsulate the various moving components. However, the particular shell structure is very inflexible for exchanging its functions. To improve the functionality of the motion simulator for conducting multi-purpose research, a modular cabin structure with flexibility and time efficiency when exchanging setups is demanded.

This research project is based on a practical design task of a multi-purpose research cabin for a hexapod motion simulator installed at the Max Planck Institute for Biological Cybernetics. It is aiming to develop a simple cabin structure with more modularity while maintaining acceptable dynamic capabilities. In this project, a detachable structure concept is proposed based on a systemic assembly break down of the cabin entity into a base frame, an outer structure frame assembly and filling-in panels. Each part is designed as a self-supported substructure that could provide sufficient stiffness individually. Connections between each substructure is proved to be stiff and will not reduce its stiffness during motion also at higher frequencies. Various design constraints and objectives are considered with specified boundaries and priorities during design process, which has formed the basic logistics behind each design choice.

The overall design of a multi-purpose research cabin can access the limited motion lab entrance as disassembled parts and can be reassembled again inside the room. It has optimized setup positioning and high modularity for exchanging its functions. With bolted connection, the side panels can be removed fast for exchanging setups and repositioned back easily. The stiffness and natural frequency of both substructures and the assembly is verified in FEM analysis software with user acceptance. The stiffness of the connection is also verified with calculations and tests. The dynamic capabilities of the hexapod motion simulator is validated for the payload mass properties. The discovery of a modular cabin structure has contributed to the development of multi-functional research motion simulators.

Acknowledgements

First I would like to thank dr. ir. Joost Venrooij and ir. Frank Drop, for the opportunity to carry out this thesis project at Max Planck Institute for Biological Cybernetics located at Tuebingen, Germany. Especially their patient supervision and generous support during the project. In addition, my special thanks to the whole motion perception and simulation group, I've learned a lot from their work and have a lot fun during the time at the institute.

My sincere gratitude goes out to my academic coach ir. J.W. Spronck and ir. Werner van de Sande for their indispensable guidance and inspiring discussions throughout the project. Also special thanks to Prof. dr.ir. Just Herder for his valuable feedbacks during review meetings.

In addition, I would like to thank all the colleagues and fellow students that had helped and encouraged me during the project, and last but not least, my family for their support and love.

Delft, University of Technology   Mengying Zhang
September 23, 2016

Table of Contents

Chapter 1

Introduction

In this chapter, the state-of-art multi-purpose research motion simulator is introduced with examples applied at Max Planck Institute for Biological Cybernetics (MPI). The thesis topic is then specified by indicating a strong demand on a modular cabin structure. The motivation of this research project with a problem statement is presented, followed with the research objectives and methodology proposal. In the end, an outline of the thesis structure is laid out.

1-1 The state-of-art multi-purpose research motion simulator

A motion simulator is generally known as a mechanism that encapsulates the occupant compartment and creates a moving experience of being in a real vehicle. Various applications have classified the motion simulators into three main categories: examination simulators for vehicle training, engineering simulators for vehicle design and research simulators for simulation design[1]. With the development of control technology, new types of motion simulator with remarkable motion capabilities have been applied for multiple research purposes. At the Max Planck Institute for Biological Cybernetics (MPI), motion simulators are used for research ranging from human self-motion perception studies to experiments on control behavior in virtual environments.[1]

Obviously for different type of experiments, the installed devices and their positioning requirements are different. For example, motion perception studies use the motion simulators to conduct psychophysical experiments, which would require a good projection system. While for vehicle simulations, a group of monitors as well as various control devices will be installed (refer Figure 1-1).

At MPI, the motion simulator is frequently occupied for multi-types of experiments, thus the exchange between different setups is relatively often. This has revealed an increasing demand

---

[1]http://www.kyb.tuebingen.mpg.de/research/dep/bu/motion-perception-and-simulation.html

Figure 1-1: Setup required for various experiments: psychophysics (left), helicopter simulation (middle) and car simulation (right)

on saving the time and effort to exchange setups when a different experiment is scheduled with the motion simulator. In order to improve the functional efficiency of the motion simulator, a modular cabin structure is proposed for the multi-purpose research simulators.

1-2   Research motivation and objectives

Utilizing a motion simulator as a multi-purpose research simulator increases the demands on both the simulator's motion capabilities and simulator functionality. Thus, optimizations regarding aspects such as extending the cabin's inner volume and its structure modularity are standing out with higher priorities. This has brought new challenges of manufacturing a modular motion simulator cabin structure while maintaining sufficient stiffness and stability during motion.

Recently, a state-of-art hexapod motion simulator (refer Figure 1-2) has been installed at the MPI and will be used for multiple research purpose such as motion perception and vehicle simulation (e.g., car and helicopter simulation). Thus, a multi-purpose research cabin needs to be designed for the hexapod motion simulator. In order to conduct multiple types of experiments, the designed cabin should at least be able to accommodate a seat, various control devices, safety systems and a visualization system, and it should be convenient to exchange those components inside the cabin. Moreover, it should meet further specified requirements regarding size, weight, inertia, costs as well as stiffness and natural frequency.

For this design problem, multiple research objectives are put forward, so are the constraints. A clarification of the boundaries and priorities regarding to each requirement needs to be done before the design starts, because this gives the reasoning for each design choice. Obviously, the functionality and modularity take the highest priority as the objective, parameters regarding to dimension, weight, inertia, cost, stiffness and natural frequency are defined with acceptable boundaries. A design meets all the boundaries with optimized modularity and functionality is the goal of the research project.

Figure 1-2: System overview of the installed hexapod motion simulator (neutral pose) at MPI[2]

From the previous problem statement, a hexapod motion simulator is already installed and will be used for multiple research purpose. Thus a practical objective is to complete a top-level cabin design with drawings and specifics that is feasible to be produced eventually for MPI. However, the method and its logistics applied during design process has to be clarified, and the final product has to be identified with respect to each requirement. This has formed the academic objective that is to validate the design to be logic and effective.

1-3 Methodology aspects

In order to form a complete and logical design process, the planning of each design phase has to be proposed based on design requirements, from the problem definition with design boundaries at beginning to the validation of design choices in the end.[3]

The problem definition is proposed as the start of the project. Since this is a practical design problem, the external constraints from the environment and user wishes are very general and could not be directly used for the detailed design process. Thus all the requirements had to be specified with boundaries so that the final product can be verified with.

During the detailed design process, many choices had to be made regarding to the configuration, material, manufacture, profile, connection, assembly and estimated cost. Some aspects influence the objective with higher priority will need to be optimized, while some other aspects that do not make a difference within the constrained boundaries will be compromised as long as it is verified with requirements. In the end, the final product will be an acceptable and feasible design which meets all the requirements from the environment and user wishes.

1-4   Outline of the thesis

The thesis report consists of five chapters, including sections and subsections to elaborate with more details. The first two chapters give the introduction and literature study of the topic and background information. The third chapter starts with the problem definition. The fourth chapter goes into the detailed description of the cabin design with requirement verifications. The last chapter gives conclusion and evaluation of the final product and the whole design process. The content of each chapter is specified below:

Chapter 2

Chapter 2 focuses on the literature study of the state-of-art cabin design and manufacture. It starts with a innovated method of manufacturing a light weight and low inertia motion simulator cabin structure. Then the CyberMotion simulator[2] and the CableRobot simulator[3] designed for MPI are investigated with their innovation of cabin design. Then a specific literature study regarding to the composite material which is widely used in the simulator cabin manufacture is presented. In the end, to prepare for the starting of the project, the installed hexapod motion simulator will be identified with both its composition and dynamic properties.

Chapter 3

Chapter 3 starts the design with the problem definition. By first stating the general user wishes and design conditions, certain design aspects can be summarized. Then each requirement is qualified and quantified with specific boundaries via modeling or calculation. During this process, each boundary defined will be verified with an evaluation of the method been used. At last, all the requirements will be summarized with their priorities to optimize, and a preliminary concept of the cabin struture is proposed.

Chapter 4

Chapter 4 goes into the detailed design of each part of the cabin structure individually. With an estimated load conditions, the concept of configuration is proposed. With a list of boundaries specified for each part, discussions will go through all the aspects from selecting material, manufacture method, element profile, connection to the stiffness verification, assembly process elaboration and production cost estimation.

Chapter 5

Chapter 5 finalizes the whole design with assembly descriptions and validation regarding to each requirement. Conclusions and evaluation of the final product as well as the whole design process will be presented.

---

[2]an modified industrial robot based on design Robocoaster from KUKA GmbH, Germany
[3]http://cablerobotsimulator.org/

Chapter 2

Background information

In this chapter a literature study is conducted first with some innovations on the manufacturing of motion simulators. During this study, factors that affect the design of the cabin are addressed and the existing motion simulators with their cabin design will be discussed. The development of composite material being applied within the flight simulator cabin design is investigated. Finally, analysis of the hexapod motion simulator used is conducted.

2-1 Method of manufacturing a light weight motion simulator

One relevant patent of the method of manufacturing a motion simulator is studied[4]. Within this patent, the drawbacks of the known simulator are pointed out and the development of a motion simulator with light weight and low center of gravity is stated. The type of motion simulator been discussed within this paper is the most conventional Stewart platform[5] which is equipped with 6 linear actuators based on a hexapod design.

2-1-1 Motion simulator composition

Within this paper, the motion simulator consists several main parts as shown in Figure 2-1.

Deck

The deck is a flat and stiff plate that performs as a movable platform supported by the actuator legs from bottom side of the plate and supporting a simulation environment on its top side (refer number 30 denoted in Figure 2-1). The movement of the deck will be arranged by a group of actuators. Normally, as stated in the patent[4], the deck plate should be a strong structure stiffened by bearing beams construction.
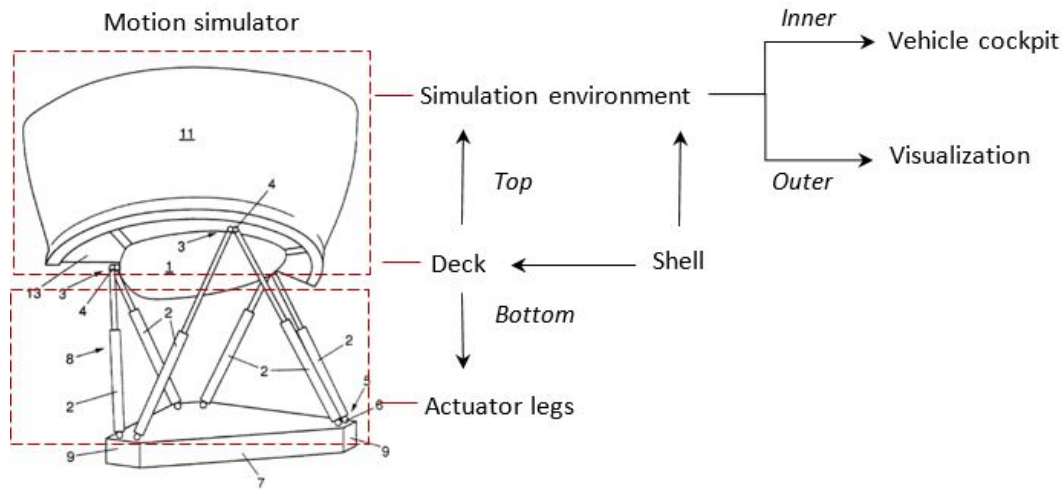
Figure 2-1: Motion simulator construction composition referred to the patent of method of manufacturing a motion simulator[4]

Actuator legs

Actuators play the role of the mechanism that generates the cues to reproduce the motions in real condition (refer number 2 in Figure 2-1). This part of the simulation directly determines how good the kinematic performance of the motion simulator is. The improvement of the mechanism design is a large topic which is out of the range of this research, since in this project design case, the mechanism part of the motion simulator is already established and all the parameter related to it is fixed.

Shell

Shell is a self-support construction which could carry the deck and is supported by the actuator leg (refer number 1 in Figure 2-1). It encloses the moving part of the motion simulator providing a simulation environment with various kinds of equipment in it. Shell is an interesting part to discuss since it plays the role of an interface that connects the moving part with the actuator mechanism. Thus a stiff, light weight shell can improve the response time of the motion simulator.

Simulation environment

The simulation environment comprises a cockpit of an aircraft or a car or other vehicles reproduced on the deck inside the shell (refer the right side picture in Figure 2-1). This part usually includes all the equipment as like in the real vehicle, for example the instructor cabin with seats, control devices, power supplies etc. Outside is the system presenting the simulated environment, also denoted as the visualization system (refer number 11 in Figure 2-1).

2-1-2 Innovation of manufacture method

Two improvements of the motion simulators have been pointed out in the patent. First is by reducing the weight of simulator cabin to improve the response time, referred as the delay time between the provision of a control signal and the reaction of the simulator. Since a high response time harms the behavior of the vehicle to become unnatural which totally goes against the fact that certain vehicles do have a very short response time in reality. In conclusion, for a simulator cabin the stiffness and natural frequency should be high while the weight should be minimized.

On the other hand, the inertia generated by the weight is also crucial. Since a high center of gravity of the moving part makes the forces and moments transmitted to the actuator legs also very high, which will definitely in turn affect the performance of the moving part. Thus, in order to improve this, the center of gravity of the moving part has to be brought as low as possible preferably close to the motion reference point of the whole simulator mechanism.

However, regarding to those aspects, there are absolute requirements, which are determined by the hexapod (such as the maximum payload). Due to the multitude of constraints, the optimal weight (for example) will be in between the absolute maximum and absolute minimum value.

Two methods to improve the manufacture of a light weight and low center of gravity motion simulator is summarized as follows:

Defining actuator leg envelops

By extending the moving structure partly under the level of the upper platform top surface (refer Figure 2-1 where part 3 and 4 defined the upper platform surface while part 1 denoted the extending part under the surface), the center of gravity of the moving payload can be brought lower to reduce the effect loads transmitted to the actuators. In order to do this, the interference between the moving structure and the actuator legs as well as all the possible obstacles should be avoided. Thus, the leg envelope is investigated to define the free interspace between the actuator legs so that in each pose of the simulator, the moving structure is clear of the actuator legs or other obstacles. This method can be applied to this design project in order to achieve a more efficient structure with low center of gravity.

By analogy, a motion envelop defined by the extreme positions of the moving structure can be performed as well. With a certain workspace of the room for the motion simulator to operate, the dimension, or the volume of the moving structure can be extended to a desired level to optimize the positioning of the equipment, especially the projector as visualization system.

In conclusion, the envelope analysis of both moving part and the actuator legs are useful tools to optimize the efficiency of the moving structure.

Applying composite material

A possible manufacture method is to have the shell at least partly manufactured with synthetic material, in particular of composite material. As well known, sandwich-shaped structure is an efficient way to reduce the weight while keep a high level of stiffness.[6] However, the selection of the type of composite material and its joining method requires custom design according to specific user wishes of stiffness and its modularity.

2-1-3   Conclusion

In conclusion, the innovated manufacture method of a motion simulator has provided some ideas for improving the weight and mass inertia of the moving structure design which could be applied in this design project. However, as observed from the setup of SIMONA[1], there are still potential to further improve the cabin design. First is the capacity of the inner volume of the cabin, which can be further extended in order to optimize the positioning of all the equipment to generate a better simulation environment. Second is the joining method which connects the parts together as the cabin assembly, since it secured part of the stiffness of the assembly. So far, glue is generally preferred and being used for such joining design due to its high resistance to loading conditions, while on the other hand, it also reduces the modularity of the simulator as a permanent connection.

2-2   Diverse simulator cabin design at MPI

The current two motion simulators for cybernetic research purpose all have a unique custom-designed cabin structure. An investigation of these two complete unique design of the cabin structure will give useful inspiration and reminders for this design project.

2-2-1   The MPI CableRobot simulator

The fist interesting motion simulator design is the cable robot simulator (refer Figure 2-2). It is actuated with 8 steel cables each can be loaded up to $14kN$ tensile strength, and it can reach very high accelerations up to 1.5g. The workspace is also very large and is only limited by the room size.[2]

This simulator uses very advanced material to achieve the best ratio between weight and stiffness. Carbon fiber is applied for the manufacture of the frame construction, which brings the weight of the simulator to 80 kg. Aluminum hoenycomb structure is applied for the manufacture of the floor. Honeycomb as a very stiff composite material compared to other type of composites.[6] As concluded from the CableRobot simulator, an aluminum honeycomb panel with thickness of 25mm can perform as floor with the necessary support from the edges.

---

[1]flight motion simulator from Technology University of Delft, the Netherlands
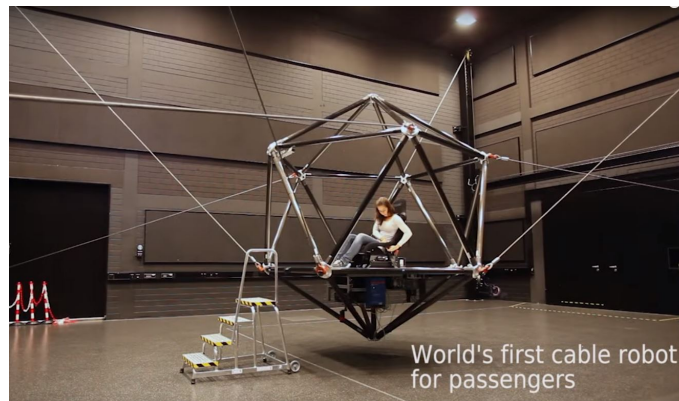[2]http://cablerobotsimulator.org/index.html

Figure 2-2: The manufacturing of the MPI CableRobot simulator

Another remark of the design is the configuration of the frame. A vertical supporting element is added to the bottom side of the seat and extends to the mounting nodes where the force is actuated (refer the lowest structure underneath the floor in Figure 2-2). This is a good way to add stiffness to the center payload from the bottom side and add stiffness to the floor panel as well.

However, the total frame is using carbon fiber pipe profile with joints to interconnect with each other, and it is not efficient for attaching further elements, interface still needs to be designed for further elements to be mounted with. Thus, the modularity of this cabin structure can be further improved.

2-2-2 The CyberMotion Simulator

Another remarkable motion simulator being used at MPI is the CyberMotion simulator[7] (refer Figure 2-3). It is designed based on an anthropomorphic robot arm[3], which has greatly extended the motion envelop with eight degrees of freedom and thus greatly improved the motion capability of the simulator for better performance of the research experiments into human perception and behavior.
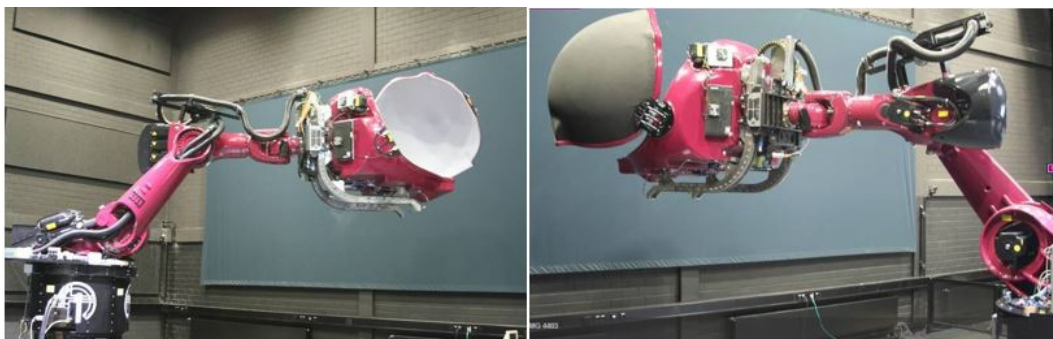

Figure 2-3: The manufacturing of the MPI CyberMotion simulator

---

[3]Based on design Robocoaster from KUKA GmbH, Germany

Within this cabin structure, the projection screen is provided by the door, which makes it structurally efficient. However, both the image size and the image stability is not optimized. Moreover, due to the door shape, the image quality is also affected with keystoning effects etc. Additionally, due to the small cabin dimension, the volume of the inner space is also small, which leads to the undesired positioning of the control devices.

2-3 Composite material applied in the flight simulator cabin design

As discussed in the previous sections, the application of the composites are remarkable especially in vehicle manufacture, and cabin structure of motion simulator as well. Here two interesting composite material are investigated.

2-3-1 Divinycell foam

Divinycell foam is one of the interesting composite with good strength to density ratio and has been already generally used in marine, land transportation, wind energy, civil engineering as well as general industrial markets[4]. Its sandwich construction consists of a core material bonded by two high strength skins (facings). The skin part take up the bending stresses and give the structure a hard wearing surface. This core construction also absorbs the shear stresses and distributes them over a large area.
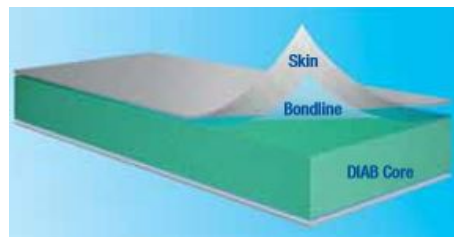
Figure 2-4: Basic concept of honeycomb sandwich construction referred in [6]

2-3-2 Aluminum honeycomb

The basic concept of honeycomb material as stated in book Honeycomb Technology [6] is the type of bonded sandwich construction with thin dense, strong facing materials and thick, lightweight honeycomb core (refer Figure 2-5). This type of material is very efficient with its strength and stiffness comparing to its weight.

The application of the first all-aluminum sandwich panel can be tracked to 1945.[6] Its application developed fast due to its light weight and excellent fatigue resistance. Due to the fact that the honeycomb panel facings are continuously bonded to the core, such that there is no stress concentrations presented through the construction and the force is well spread.

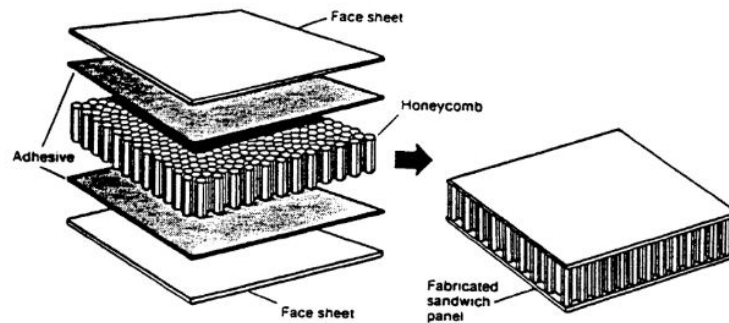[4]http://www.diabgroup.com/en-GB/Products-and-services/Core-Material/Divinycell-H

Figure 2-5: Basic concept of honeycomb sandwich construction referred in [6]

2-3-3 Conclusion

A comparison of the material properties between different type of composite material structure is shown in Figure 2-6[6].

Material	Density (pcf)	Compression		Shear	
		Strength (psi)	Modulus (ksi)	Strength (psi)	Modulus (ksi)
Aluminum honeycomb	3.1	300	75	210	45
Nomex honeycomb	3.0	325	20	175	6
Fiberglass honeycomb	3.0	410	23	195	19
Rohacell foam	3.1	128	10	114	3
Klegecell foam	3.0	69	2.7	51	1.1
Rigicell foam	3.0	80	2.5	70	2.5
Divinycell foam	3.1	100	10.2	73	2.5

1 ksi = 1000 psi.

Figure 2-6: Comparison of different composite material properties as referred in [6]

It is obvious to see that with comparable density, the aluminum honeycomb marks the top place with great strength and modulus in both compression and shear load cases. A good example is its application in the MPI CableRobot simulator functioning as the floor. In this design case, it may be a good choice for the material to build up the shell.

2-3-4 Bolted joints connection with honeycomb panels

The joining method of honeycomb material is various.[8] One way is by focusing on a local reinforcement to the core structure, usually in the form of one or more metallic inserts where the joint is to be established (refer Figure 2-7 on the left). The other way is to use out-plane joints to spread the force where the bolt is located (refer Figure 2-7 on the right).

For either type of bolting has its advantages and disadvantages. For example, the disadvantages of using inserts is that it takes more time and effort to manufacture. However, for inserts, the connection stiffness is dependent on the strength and stiffness of the glue. With
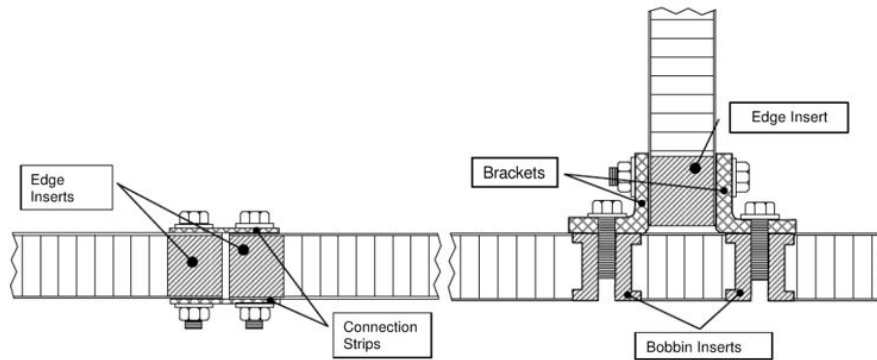
Figure 2-7: Various types of joining honeycomb with bolted connection[8]

a good quality of glue, the stiffness of the connection is very high. For the metal strip joint of mounting, it is very easy and fast, which saves cost and time. But the stiffness of the connection is depended on the compression resistance of the honeycomb structure and the size of the strip. It also add more mass to the structure.

Thus the selection of joining method with the honeycomb panels is highly dependent on the required stiffness and cost limits.

2-4   Hexapod motion simulator and the components to be mounted

After a study of the existing cabin design examples, the installed hexapod motion simulator to be designed with will be identified with both its system composition and its dynamic capabilities. Moreover, the components required to be mounted inside the cabin will be introduced as well.[2] This is the most conventional Stewart platform equipped with 6 linear actuators based on a hexapod design. Such simulators are widely used for their capability of carrying large payloads, large moment of inertia, and maintaining high rigidity. The drawback is its motion envelop (the workspace of the cabin) is highly limited by the actuator strokes.

2-4-1   Hexapod motion simulator system description

The installed hexapod is defined with this electric 6 DOF motion system consisting of a motion base assembly, system controls, motion software and documentation. The motion base assembly as referred in Figure 1-2 is the main target for the literature study to start the cabin design task. It consists of three main components:

Motion platform

The motion platform is a steel construction that comprises mounting holes (collected by 3 main mounting blocks) for the customer's cabin and universal joints to which the motion servo actuators are attached. The steel triangular structure (refer to the upper left drawing in Figure 2-8) between mounting blocks has no contribution to payload stiffness or strength
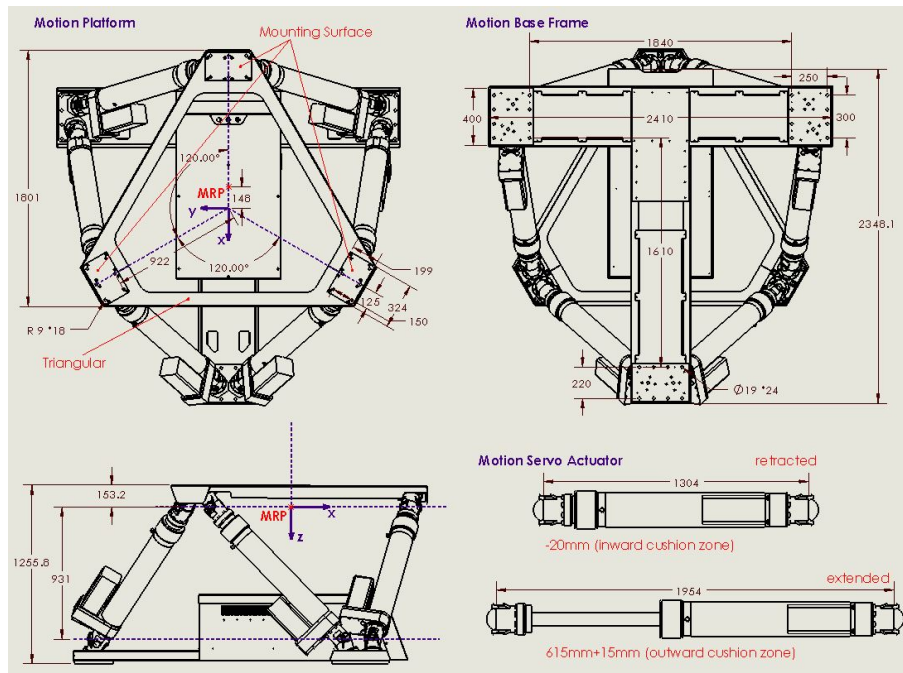
Figure 2-8: Engineering drawings of hexapod simulator with parameters referred from documents

and is only for handling and transport. Thus the cabin performed as the whole payload should be a stiff structure by itself. And any potential interference between the payload, actuators, frames and joints should be avoided by mounting the main items of the payload at or above the level of the upper platform top surface.

Motion base frame

The motion base is a steel construction (refer to the upper right drawing in Figure 2-8) that comprises mounting holes (collected by 3 floor mounting pads) for the customer's floor and universal joints to which the motion servo actuators are attached. The motion base is already installed and could not be changed. The floor is assumed to be able to provide sufficient strength, stiffness and stability to support the motion system under all conditions.

Motion servo actuators

The actuator as referred in the lower drawings in Figure 2-8 has a maximum stroke of 650mm including a total of 35mm safety zones. Each actuator is equipped with two joints. The design allows the platform to move freely within the maximum excursion envelope without mechanical interference. The velocity of each actuator is 450mm/s.

2-4-2   Hexapod motion simulation dynamic capabilities

Motion Reference Point for maximum excursions, velocities and accelerations (MRP)

The Motion Reference Point for maximum excursions, velocities and accelerations (MRP) of the motion system denotes the reference point for maximum excursions, velocities and accelerations. It lies 148mm toward the +x direction with respect to the geometric origin of the upper joint plane, and 153.7mm below the top surface of moving platform as referred in Figure 2-8.

Axis system definition

The axis definition of the system is shown in Figure 2-9. The names used for the six degrees of freedom are: 1)Surge: translation in X direction; 2)Sway: translation in Y direction; 3)Heave: translation in Z direction; 4)Roll: rotation around X-axes; 5)Pitch: rotation around Y-axes; 6)Yaw: rotation around Z-axes.
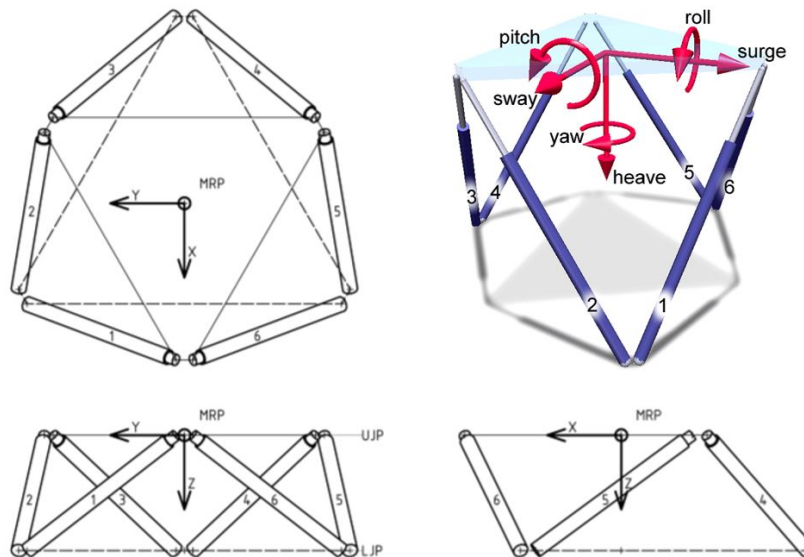
Figure 2-9: The hexapod system axis definition

Moving platform coordinate system

The moving platform coordinate system is fixed to the moving platform of the motion system. It has its XY plane fo the moving platform coordinate system lies in the Upper Joint Plane and Z axis points downwards (refer Figure 2-9). The origin of th moving platform coordinate system is located at the MRP.

Gross moving load

The mounted payload can have its weight maximumly at 1500 kg and its moment of inertia maximumly at 2000 kgm^2 for Ixx, Iyy and Izz while maintaining a good dynamic capabilities.

The payload center of gravity should be lower than 1m above the mounting surface and should lie -0.148m in X with respect to the motion reference point, which is right the upper joint plane center point.

Non-simultaneous velocities and accelerations

The accelerations are defined relative to the motion reference point with the motion system in its neutral position. With the designed gross moving load, the system can provide the non-simultaneous accelerations and acceleration onsets as shown in Table 2-1.

Direction	Velocity		Acceleration		Acceleration onset
Surge	± 0.79 m/s	± 31.1 in/s	± 7.000 m/s²	± 0.714 g	± 10.0 g/s
Sway	± 0.81 m/s	± 31.8 in/s	± 7.000 m/s²	± 0.714 g	± 10.0 g/s
Heave	± 0.55 m/s	± 21.6 in/s	± 10.000 m/s²	± 1.020 g	± 10.0 g/s
Roll	± 34.3 °/s		± 250 °/s²		± 600.0 °/s²/s
Pitch	± 37.4 °/s		± 250 °/s²		± 600.0 °/s²/s
Yaw	± 41.3 °/s		± 500 °/s²		± 600.0 °/s²/s

Table 2-1: Non-simultaneous velocities and accelerations defined by the hexapod

Frequency response and resonance

The frequency response is measured at the motion reference point with the system in the neutral position. The frequency response specified is valid for payloads with a minimum resonance frequency of 10 Hz. When the stiffness of the payload is higher, the frequency response of the system can be further improved.

Chapter 3

Cabin design problem definition

The previous chapter has given the literature study about the state-of-art method of manufacturing a motion simulator cabin. In the last section, the installed hexapod system which is to be designed with is identified with its system description as well as the dynamic capabilities.

This chapter will start the multi-purpose research cabin design with a problem definition. Each requirement from the user wish will be translated into specific parameter, which can be identified via calculation or analysis. The goal is to qualify and further quantify the design constraints and objectives with specific boundaries and magnitudes. The ultimate goal of the project is to complete a modular cabin structural design that could meet the defined boundaries and objectives presented in this chapter.

3-1 Statement of general requirements

Design problems are generally defined by environment conditions and user wishes. By summarizing the problems as statements, a more systemic approach can be conducted to translate the general requirements into specific design constraints and objectives. The general requirements can be stated as follows from the user:

1. Designed cabin should be safe to operate inside the laboratory room without collision

2. Designed cabin should be capable of accommodating seats, various control devices, safety systems and visualization system with optimized positioning

3. Designed cabin should meet the maximum weight and moment of inertia requirements which is checked against the hexapod's dynamic capabilities

4. Designed cabin should be cost-effective with respect to its material and manufacture method to meet the maximum production costs

5. Designed cabin should meet the required modularity for frequent adjustment and re-placement of the equipment mounted inside it for multiple research experiments and participants

6. Designed cabin should be stiff enough to safely support all the components in the determined positions with minimized deflection also at higher frequencies

The general statements can be translated into design parameters of cabin's dimension, inner volume, mass properties, production costs, modularity, stiffness and eigen-frequency. The limited work space condition together with the required inner volume, which is defined by the optimal positioning of components, will determine the preliminary cabin concept with dimensional boundaries. The mass properties and natural frequency limited by the hexapod motion simulator system will have their boundaries defined in order to maintain a good dynamic capability of the hexapod. The budget of production costs is defined by the user, as well as the modularity and stiffness. All the requirements play a role when making a design choice, however with different priorities. This will also be specified in the following sections. In the end, the design has to meet the boundaries of all the requirements.

During each boundary definition, due to the practicality of this project, the method been selected is not necessarily the most accurate but the most effective regarding to time and effort efficiency. The purpose of using each approach will be illustrated and the credibility will be verified for each result.

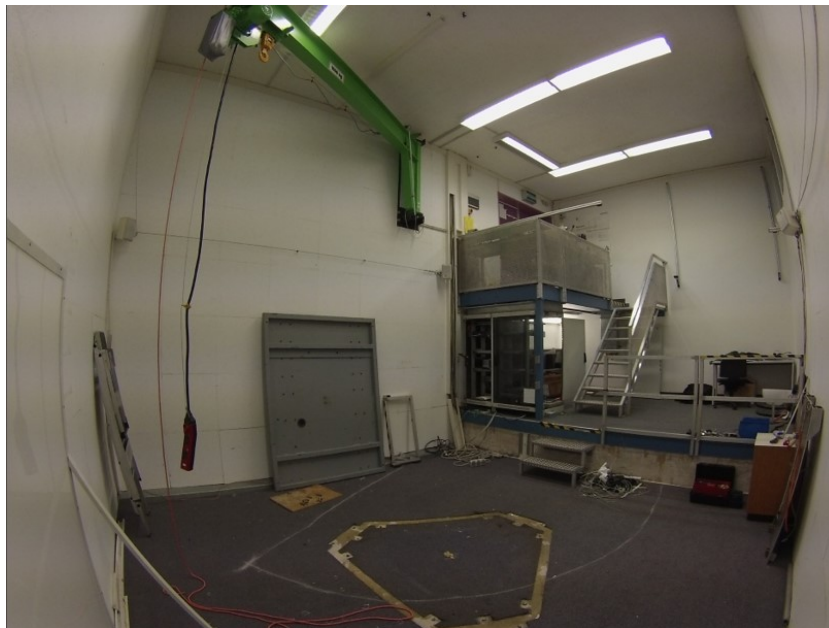## 3-2   Dimensional constraint analysis

Figure 3-1: Limited work space inside the motion lab for hexapod motion simulator to operate

A main constraint from the local environment condition is the work space limitation. In Figure 3-1 showed the work space of the motion lab room, its size is relatively small compare to other motion simulator labs. A measurement of the room size is approximately 4.9m*4.9m*4.9m, which determined the maximum dimension of the cabin without collision with walls or other obstacles inside the lab room. However, the boundary requires a motion envelope analysis together with the room model to quantify its magnitude.

Furthermore, multiple research purpose requires different experiment setups to be installed inside the cabin, and their positioning has to meet certain criterion defined by experimenters. This has provided with the cabin's inner volume a range to be optimized with. Thus, the specifics of the positioning of each critical component has to be defined to quantify the boundary of the optimal inner volume of cabin.

In this section, the definition of boundaries about dimensional aspect will be conducted, in the end a preliminary concept will be proposed.

3-2-1   Motion envelope analysis of hexapod system

The cabin dimension is constrained by the lab room in which the hexapod is installed. The cabin needs to be designed such that collisions with walls or other obstacles cannot occur at any time, even in extreme hexapod positions. (The extreme hexapod positions are defined as the combinations of actuators' states. Each actuator has two extreme states of completely extended or retracted including conditions that the stroke is within the cushioning zones. Thus 6 actuators in total give 64 combinations which are defined as the 64 extreme positions.) For this purpose, a motion envelop analysis model is required, in which the motion envelope of the hexapod with the envisioned payload is determined using a dynamical model of the hexapod.

The approach (refer Appendix D) is to first have an envisioned payload available in 3D drawing software, then attach a moving platform coordinate system (refer Figure 2-9) to the payload that has its origin in the MRP, after the MRP can be transformed with the excursions in 6 degree of freedom at 64 extreme poses available in Appendix A-2-2, consequently the payload can be transformed to the extreme positions, in the end by overlaying all results, the complete envelope can be determined. A modular motion envelope model with an envisioned payload sample of 2.2*2.0*1.8 m can be seen in Figure 3-2. At a later stage, after a finalized cabin design is achieved, the dimension can be checked by simply replacing the envisioned payload with the designed cabin structure. If the imported cabin envelope model exceeded the wall of the room model, then adjustment need to be made. Otherwise, the designed cabin is proved to be validate with the dimension, since this modular check model is a conservative model, thus as long as the imported cabin envelope does not exceed the room boundary, it is safe to operate.

A first estimation of the dimensional boundary is around 2.1m*2.3m*2.1m (width*depth*height). However, this has to be further specified with the positioning of cabin center with respect to the MRP. This has to be rechecked after the analysis of positioning of the components.
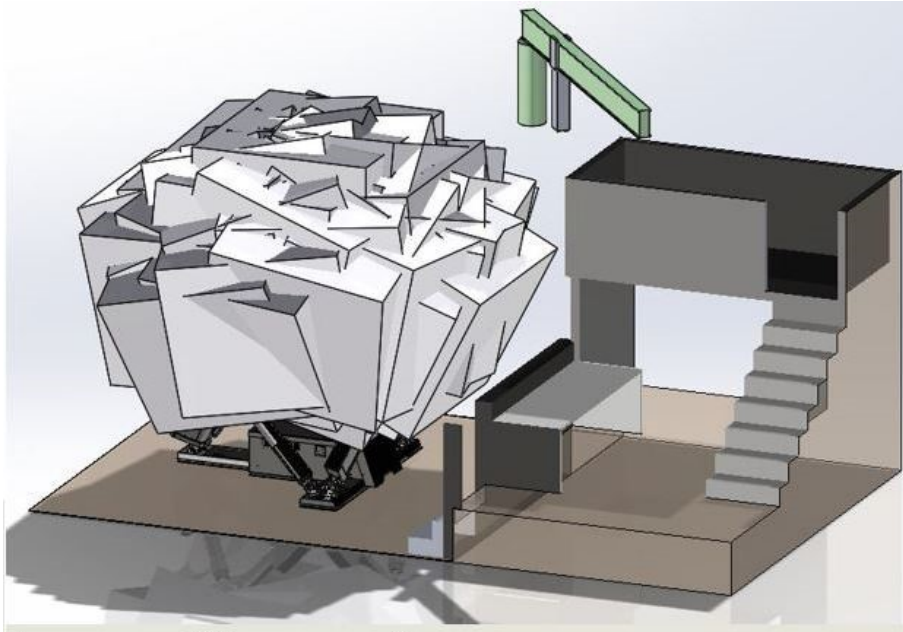
Figure 3-2: Motion envelop analysis model with an envisioned payload

3-2-2   Leg envelope analysis of hexapod actuators

In the definition from the hexapod, main items of the cabin should be mounted at or above the hexapod mounting surface, however, some elements can also exceed to the inner space between the actuator legs below the hexapod mounting surface as long as it is validate that no interferences will happen. For this purpose, a leg envelop analysis model is conducted using the same approach from last subsection. The main change is to fix the motion platform while make the base frame float instead of fixing the base frame. A region free from the actuators envelope is analyzed as shown in Figure 3-3. After the cabin is designed, it can be quickly checked with this leg envelope model.
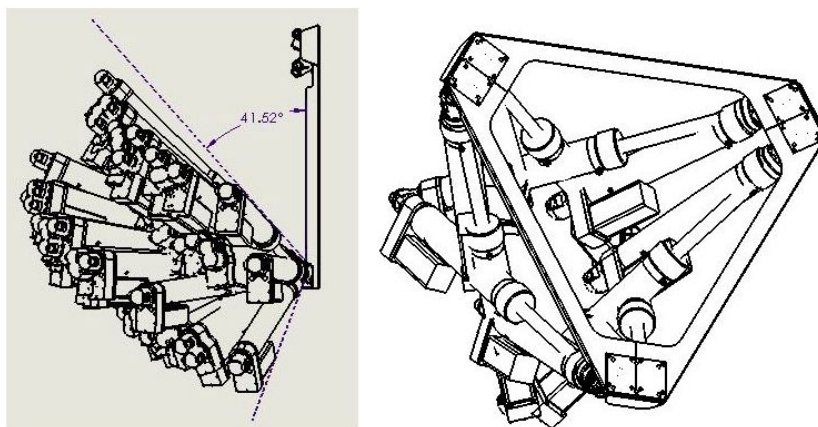

Figure 3-3: Leg envelope analysis model with 1 leg on the left and 6 legs on the right

3-2-3   Optimal positioning of components

As the problem stated from Chapter 1, the hexapod motion simulator being designed with will be used for multiple research purpose such as motion perception and vehicle simulation. And the multi-types of experiment require the designed cabin to be able to accommodate setups including at least a seat, certain control devices, safety devices and a visualization system. Moreover, these components have specific positioning requirement and can be optimized regarding to certain experimental aspect. In this subsection, each component will be identified individually with its optimal positioning.

Seat positioning and optimization

The seat component has the properties defined in Table 3-1.

Weight	13.6kg	
Dimensions	Bounding: 556*665*1032 mm (w*d*h)	
Position requirements	Horizontally: the head of the simulator occupant should be centered with respect to MRP; Vertically: the head of the simulator occupant should be as close to the MRP as possible, with boundary of less than 1m	
Mounting method	Bolts + nuts on slide blocks; removable in both x and z axis	

Table 3-1: Seat component properties and positioning summary

The seat can be centered with respect to the MRP easily in horizontal point of view, such that the head of the simulator occupant is over the MRP. Then the boundary of the inner volume depth is determined with the space required from the front and back of the seat. While, in the vertical positioning point of view, it can be optimized with minimum distance from simulator occupant head to the MRP. Because for motion perception experiment, with a minimized head-to-MRP distance, the pure rotational excursion at head can be maximized. For example, when an occupant's head is away from the MRP, a pure rotation at MRP will be transmitted as a mixed motion of rotation and translation at the occupant's head, in order to compensate the translation to obtain a pure rotation at occupant's head, the platform needs to move backwards which also eliminates certain excursion of the rotation. However, as the seat moves closer to the MRP, it adds difficulties to design the cabin structure. This is because the MRP is located 153.7 mm below the mounting surface of motion platform (refer Figure 2-8). Thus an investigation is conducted to understand how much gain can be achieved by changing the head-to-MRP distance.

A dynamical hexapod model in SolidWorks is used. The hexapod's top frame is rigidly connected through a rod with a single degree-of-freedom joint, which is located at the position of the occupants head. In this condition, the hexapod motion results in pure roll or pitch rotation at the occupant's head can be simulated (refer Figure 3-4).

A measurement of the difference between maximum rotational excursion can be seen in Figure 3-5, for roll excursion, the gain of changing head-to-MRP distance from 1.3 m to 0.9 m is

Figure 3-4: Models to check the maximum pure roll and pitch excursion at head with different head-to-MRP distances of 1.3m and 0.9m

6° in roll and 2.5^o in pitch. Compare to the difficulties added to the design and manufacture of the cabin structure, the rotational excursion gain is not revolutionary and is not convincing enough to have high priority of the requirement to optimize it.
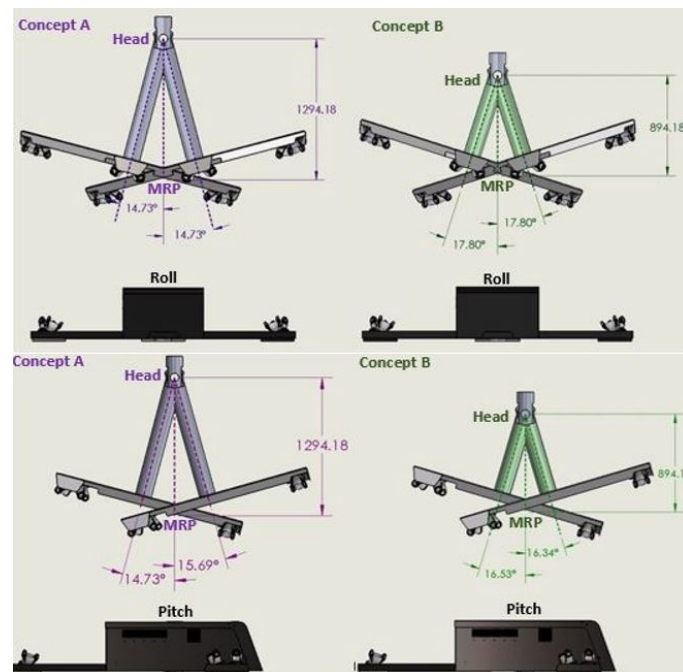

Figure 3-5: Results of the rotational excursion gain regarding to different head-to-MRP distance

In conclusion, the positioning of seat will be centered with MRP in the horizontal plane while vertically no further than 1 m above the MRP.

Projector positioning and optimization

Regarding to the visualization system aspect, the requirement from experimenter will be evaluated first. With the two mentioned types experiment (refer Chapter 1), psychophysics experiment requires the visual display to have a high resolution, processing speed and low physical production (e.g., heat, magnetic and noise). Meanwhile, vehicle simulation experiment requires a wide field of view, which indicates the requirement of an maximum image size of projector or multiple monitors display setup. A comparison between different visualization system is summarized in Table 3-2.

Properties	Projection	TV Monitor Display	Head Mounting Display
Total Weight	(screen) <25kg	<40kg	<1kg
Image Quality	1920*1080	3840*2160	relatively low
Image Processing	high	input lag 20ms	qualified
Physical Effect	magnetic, noise	noise	magnetic, noise, heat
EEG recordings	Highly preferred	preferred	unavailable
FOV	84°*53°	73°*45°	no limits but can't see real setups
Side-view	multiple projectors	multiple monitors	available
Stability	stiff mounting	stiff mounting	no limits

Table 3-2: Visualization system properties comparison between different options

From the comparison, projection system is preferred first for its high image qualities regarding to the requirement from psychophysics experiments. It is also very flexible to adjust both the image size and position by changing the throw distance. Multiple projectors setup makes it possible to have also side views. However, the occurrence of shadows should be avoid and its supporting structure should have sufficient stiffness to keep it moving stably.

The selected projector is a PROPixx DLP LED projector from VPixx[1] with high resolution and projection quality especially for conducting psychophysics experiment, and it is preferably mounted inside a ShieldPixx enclosure[2]. With a VPX-ACC-6506 short-throw lens, which has a throw ratio of 0.84:1 - 1.03:1, focus range of 0.5m - 4m and a fixed vertical lens shift of 45%. After communication with the vendors from VPixx and some hand-calculation, 1.5m was chosen as the optimal throw distance together with the vertical lens shift. Assuming the eye-to-screen distance is 1m, a shadow check was performed shown in Figure 3-6.

The projection screen size has been maximized up to 1.79m*1.0m, resulted from considerations of both the estimated maximum cabin dimension boundary and the projector capabilities. As checked in Figure 3-6 the occurrence of shadows is minimized to zero.

---

[1]http://vpixx.com/products/tools-for-vision-sciences/visual-stimulus-displays/propixx/
[2]http://vpixx.com/products/tools-for-mri/mri-visual-stimulusdisplays/shieldpixx/
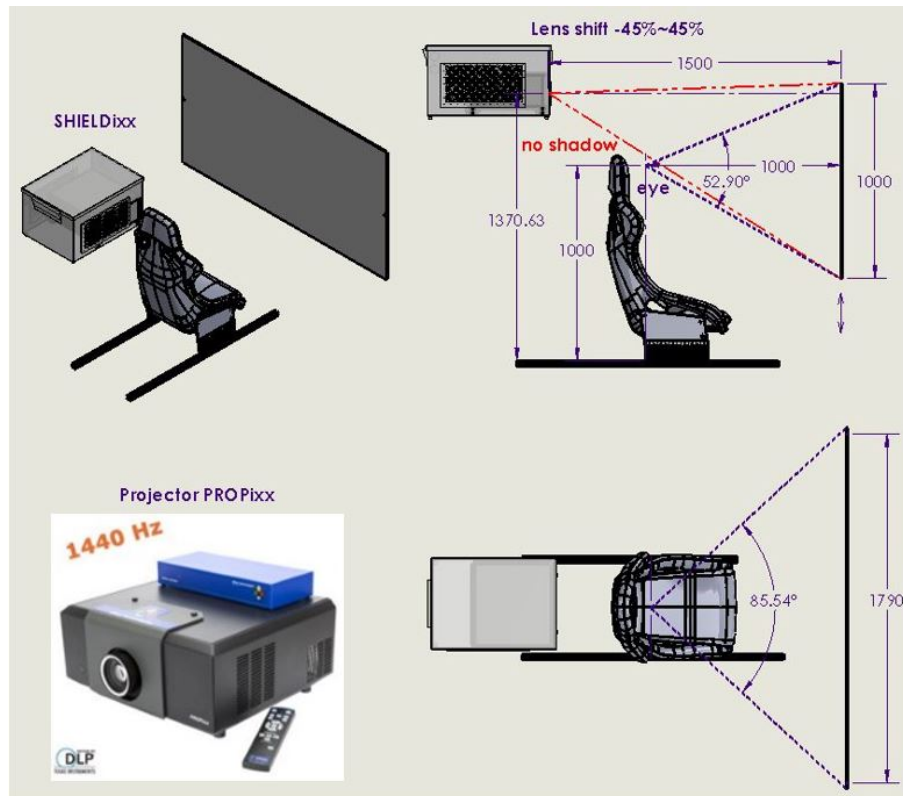
Figure 3-6: Shadow check of projection visualization system with PROPixx

In conclusion, through the selection and optimization of the projector, its position is determined with respect to the seat, which is horizontally centered with the MRP. The positioning of projector requires the cabin to extend behind the MRP to be around 910mm, while the positioning of the projected screen requires the cabin to extend in front of the MRP to around 1m. The relative height on the front is about 1.5m from the seat and about 1.6m height on the back. This determines the required depth of the inner volume to be at least 1.91m, a height of the inner volume to be at least 1.6m and a width of the inner volume to be at least 1.79m.

3-2-4 Positioning of control devices and safety features

A description of the car and helicopter setups to be used can be seen in Table 3-3. The positioning of the devices is determined according to a measurement of the current setups in other applied simulators (the CyberMotion simulator), and their adjustable ranges is determined from the user wishes (refer Appendix C). As a result, the depth of inner volume of cabin to the front from the MRP is required to be maximum 1.33m and the space below the seat is required to be at least 200mm height. This has finally determined the required inner volume of the total cabin to be 1.82m height, 2.24m depth and 1.79m width.

The safety systems include a seat belts with lock detector,an emergency button within arm's reach, a fire extinguisher and a sensor alarm for crane secure position test. All the safety
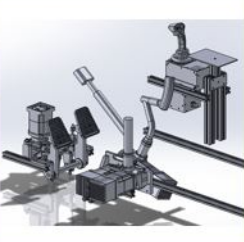
Weight	25kg	
Dimensions	Bounding: 515*704*835 mm (w*d*h)	
Position requirements	Centered with respect to the seat; Frame 400mm from the fixation points to the seat	
Mounting method	Bolts + nuts M6 *4 on slide blocks; removable in x axis	

Weight	48kg	
Dimensions	Bounding: 1041*1130*861 mm (w*d*h)	
Position requirements	Collective stick on let-hand side; cyclic stick and pedals centered with respect to the seat	
Mounting method	Bolts + nuts M8 *15 on slide blocks; removable in both x and z axis	

Table 3-3: Car steering and helicopter setups properties overview

features are easy to position with less requirements from the experiment. Supporting systems such as the SCM (system control module) and the PS (power supply), which weigh 2kg and 6kg respectively, will be positioned on the back side of the seat together with ballast means (if necessary) in order to bring the COG of the cabin to the vertical line along MRP and balance the weight of control setups on the front of the seat.

3-2-5   Conclusion

Inner volume boundary definition

After the optimal positioning of all the components required to be mounted inside the cabin, a summary can be seen in Figure 3-7. This has defined the optimized boundary for the required inner volume with 2.04m height, 1.35m depth from the MRP to the front, and 1.79m width. The red arrows has indicated the desired adjustable range for each components, which gives further flexibility to change the required inner volume.

With this positioning of the components, the distance between the occupant's head and the MRP is around 1.3m, which allows a maximum pure rotational excursion of 30° in roll and 30.4^o in pitch.

Outer dimension boundary definition

With the definition of inner volume of the cabin, its maximum dimension can be specified again with the motion envelope model and the result is shown in Figure 3-8.

The cabin has a maximum depth of 2.25m with 1.35m extending to the front and 0.9m extending to the back. In the front, the height is constrained to 1.76m while on the back, the
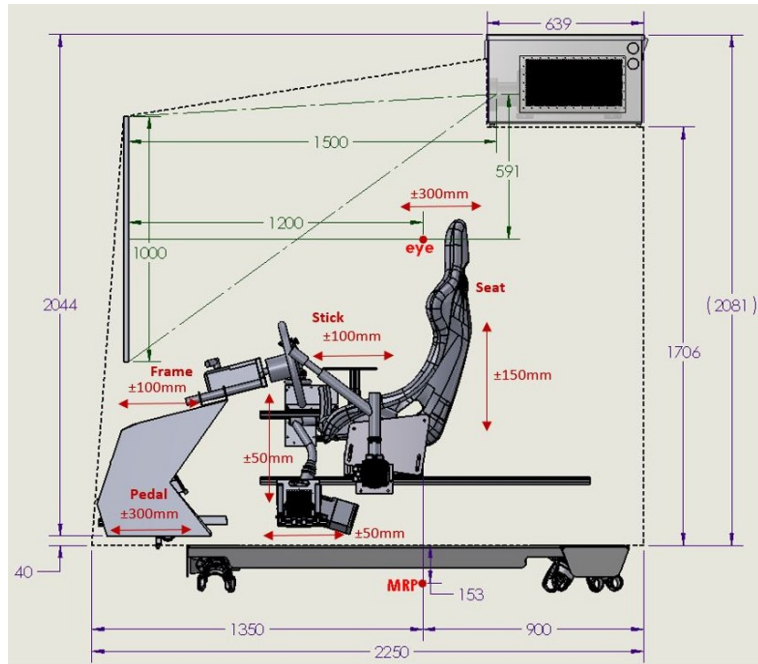
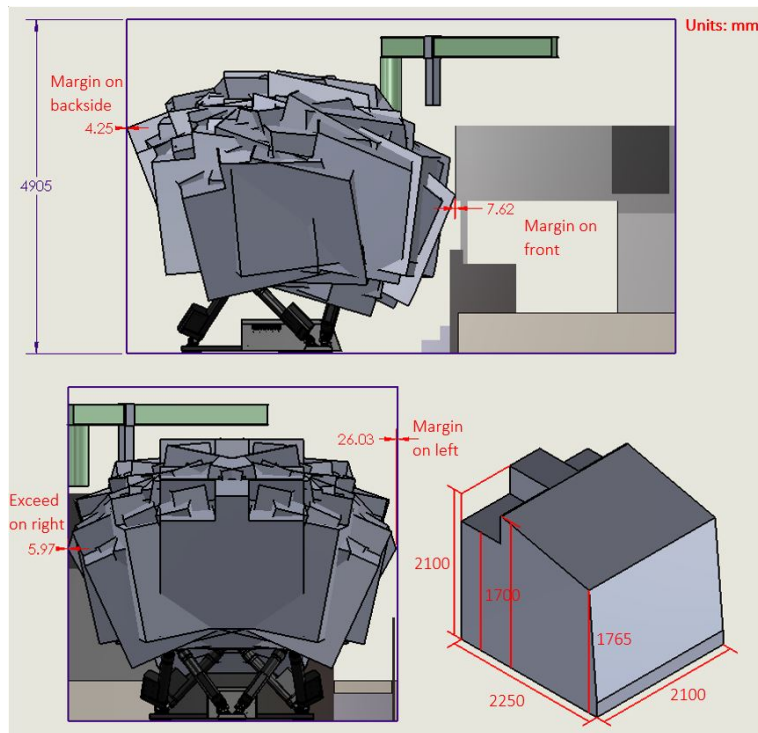**Figure 3-7:** Inner volume boundary defined with optimal positioning of the components

Figure 3-8: Dimensional constraint of cabin structural definition

height is constrained to 2.1m. The width of the cabin can be extended up to 2.1m. This has given a more specific boundary for the dimensional parameter of cabin structure design.

3-3   Cabin structure assembly break down

In Figure 3-9 showed the path to access the motion lab room where the hexapod motion simulator was installed. A measurement with 2m*2.15m showed the boundary of dimensions of each part that could be brought into the motion lab. Obviously, the cabin could not be able to enter the motion lab as a single entity. Thus, the total cabin structure has to be broken down in to parts and reassembled within the motion lab room. Each part of the cabin assembly is constrained with their size smaller than 2m*2.15m as its boundary.
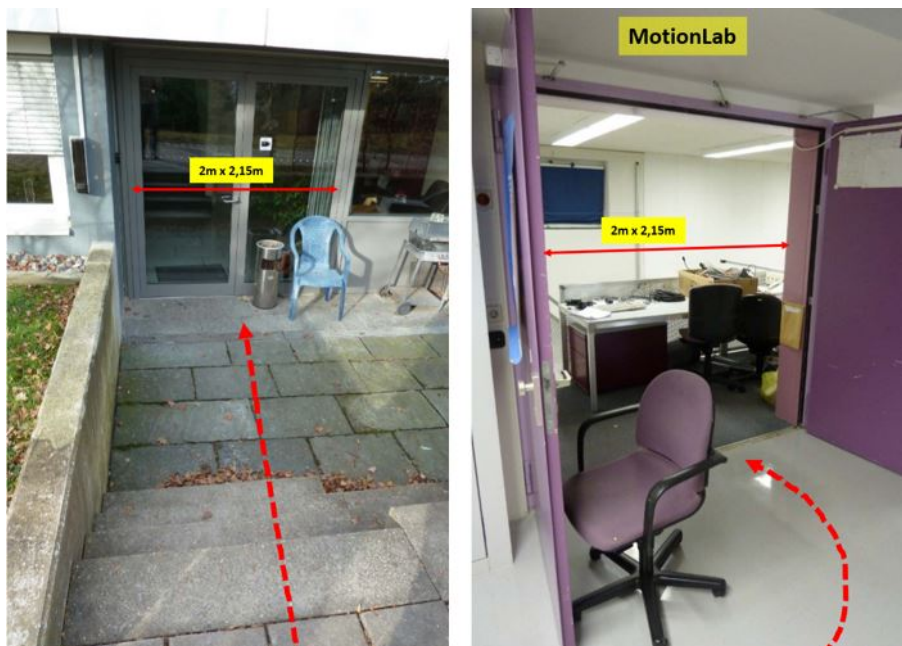

Figure 3-9: Limited path and entrance for cabin structure parts to access the motion lab

Consequently, the whole cabin structure can be preliminarily decomposed into three parts: a base floor, outer structure and supporting items (to mount the components). The boundary for the base floor is approximately 2.1m x 2.25m x 0.05m which can be brought into the lab as one entity. The outer structure with a total size of 2.1m x 2.25m x 2.04m exceeded the limitation of the entrance size, thus it should be further decomposed into several frames and reassembled within the lab. The supporting items can be easily brought into the motion lab as beam elements. A more detailed assembly break down is shown in the next section.

3-4   Cabin modularity definition

After a preliminary assembly break down in the last section, each part is further identified with its required functionality and modularity.

Permanent parts (to be used for every experiment)

1)Base floor; 2)Seat with its supporting structure

Semi-permanent parts (to be used for part of experiments)

1)Outer structure; 2)Visualization system with its supporting structure

Flexible parts (will be adjusted or exchanged according to specific experiments)

1)Mounted components (participants, control devices, power supply, etc...);

2)Supporting items for the mounted components

Firstly, the base floor will be needed for all kinds of experiments, thus it is defined as a permanent part of the cabin structure. Which means the selection for its connection method can be more permanent. Secondly, due to the requirement that the components inside the cabin may change regarding to different experiment requirements, as well as the projector it self, the outer structure which supports projectors and screens is defined as a semi-permanent part of the cabin structure. Especially the panels functioning as the walls should be removable to make more space for exchanging devices. This also means the connections between outer structure and base floor will prefer non permanent methods such as bolts. At last, supporting items structure has to meet requirement of adjustability and exchangability of the components, thus it is defined with the flexibility for making changes. This means the connection methods have to be non permanent connection like bolts. An overview of structure assemby is illustrated in Figure 3-10.
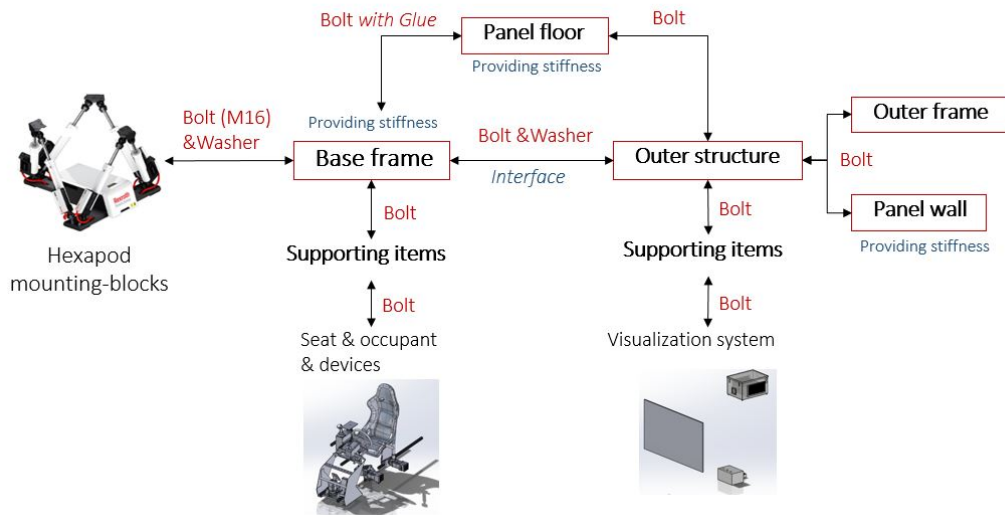

Figure 3-10: Assembly break down of cabin structure

The definition of the modularity required from the cabin structure has constrained the joining method between each part of the assembly. Connections within the base floor has the least constraint that it can be permanent. However, connection between outer structure and the base floor, connection between the outer structure assembly, connection between the wall

and frame and connection between the supporting items and the components should be non permanent.

3-5   Mass properties definition

From the hexapod motion simulator system description, the mass of the payload is defined with a maximum boundary of 1500kg, and the center of gravity is defined with maximum 1m above the mounting surface, the moment of inertia at the object's center of gravity is defined with maximum $2000kgm^2$ in its Ixx, Iyy and Izz components. It is assumed that within this defined boundary of mass properties, the hexapod's dynamic capabilities will not be affect dramatically. (This will be validated in Chapter 5.) However, by improving the mass properties with a lighter weight and lower center of gravity structure, the frequency response time of the system can be further improved. Thus, the optimization of the weight and center of gravity is required but will have lower priority.

Lightweight structure objective requires the design of each part to be efficient structure. Thus, sandwich concept[6] are applied for all the cabin structure design by combining beam frames and filling-in panels.

3-6   Frequency response and stiffness requirement definition

As specified in Chapter 1, both for motion perception simulation and vehicle simulation want the simulator to operate as naturally as possible compared to reality. This has indicated the response time of the system has to be low to keep the simulation efficient. The hexapod system has defined its frequency response to be valid for payloads with a minimum resonance frequency of $10Hz$. Thus the natural frequency of the designed cabin system has to be higher than 10 Hz. However, by designing a payload with higher stiffness, the frequency response of the system can also be improved.

The requirement of the structure's stiffness is defined with the undesired deflection of critical components under worst load cases. The most critical component is the projector and screen. The translational deflection of the projector in y and z axis will cause the image to shift with the same magnitude, while deflection in x axis is more critical since it will cause the change of throw distance, consequently the image can lose its focus when this deflection is too large. The rotational deflection of the projector around x axis will cause the image to rotate with the same magnitude while rotation in y and z axis is more critical since it will cause the throw distance to be different along the screen, where keystone effect will occur. In order to keep the projection image quality, the allowed deflections of projector are constrained to 1mm in translational degree of freedom especially in x axis. The allowed rotational deflections of projector are constrained to 0.003 rad especially around y and z axis. With a throw distance of 1.5 m, 0.003 rad defection of projector will cause 5mm shift at the screen.

The deflection of screen is define with 1mm maximum in translation and 0.005 rad maximum in rotation under any worst load conditions.

3-7   Conclusion

In this Chapter, the constraints and objectives are defined with specific boundaries which can be directly used for the detailed cabin structure design. A summary can be seen in Table 3-4.

| | Modularity | Dimension | | | Stiffness | | | Mass properties | | Production costs |
		Access	Work space	Inner volume	Axial	Rotational	Dynamical	Weight	Moment of inertia	
Cabin structure assembly	detachable	detachable	2.1*2.25*2.1 (m) (w*d*h)	1.8*2.2*2.05 (m) (w*d*h)	defined by critical components: projector translational < 1mm, rotational < 0.003 rad; screen translational <1 mm, rotational < 0.005 rad		defined as natural frequencies	< 930 (kg)	< 1.3*1.2*1.6 (10³) (kgm²)	< 20 (keuro)
Base frame	permanent	< 2*2.15 (m)	thickness < 50 (mm)				> 10 Hz	< 450 (kg)	COG -to- MRP distance < 1m	< 10 (keuro)
Outer structure frame	removable	< 2*2.15 (m)	thickness < 25 (mm)				> 10 Hz	< 100 (kg)		< 4 (keuro)
Panels	removable	< 2*2.15 (m)					> 10 Hz	< 200 (kg)		< 2 (keuro)
Mounting items	removable & adjustable	< 2*2.15 (m)	**				> 10 Hz	< 180 (kg)		< 4 (keuro)
Design Priority	high during concept design phase				high during detailed design phase			high during evaluation phase		

Table 3-4: Problem definition of cabin structural design with specified boundaries

Clearly, the modularity requirement has determined the preliminary concept of the cabin structure with the highest priority. And the concept is further modified with the dimensional constrains. Detailed structure design are leading by the stiffness constraint. And the resulted design has to be checked with the defined boundaries of mass properties and production costs.

In next chapter, detailed design will be conducted to achieve the ultimate goal of the project, that is to complete a modular cabin structure design with specifics of major parts that could meet the defined boundaries and objectives presernted in this chapter.

Chapter 4

Structural design of cabin

In the previous chapter, the design problem was well defined with specific boundaries. In this chapter, a top-level cabin design will be completed. It includes a 3D drawing of the cabin and design choices regarding to material, manufacture method, joining method, assembly process and etc. It also includes the identification and functional description of each assembly part. During the design process, every choice that has been made will be clarified with its reason and will be checked with the requirements defined from last chapter.

4-1 Planning of design process

Due to the requirement of modularity, the total cabin structure is detached into three parts: base frame, outer structure and supporting panels. Similar design process will go through each substructure as summarized in the following points:

1. Concept design: based on the defined dimensional boundary and load distribution, the configuration is proposed and selected

2. Detailed design: based on the required stiffness, the specifics of the structure elements is decided and its joining method is designed

3. Stiffness verification: based on a FEM analysis tool (COMSOL), the stiffness in both static and dynamic cases will be verified, including the deflection under worst load cases, the response of components under maximum accelerations and the eigen-frequencies of the structure

4. Requirement evaluation: mass properties and production costs will be evaluated with the required boundaries in the end

4-2   Cabin load condition analysis

The analysis of load condition depends on the definition of the components mounted inside the cabin and the motion of the hexapod. Since the simulator is designed for multiple types of experiments, the setup of components inside cabin is changeable. The motion of simulator is also unpredictable at the moment. Thus, several assumptions are made to define the load cases.

Assumption 1: the total cabin payloads used for load calculation are defined by taking into account all the possible components and giving the conservatively estimated value of weight of each component. The defined payload model can be seen in Figure 4-1.
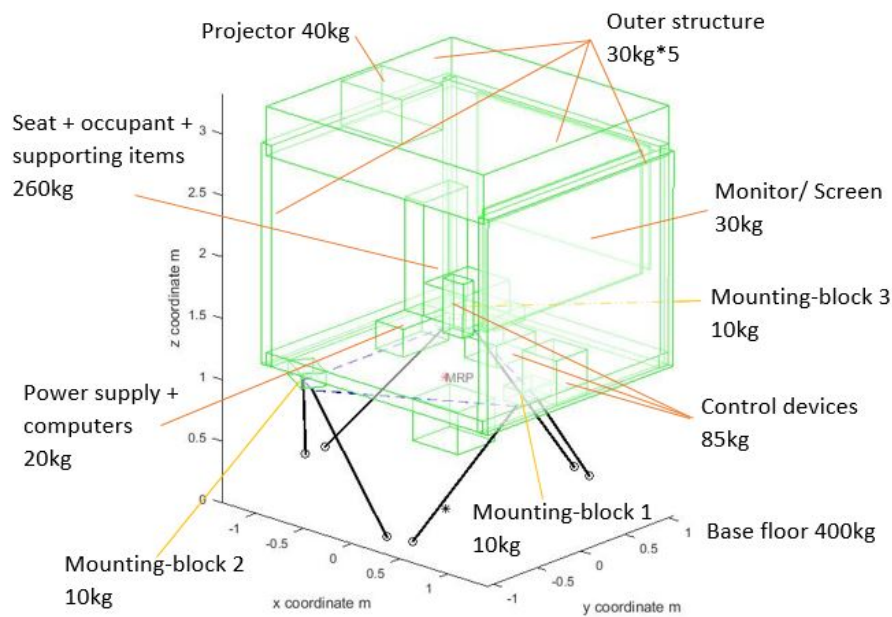
Figure 4-1: Cabin payload model for loads calculation

Assumption 2: the hexapod is rigidly supporting the cabin payloads, with which the deformation of the actuator legs can be eliminated.

Assumption 3: only specific load conditions are defined and applied to check the stiffness of the cabin structure, and they are proved to be the worst load conditions that could happen.

4-2-1   Stationary load conditions

In stationary conditions, the load condition for the cabin structure is to support all the payloads at any hexapod poses, among which the 64 extreme poses are the most critical ones where the worst case will occur. In order to calculate the gravity effect from the payloads at extreme hexapod poses, a coordinate system transformation model is built to transform gravity vector from the generalized coordinate system to the moving platform coordination system at extreme hexapod poses.(details refer Appendix A-3-1) These values can then be

applied for checking the stiffness of the designed cabin with its structure. Some critical poses can be seen in Figure 4-2.
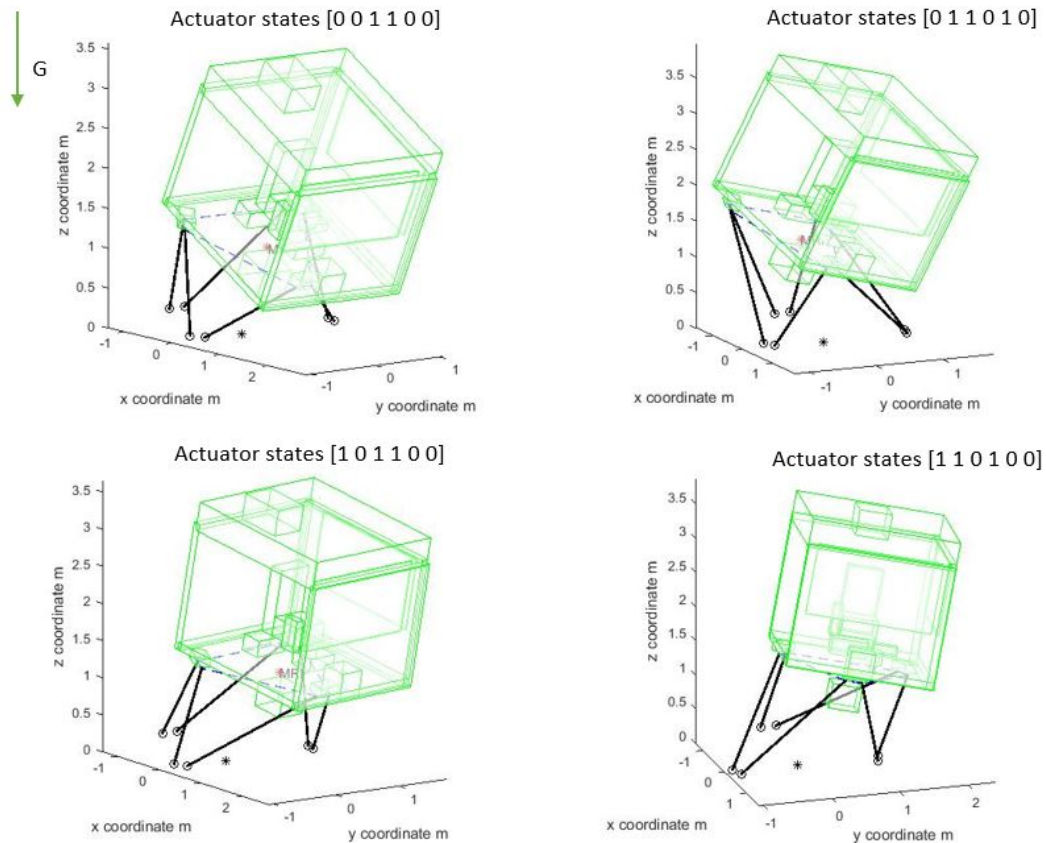

Figure 4-2: Critical pose examples for stationary load conditions

4-2-2   Dynamic load conditions

In dynamic load conditions, cabin structure has to transmit the forces exerted from the actuators to accelerate or decelerate the components rigidly. The response of the components due to the applied loads determines the stiffness of the design cabin structure. And the vibration of the components due to the acceleration is also involved.

In order to calculate the dynamic load conditions, the maximum acceleration and velocity per each degree of freedom is defined with reference from the hexapod system description[2].

Assumption 5: The worst dynamic load conditions happen when accelerating the payloads with the maximum non-simultaneous velocities and accelerations (defined relative to the MRP with the motion system in its neutral position) per each degree of freedom with the motion system in its extreme poses (refer Table 2-1).

With this definition, the force exerted from actuator to accelerate the payloads at the extreme poses can be calculated use inverse dynamics theory[9]. Some critical poses can be seen in

Figure 4-3 and Figure 4-4. For all the figures, the upper left plot visualized the hexapod pose and the force vector exerted by the actuators; the upper right plot showed the acceleration and velocity with the degree of freedom they applied to components; the lower left plot showed the actuator states which details of which actuator is fully extended and which actuator is fully retracted; the last plot showed the force values within each actuator.
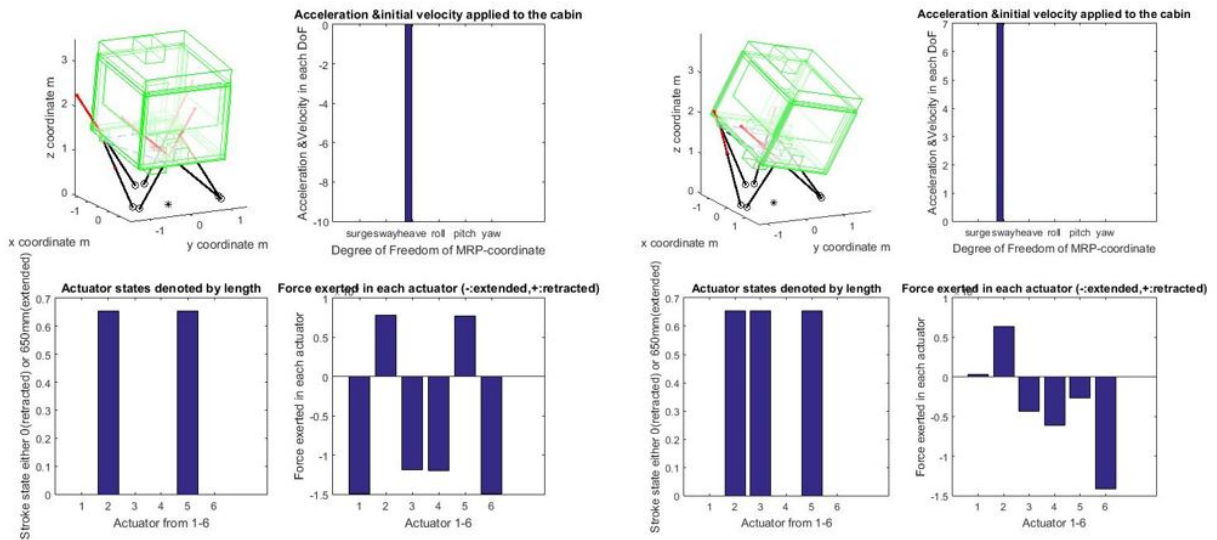

Figure 4-3: Worst dynamic load case with hexapod pose when forces is maximum
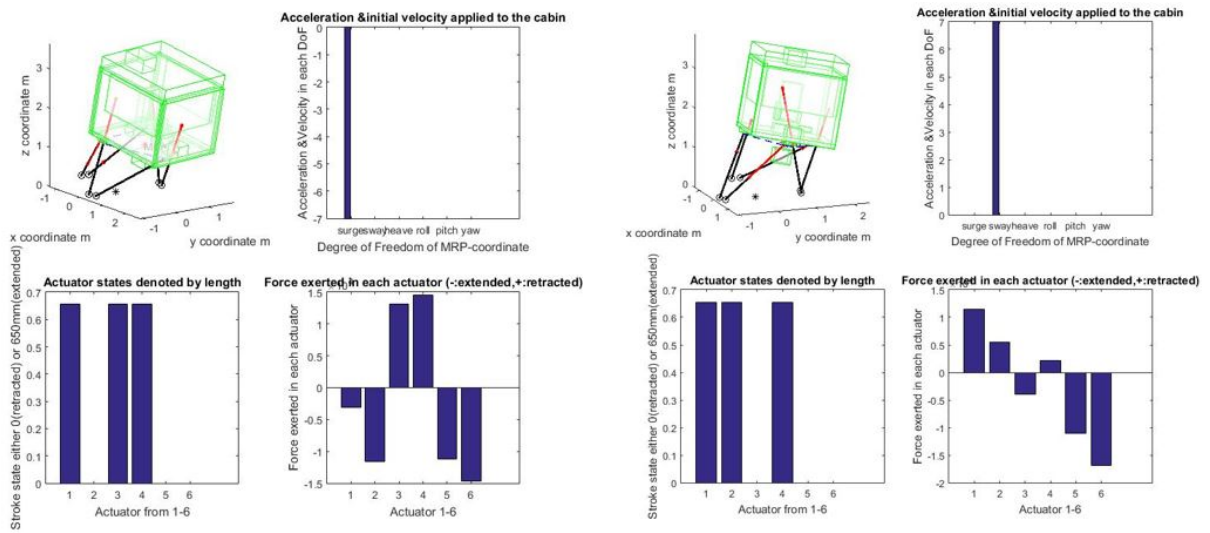
Figure 4-4: Worst dynamic load case with hexapod pose when moments is maximum

The detailed calculation model can refer Appendix A-3-2.

4-3   Design of base frame

The base frame as the most important part should be able to provide sufficient stiffness for the rest of the structure and cabin components under any load conditions. It is also a permanent part that will be mounted on the hexapod and will be required for all types of experiments, which gives more flexibility when selecting the manufacture method. The limits and boundaries for the base frame design can be checked in Table 3-4. In a later stage, panels will be added to filling-in the gaps of the base frame in order to provide a flat floor.

4-3-1   Concept design

The base frame will be designed to support the components mounted with it, including the cabin outer structure. In Figure 4-5 has showed the potential distributed loads on base frame in static case (see arrows) and the proposed beam element configuration to transfer the loads (see dashed lines). According to Figure 3-7 the optimal positioning of the components, firstly the seat and occupant are represented by the center payload loaded upon the MRP (indicated by the red arrow in Figure 4-5); secondly, the control devices such as pedal loaded at the front center are represented by the front payload (denoted by the blue arrow in Figure 4-5); moreover, the cabin outer structure mounted with the base frame at its edges is represented as the edge payload (refer orange arrows in Figure 4-5); at last the base frame is supported (or actuated) by three mounting blocks from the hexapod (refer the green arrows in Figure 4-5).
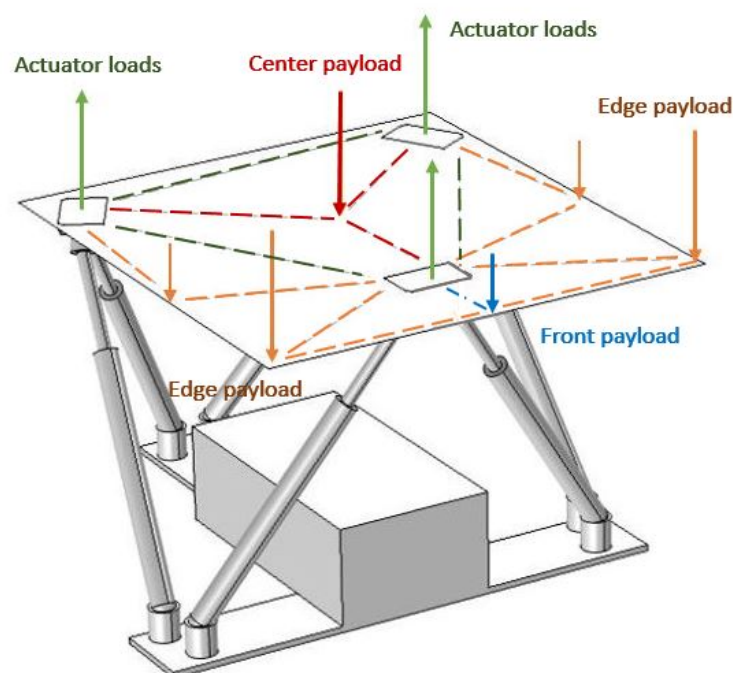

Figure 4-5: Base frame concept with load distribution (arrows) and proposed beam element configuration (dashed lines)

The worst dynamic load conditions created by each payload that acted on the base frame structure is calculated in Appendix A-3-2 and is summarized in Appendix B.

The sketch in Figure 4-5 was first illustrated with the concept in the upper left side of Figure 4-6, where a 'Mercedes-star-shape' element was designed to transfer the center payload to the three mounting block supports. A triangular element (reinforcing the original triangular steel structure from the hexapod system, refer Figure 2-8) was designed to stiffly collect actuators and maintain the configuration of the hexapod moving platform (refer Figure 2-9). A square element with side beams extending from the back mounting blocks to the front edge and beams connecting front mounting block to the front center was designed to support the front payload and edge payloads from the outer structure.
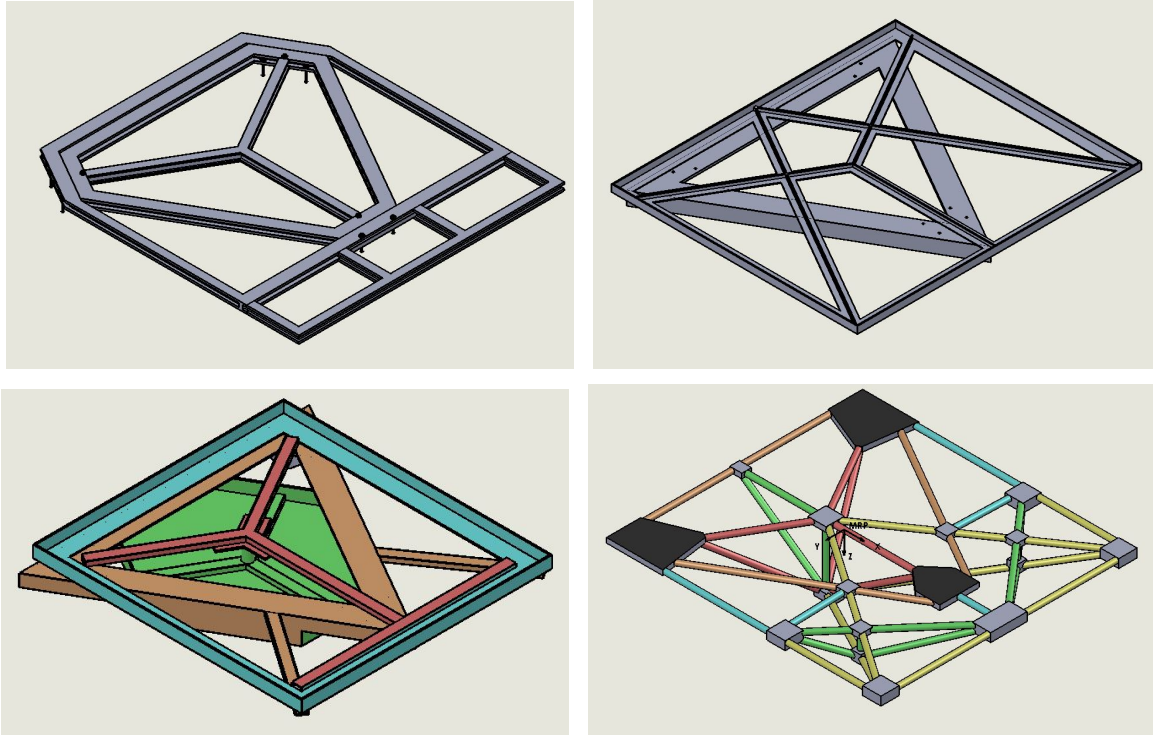
Figure 4-6: Base frame configuration concept proposals

However, the center star-shape element is not very stiff with elastic mode along z direction (refer upper left plot in Figure 4-7). The front corner is also critical with the mode showed in upper right plot in Figure 4-7. Consequently, reinforce beam was designed to connect front corner to the back support element to add stiffness, as shown in the second concept on the upper right of Figure 4-6. And a stiffener was designed to reinforce the center star-shape element from below as shown in the third concept on the down-left of Figure 4-6. However, the side beams of the square element extending from back to front still lacks torsional stiffness as shown in the lower two pictures of Figure 4-7. Stiffeners need to be designed to support the side beams. As is known, a common way to add shear and torsional stiffness to a cantilever beam is to add a reinforce beam from the free tip to the place below the support to form a truss structure. This has eventually lead to the last concept with a truss structure design as shown in the down-right of Figure 4-6. Vertical beam elements (refer green beams in the last picture of Figure 4-6) are placed to reinforce the center payload as well as the front corner and square side beams.
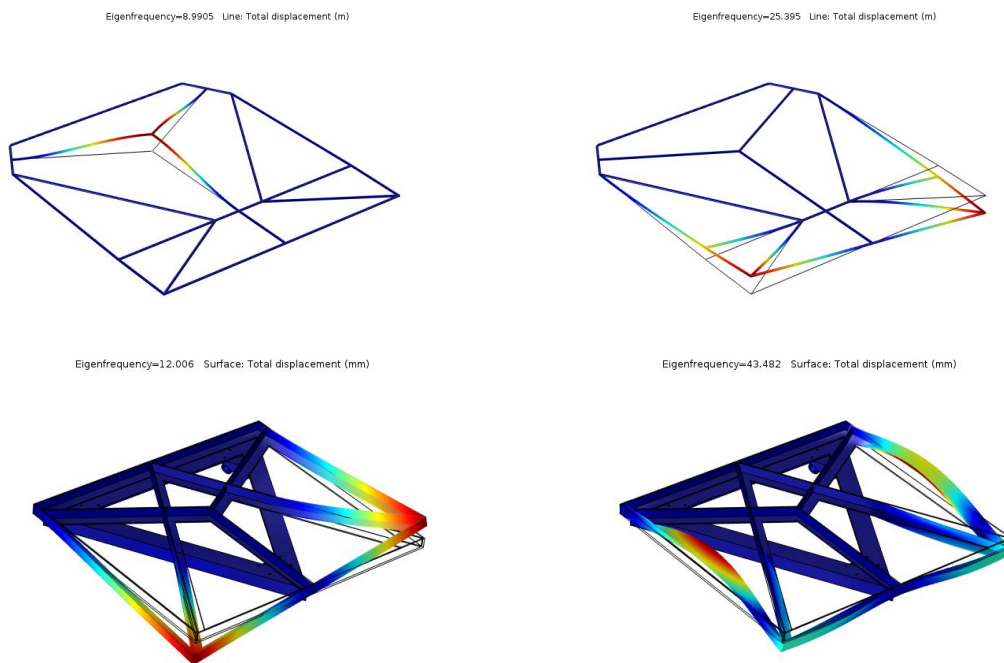
Eigenfrequency=8.9905 Line: Total displacement (m)   Eigenfrequency=25.395 Line: Total displacement (m)

Eigenfrequency=12.006 Surface: Total displacement (mm)   Eigenfrequency=43.482 Surface: Total displacement (mm)

Figure 4-7: Base frame configuration concept proposals

4-3-2   Manufacture method

Since the base frame is defined as a permanent part and can be brought into the motion lab as a single entity, the joining method can be permanent. Welding is selected due to several advantages: firstly it can create a continuous joint with lower stress concentrations compare to bolting; moreover it connects the same material by combining their atoms which gives a higher strength compare to glue, since the tested shear strength with normal glue [1] is about 17 MPa, which is much lower than the steel material shear strength (400 MPa). However, for glue with a higher quality, the strength of both connections can be comparable. Then the cost becomes the issue, since welding requires high specialized site labor and inspection with scientific instruments which will also rise the cost.

4-3-3   Material selection

Common materials for structure design like steel and aluminum are considered to keep the price low. Structural steel has a high Young's modulus and also a high density. Aluminum are light weight material and has lower buckling risk. However, base frame is positioned relatively close to the MRP compare to other components, and its dimension, especially height, is constrained by the required cabin volume for positioning of components (refer Table 3-4). Thus its inertia is less critical constraint compare to the dimensional requirement and stiffness. In this point of view, a more condensed material, steel, is selected.

---

[1]http://www.adhesivehelp.com/productdatasheets/huntsman-a2014.pdf

On the other hand, suppose the base frame will be manufactured by welding, steel is also highlighted with a relatively low manufacture cost compare to aluminum.[10] Furthermore, there are quite limited types of aluminum that can be welded which added limitations to select a proper type of aluminum alloy with required yielding stress properties. In this point of view, steel is also a better choice for manufacturing base frame.

4-3-4 Profile selection

Profiles of the base frame beam elements will be selected from most regular cross section type with standard sizes in order to keep the cost low. The selection of section shape has to be discussed since the modulus and strength of a material can be made stiffer and stronger by shaping it into I-beam or a hollow tube when loaded in bending or twisting.[11] Thus solid rectangular profile is not considered due to its inefficient section shape.

For different loading mode, the most efficient section shape is different. From Table B-1, for the base frame beam elements, the bending load in both orientation (x and y axis) with comparable magnitude are the critical load modes. As well as the torsional loads especially for side edge beams. Thus, I-profile and L-profile is not preferred. Since L-profile is weak in torsional load, and I-profile is highly asymmetric with its strength resisting bending moment both along x-axis and y-axis (refer Figure 4-8 on the left). Thus, profile with hollow section shape are preferable (for example the pipe and hollow square shown in Figure 4-8 on the right). Pipe profile is further selected due to its higher efficiency of section area and strength resisting torsional loads.
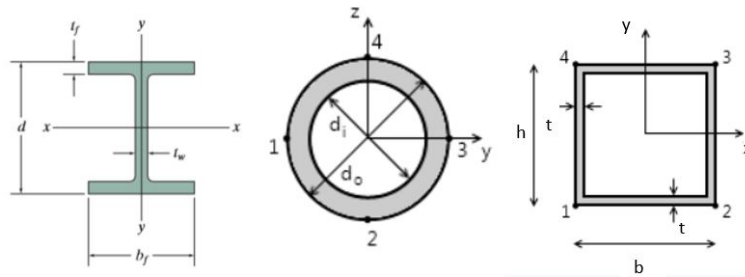

Figure 4-8: Cross-section properties of hollow tube, hollow square and I profile

The section moment of inertia I of pipe profile is calculated with equation 4-1.[11] Parameters d_o and d_i can be referred in Figure 4-8. From the equations, it can be concluded that profiles with large outer diameter but smaller thickness can achieve both a higher section moment of inertia and a smaller section area than profiles with smaller outer diameter but larger thickness. For example, a 60mm*5mm pipe has its moment of inertia of $3.3(10^5)mm^4$ which is $2(10^5)mm^4$ larger than a 40mm*10mm pipe with its moment of inertia of $1.18(10^5)mm^4$, while a section area with $864mm^2$ is $78.5mm^2$ smaller than the 40mm*10mm pipe with $942.5mm^2$.

$$I_{pipe} = \frac{\pi}{4}((\frac{d_o}{2})^4 - (\frac{d_i}{2})^4)$$

(4-1)

Thus, the beam element of base frame is designed with its profile outer diameter directly determined by the boundary of maximum base height, while with its profile thickness selected according to the calculation with required stiffness. The boundary of maximum base height is 50 mm (refer Table 3-4) that is defined in order to achieve an optimal positioning of the control devices. Thus, except for the metal mounting plate which will occupy around 10 mm, 40 mm is determined as the outer diameter of the base frame profile. The thickness is determined based on the calculation according to the required stiffness part by part. Details are in Appendix B.

As a result, a pipe profile of 40mm*10mm with outer-diameter of 40mm and thickness of 10mm is selected as the element profile for the base frame.

4-3-5   Base frame entity stiffness verification

The stiffness verification of base frame entity is conducted in FEM software COMSOL.

Stationary test of base frame design

In stationary, three mounting blocks which connect with the hexapod mounting surface are defined as the fixed constraints. The loads are defined by the self weight of masses mounted upon base frame. The simulation consists of load conditions in 64 extreme hexapod poses. In COMSOL, the base frame geometry is imported from the SolidWorks model as a solid entity (form union). In the model, simplified mass representing the payloads mounting upon the base frame is added. A description of the simulated model can be seen in Figure 4-9.
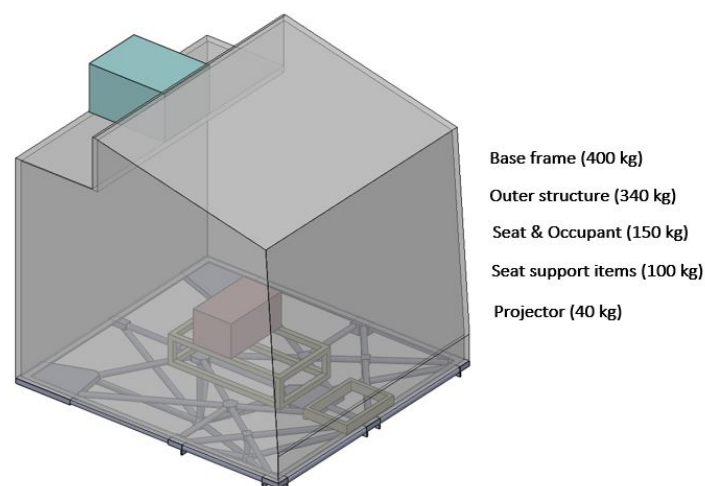

Base frame (400 kg)

Outer structure (340 kg)

Seat & Occupant (150 kg)

Seat support items (100 kg)

Projector (40 kg)

Figure 4-9: Description of base frame model simulated in COMSOL

Since the simulation will focus on the deformation of the base frame, thus the mass added to it as defined in Figure 4-9 will be meshed only as one element, indicating that their deformation is not interesting for this simulation.

In order to describe the load condition in different hexapod poses, it is more convenient to transform the gravity from the global coordinate system to the moving platform coordinate system which is fixed to the moving platform of the motion system. Thus by inversely calculate the gravity vector components in x, y and z axis in the moving platform coordinate system, the stationary self-weight load condition can be realized for various hexapod poses. The values of each component in x, y and z direction of the gravity vector with respect to the moving platform coordinate system is shown in Figure 4-10.
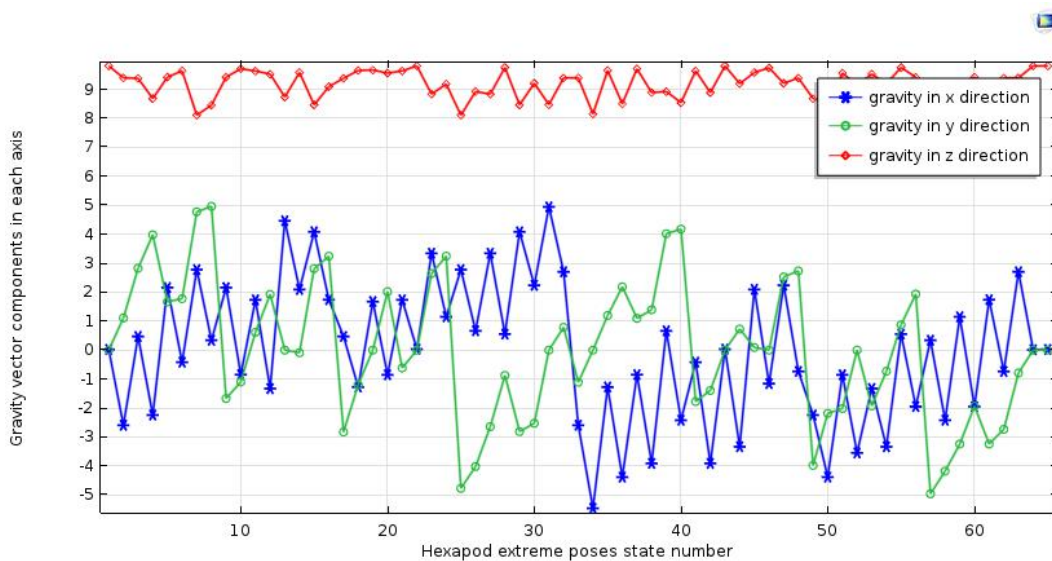
Figure 4-10: Gravity components in moving platform coordinate at 64 extreme hexapod poses

Thus, the analysis will be conducted with a series of stationary solutions, controlled by a sweep over the 64 parameter combinations. The parameters used are the decomposed components of gravity vector within the moving platform coordinate system.

The maximum deflection of the base frame structure surface in each of the 64 extreme hexapod poses are shown in Figure 4-11. The highest value generates at pose number 19 (with only actuator 2 and 5 extended), and the value is about 0.15mm (Figure 4-12). This deflection is hard to be perceived by the occupant, thus the designed structure satisfies the required stiffness in stationary.

The maximum stress along the base frame structure surface is also evaluated in each of the 64 extreme hexapod poses as shown in (Figure 4-13). The worst case with 54 MPa is at pose number 7 (when only actuator number 4 and 5 are extended) which is illustrated in Figure 4-14. This value is under the allowable yielding stress of steel, thus the design is acceptable.
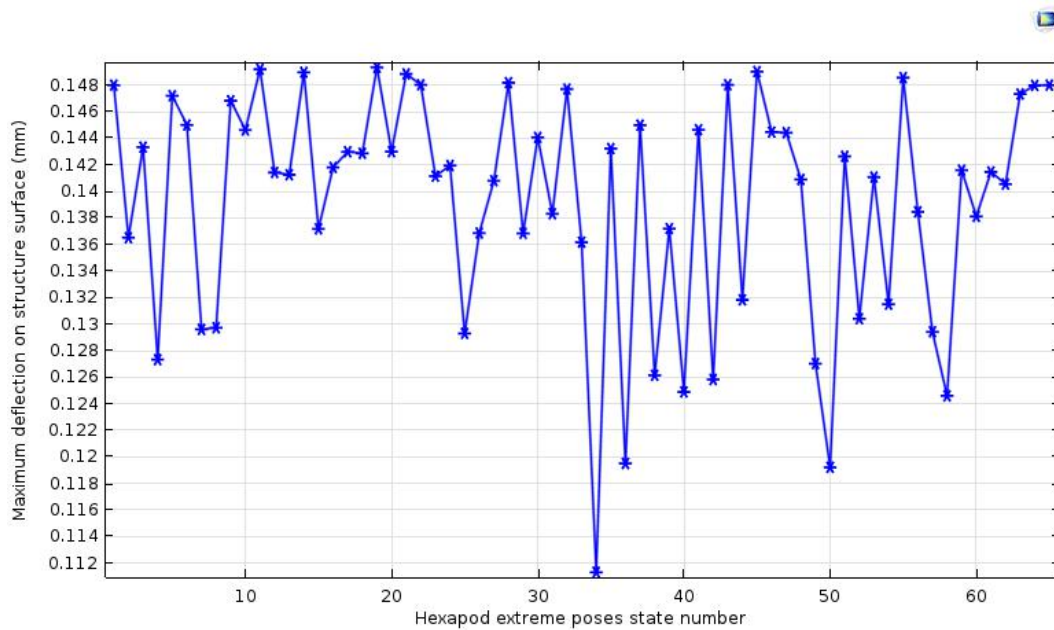
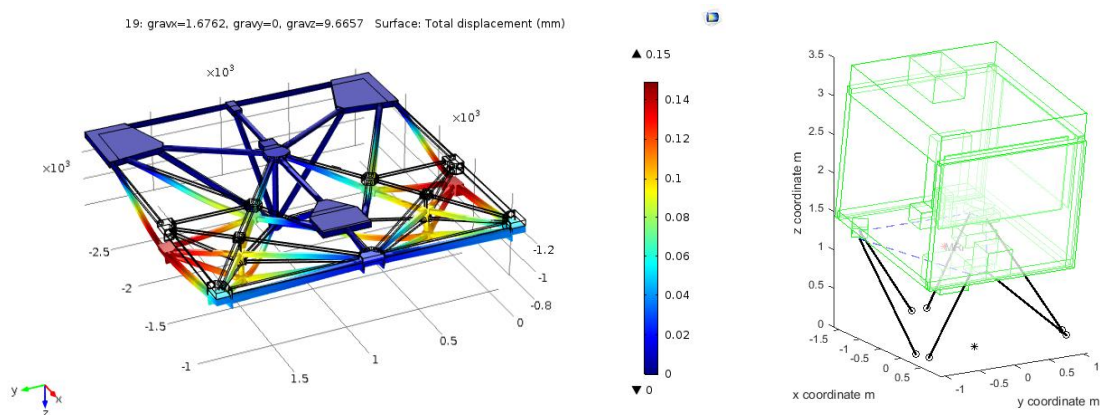**Figure 4-11:** Variation of maximum deflection on base frame structure surface through all 64 extreme hexapod poses

Figure 4-12: Base frame structure performance under worst stationary load cases

Transient dynamic test of base frame design

From the analysis in the last section, the designed base frame performs quite good under the static load conditions. However, in the dynamic cases, the response of a structure to the time dependent varying loading is hard to predict. From the documents provided with hexapod manual, at its neutral pose, the maximum acceleration would reach 1g in heave and the acceleration onset is about 10g/s. Thus one simulation could be conducted with transient analysis to check the structure response when actuating the base frame to the required maximum non-simultaneous acceleration in each degree of freedom within 0.1s at its neutral pose. 0.1s are selected from the maximum velocity defined by the heaxpod (refer Table 2-1)
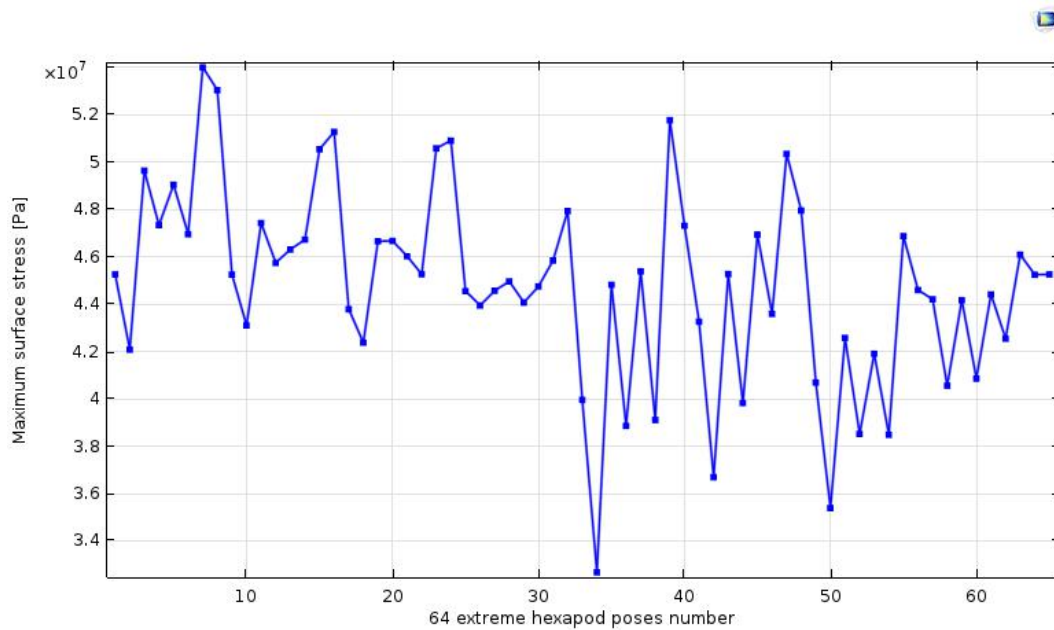
Figure 4-13: Variation of maximum stress of structure surface during different extreme poses
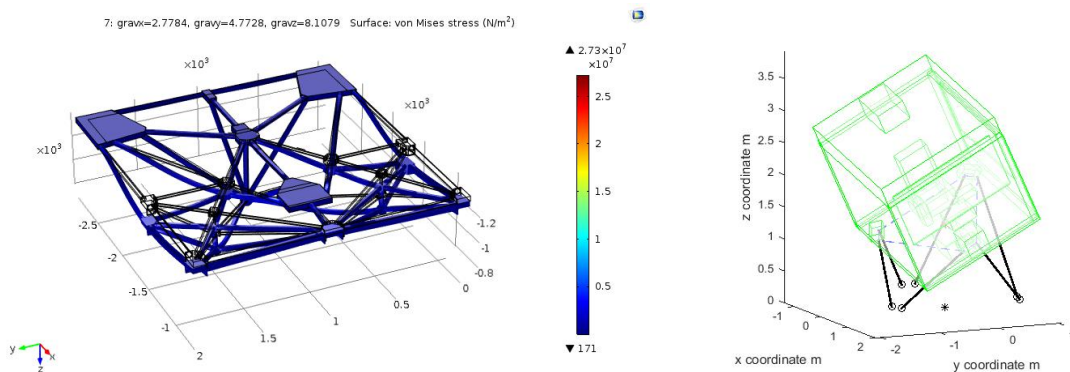

Figure 4-14: Base frame structure performance under worst stationary load cases

In COMSOL, the actuation of the base frame carrying the payloads can be realized by adding a prescribed acceleration to the mounting surface. The maximum stress generated within the base frame has to be under the maximum allowable stress from the material. With a safety factor of 2, the maximum stress can generated is as 270 MPa (assuming the yielding stress is 550 MPa [11]) Thus the stress generated in each acceleration condition within 0.1s is shown in Figure 4-15. And the structure response can be collected within 0.1s by running the simulation, the center payloads response within 0.1s is shown shown in Figure 4-16.

As seen from the results, in dynamic load cases, the stress of the structure surface are under 200 MPa, which is under the material yielding stress level.
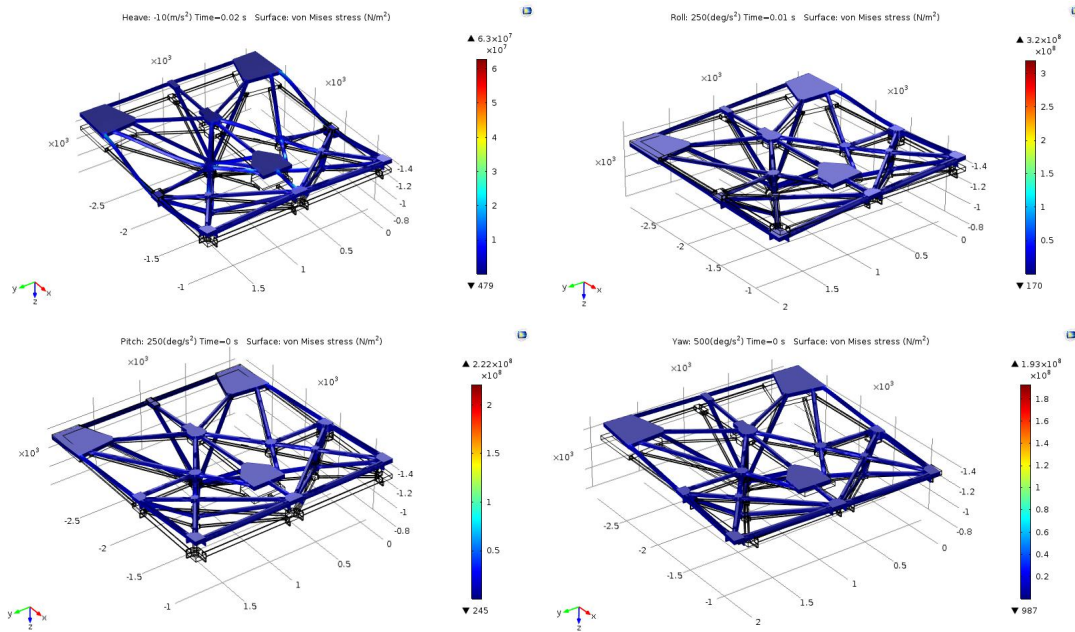
Figure 4-15: Transient FEM analysis with base frame under worst dynamic load cases under maximum accelerations
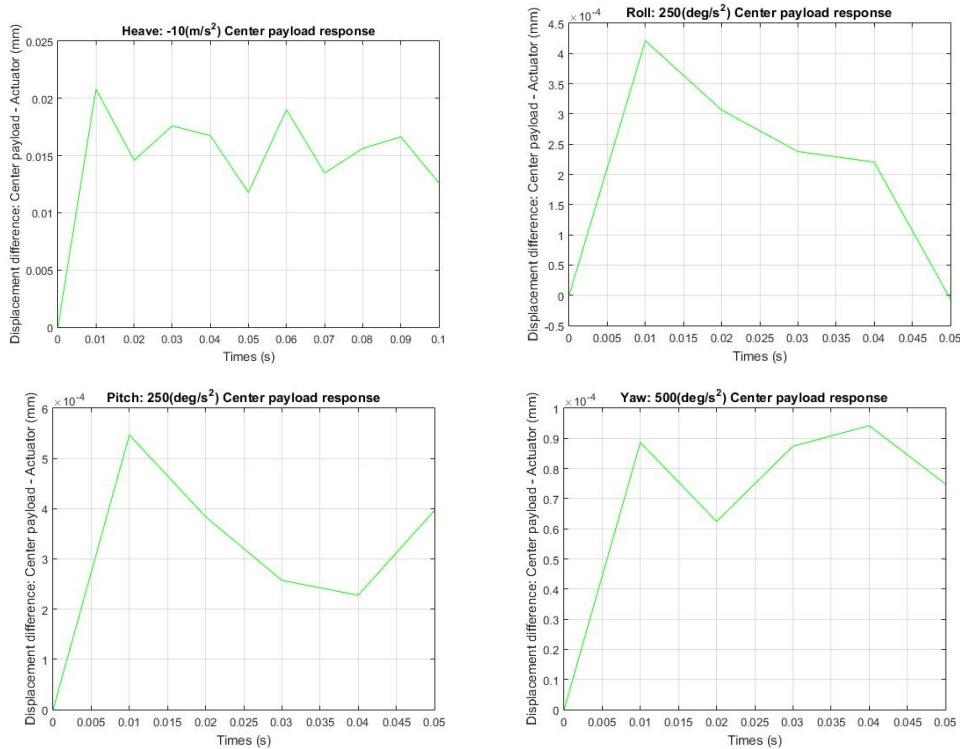

Figure 4-16: Transient FEM analysis with base frame under worst dynamic load cases at hexapod's neutral pose

Eigen-mode analysis

In dynamic cases, the eigenmodes of base frame with loaded masses under maximum accelerations are also checked in COMSOL. As seen in Figure 4-17, the first elastic eigenmode generated when applying maximum acceleration at MRP in sway, heave and roll is plotted. The lowest eigen-mode is 37 Hz which is higher than the operating frequency of 10 Hz.
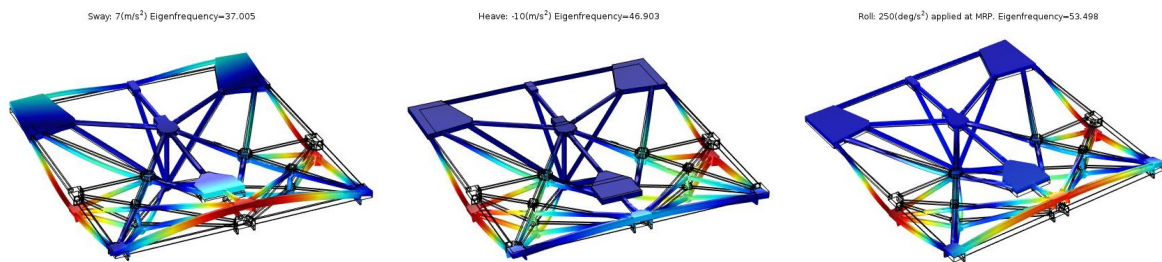
Figure 4-17: Modal analysis of the base frame with loaded masses under different accelerations

4-3-6   Base frame mass properties evaluation

Some modifications are added to the preliminary concept, and an overview of the detailed base frame design can be seen in Figure 4-18.
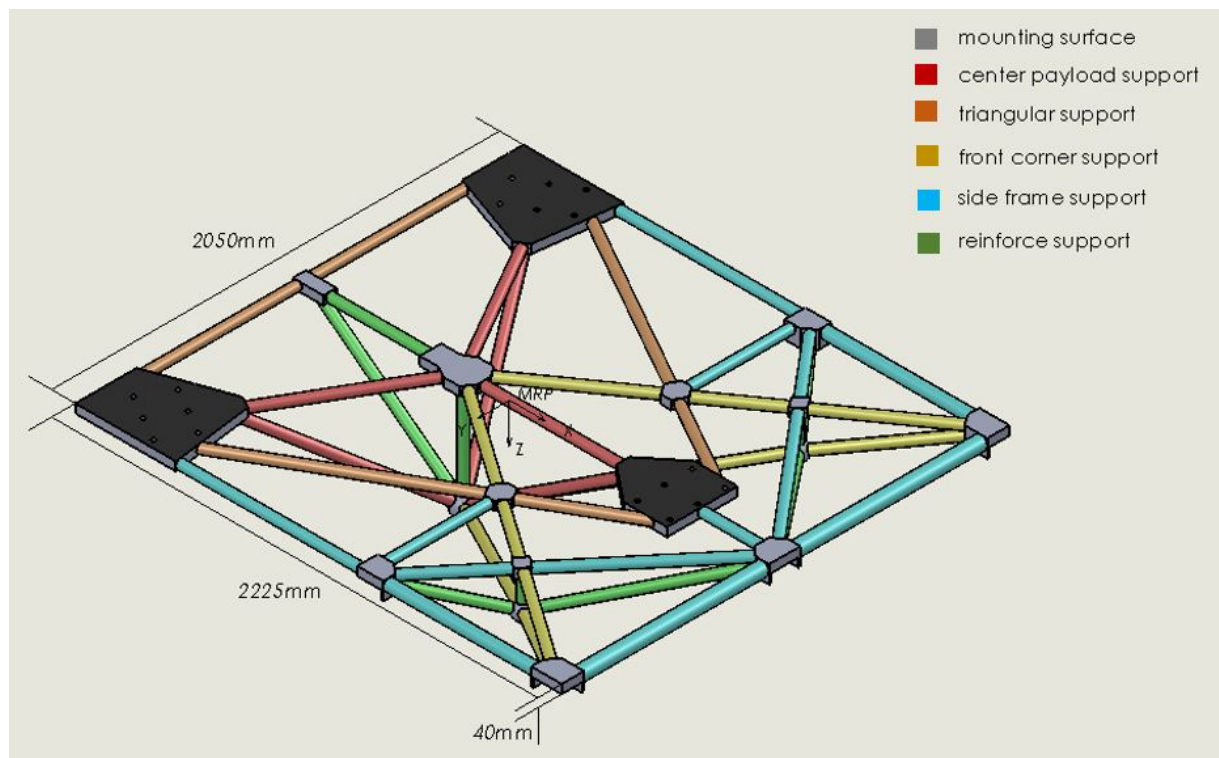

Figure 4-18: Base frame design of cabin structure

Some conclusions can be referred in the following descriptions (the values are collected from the SolidWorks evaluation):

- The total dimension of the base frame is 2000m width, 2225m depth and 40mm height mounting upon the hexapod mounting surface.

- The material is selected as Steel, and the joining method is selected as welding.

- The resulted mass is under 400 kg (372 kg).

- The resulted moments of inertia (when taking at the center of mass and aligned with the motion reference point (MRP) of hexapod) in Ixx, Iyy and Izz are 20.3, 24 and 43 (kgm^2) respectively.

- The resulted center of mass lies around +130mm in X direction from the MRP and 50mm in Z direction left 100mm above the MRP. The only problem with the center of mass might be the position in X direction, thus later the center of mass should be ideally adjusted to align the origin of the MRP along x-axis.

4-3-7 Assembly with hexapod mounting surface

This base frame design has to be evaluated with the ability of assembling with the hexapod motion simulator. One problem is the interference with the exist steel triangular structure from hexapod (refer Figure 2-8) when uploading the base frame. Thus adjustment have been made by separating the two reinforce beams (which created the interference) from the entity. By doing this, the base frame entity is able to be uploaded upon the hexapod top platform with no interference with the original triangular structure on the platform. Then the reinforce beams can be bolted with the previous structure. The assembly process has been illustrated in Figure 4-19. The left picture showed the separated entity being uploaded from the top of the hexapod motion simulator. The right picture showed the reinforce beam elements being mounted within the base frame entity from the bottom side of the hexapod platform.
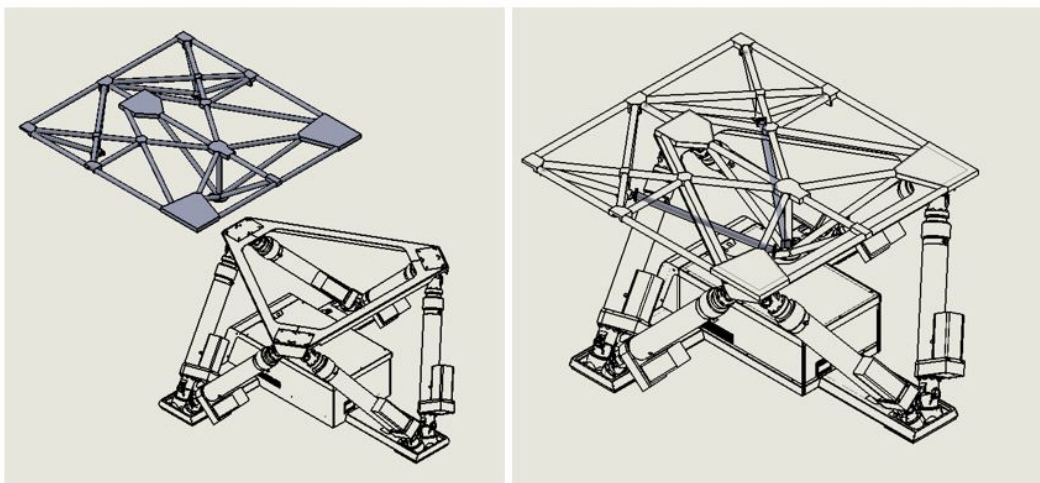

Figure 4-19: Base frame assembly process upon the hexapod motion simulator original platform

In order to realize this, some interface has to be designed for the assembly convenience. A common way to solve the bolted interface problem between the welded part and the reinforce beam elements is to provide a plate and then bird-mouth the pipe.[2] An application of this method is illustrated in Figure 4-20.
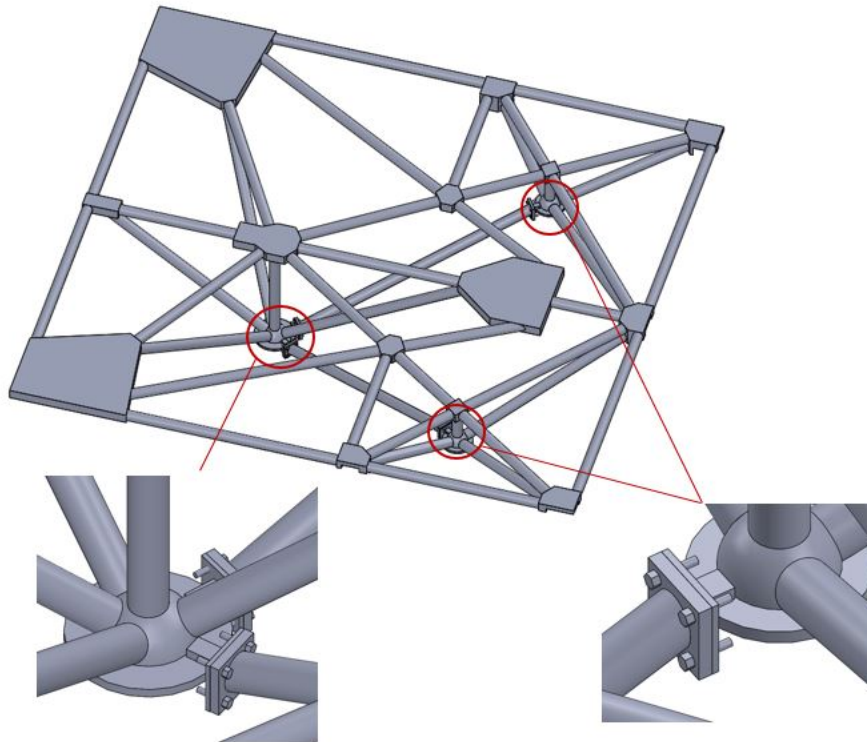

Figure 4-20: Interface between welded base frame part and the bolted reinforce beam elements

4-3-8 Production costs estimation

The production costs includes the cost of material, cost of manufacture and cost of coating. The cost of 40mm steel pipe is 0.3-1 euro per meter, however, the manufacture costs of the base frame can be hard to estimate. The smaller nodes can be cut from plate which is thick enough to weld the full profile of the pipe to the node. However, for some of the smaller nodes flanges on the edge of nodes are added to fit the face of the node at the assumed thickness. In fact, it will be less expensive to make the node just thicker, but this will add weight. Externally, the nodes can be manufactured with hole burned or drill thought the node to reduce the weight. The node at the base and the other two that receive the members that frame vertically but obliquely will be the most expensive joints. However, the expense can be reduced as well by oversize the nodes to provide better access for welding.

---

[2] http://www.ecs.umass.edu/cee434/tour/ScienceSteel/

4-4   Filling-in panels as floor of base frame

The base frame needs to be filling-in with panels for people for walk around and for mounting the equipment as well. Thus two parts of the filling-in floor is considered in this section.

First, in order to provide convenience for mounting components on the base floor, a metal plate is attached to the base frame in the region where the seat and equipments are mounted. This metal plate is mounted with the base frame at four nodes on the frame located at front, back, left and right respectively. Second is the filling-in floor, sandwich material are aimed for the floor design of the base frame. In order to add more stiffness to the base floor, aluminum honeycomb panels is selected as the filling-in panels for the base floor. The weight saved by using the honeycomb panels (with a thickness of $25mm$) instead of a metal panel (with a thickness of $10mm$) to cover the entire base frame is 78.8 kg. The design can be seen in Figure 4-21.
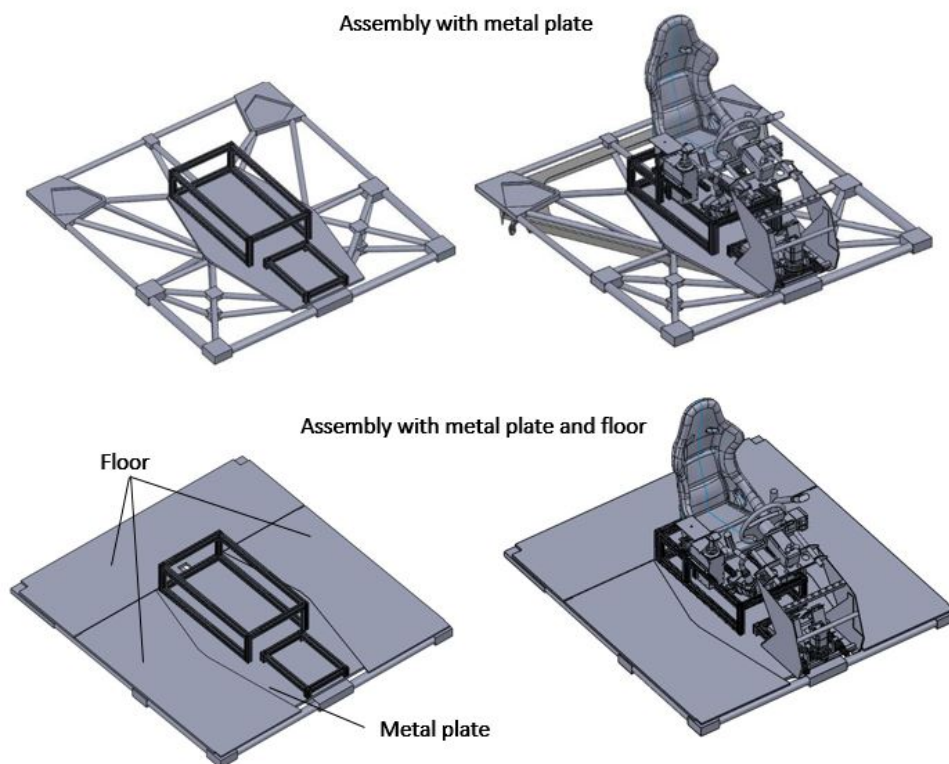

Figure 4-21: Base floor assembly with frame, metal plate (up figures) and filling-in panels (down figures)

The interface between metal plate and aluminum honeycomb to the base frame are using bolt to add modularity of the base frame. According to the experimenter's preference, the filling-in panels and metal plate can also be connected stiffer by adding glue together with the bolt.

4-5   Design of outer structure

The outer structure as a self-supported structure is usually designed as an enclosed shell to optimize the stiffness. In this design case, the cabin outer structure couldn't be brought into the motion lab as a single entity, thus an assembly break down of the outer structure is necessary (refer Table 3-4). Moreover, as concluded from the modularity requirement, the wall of the outer structure is preferably removable to provide convenience for exchanging experimental setups. For these reason, flat panels filling-in as the shell is very simple design and easy to be assembled with. Thus the outer structure will be proposed as a box that directly mounted upon the base frame. A sketch of the outer structure configuration proposal can be seen in Figure 4-22. Some reasoning to the shape of the concept is summarized in Table 4-1.
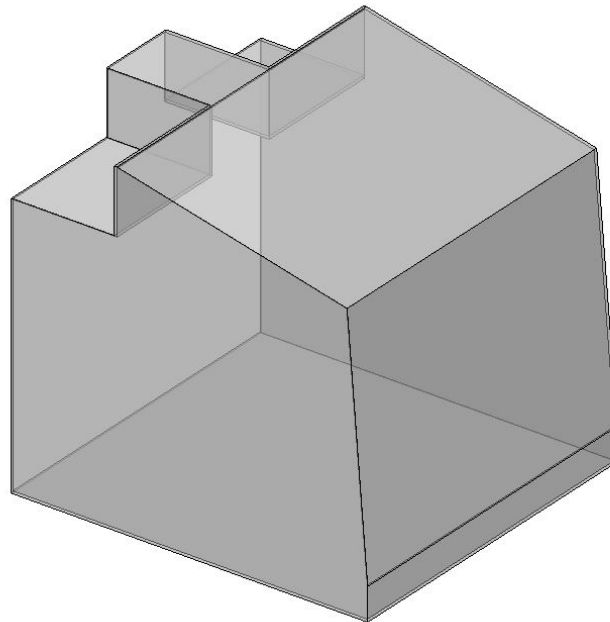

Figure 4-22: Outer structure frame concept sketch

As mentioned, the outer structure as the main supporting structure of the visualization system should be designed with sufficient stiffness to support the projector, screen and ceilings under any load conditions. The projector is the most critical component which requires high stiffness during operation, since any deflection or vibration especially in pitch and yaw will damage the projection qualities due to keystoning effect. Thus, evaluation of the projector modes require special attention in a later validation stage.

To make the structure more efficient, frame filled by panels are applied to outer structure design as the same procedure as base floor. However, the joining method design is greatly constrained to non permanent connection, for example bolts.

Decisions made of cabin concept	Reasoning from certain requirement
Flat-square-shape base	Flatness of the cabin mounting surface with hexapod
	Flatness of cabin floor surface for walking convenience
	Difficult to remove the original steel triangle platform on hexapod
Square-shape walls	Easy to assembly break down for transportation
	Easy to mount side monitors for capability of multiple visualization systems
Stair-shape ceiling	Ventilation of the projector device during operation
	Easy access of projector's top control panel for adjustment of projection

Table 4-1: Reasoning of the promoted outer structure preliminary concept

4-5-1   Concept design

The proposed outer structure is a box which is very simple and convenient to manufacture. Main components need to be supported are the projector on the back side and the screen (or monitor) on the front side. Refer back to the modularity specifics and dimensional requirements from the lab room entrance, the outer structure can be designed as five individual frames connected together as referred in Figure 4-23.
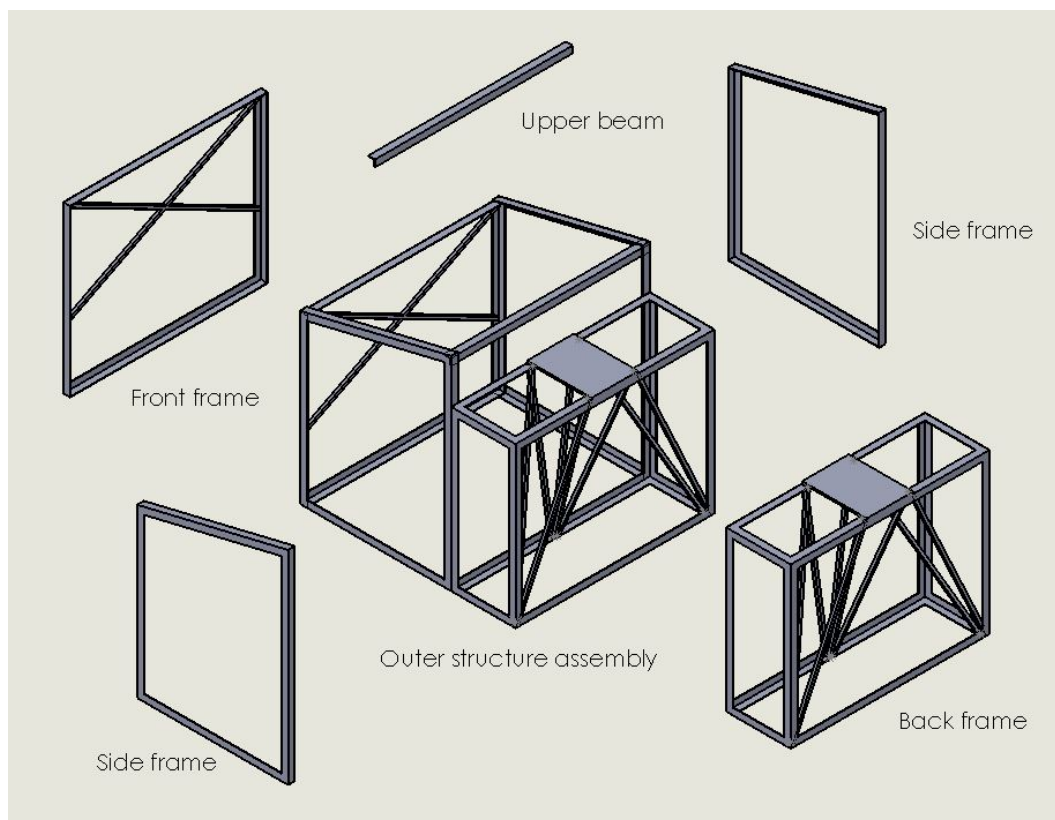

Figure 4-23: Outer structure frame concept sketch

4-5-2   Manufacture method

The outer structure, as a semi-permanent part of the cabin that requires both assembly break down in order to access the part into the motion lab and modularity in order to replace the shell for mounting setup convenience. Thus the manufacture of the whole base frame will be partly welding and bolted as an assembly. As seen in Figure 4-23, the whole outer structure is assembly break down into five parts that each can be brought into the motion lab as an entity. The five individual parts consist a back frame as welded as a closed box with reinforce beams to support the projector stiffly; two side frames to enclose the cabin; front side frame to support the screen or potential monitor and an upper beam to interconnect the side frame from the top view. Each individual part is manufactured by welding as an entity. And they are bolted together within the motion lab room to form the outer structure assembly. Later, the filling-in panels will also be bolted to the outer structure frame with bolts or special joining design.

4-5-3   Material selection

As the outer structure frame will be relatively high with respect to the motion reference point of the hexapod simulator. Thus to reduce the moment of inertia during motion, the material for the outer structure is selected with Aluminum. Since Aluminum is a proper material considering the price, density as well as stiffness. The material for the filling-in panels can be composite material or metal honeycomb material.

4-5-4   Profile selection

For outer structure frame, L profile is selected as the elements compare to the other cross-section shape, since L profile is a relatively more efficient profile for mounting convenience. However, the torsional stiffness of L profile is very weak. Thus filling-in panels have to be added to provide more stiffness to this structure. Since the main stiffness of the outer structure is provided by the panels, thus honeycomb, preferred with its relative high elastic stiffness is selected as the profile for the panels of the outer structure.

A brief proof can be seen in the following identification of the outer structure. It starts with the backside frame, since it supports the projector which requires high stiffness to guarantee the projection image quality. With a simple backside frame as a box (refer Figure 4-24 on the left side), the torsional stiffness is very low. When apply a torsional moment of 560 Nm at the projector (as projector has a maximum rotational acceleration around Z axis), the stress in the structure can reach $6(10^6)GPa$. However, by assembling the whole outer structure frame with the front frame as well as side frames, the torsional stiffness can be greatly improved (refer Figure 4-24 in the middle). Under the same load condition, the stress in the structure has been reduced to $5MPa$. When adding panels on the side (refer Figure 4-24 on the right side), the stiffness are even stronger. Under the same load condition, the stress reacted in the structure is $1MPa$ maximum.

Aluminum L profile with size $70mm * 6mm$ is selected as the basic element for outer structure assembly. Aluminum square profile with size $30mm$ is selected as the reinforce beams on both
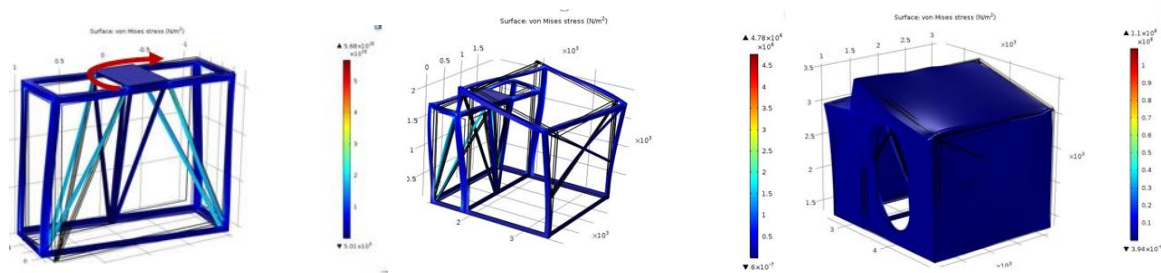
Figure 4-24: Weak of torsional stiffness of the L profile back frame compare to adding filling-in panels

the back side frame and front side frame. Aluminum honeycomb panels are selected as the filling-in shell to stiffen the outer structure with thickness of $25mm$. This selection is based on the dimensional requirements to the outer structure.

4-5-5   Outer structure design and stiffness verification

In COMSOL, the outer structure geometry is imported from the SolidWorks model with simplified joining connection between each beam element. By doing this, the connection are defined as bonded contact in FEM analysis by assuming the both the welding and the bolting joint is performing as rigid connection. In the model, simplified mass representing the payloads mounting on the outer structure is added. An identification of the outer structure simulated model parts can be seen in Figure 4-25.
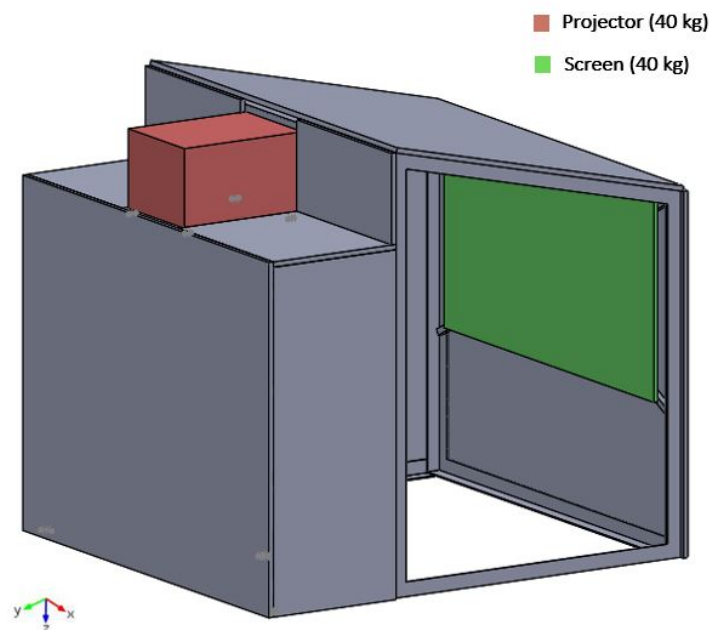

Figure 4-25: Description of outer structure model simulated in COMSOL

Stationary test of outer structure

In stationary test, the bottom of outer structure which is supposed to be mounted with the base frame upper surface is defined as the fixed constraints. The loads are defined from the self weight of the structure itself as well as the payloads in the positive Z direction (pointing downwards). The simulation consists of positioning all the payloads in 64 extreme hexapod poses. Similar procedure is applied with the same series of stationary solutions, controlled by a sweep over the 64 parameter combinations. The parameters used are the decomposed components of gravity vector within the moving platform coordinate system.

The maximum deflection through all the structure surface in each of the 64 extreme hexapod poses are shown in Figure 4-26. The highest value generates at pose number 7 and 25 with about 0.15mm. And the stress along the surface also has its values under 13 MPa. The worst case is illustrated in Figure 4-27.
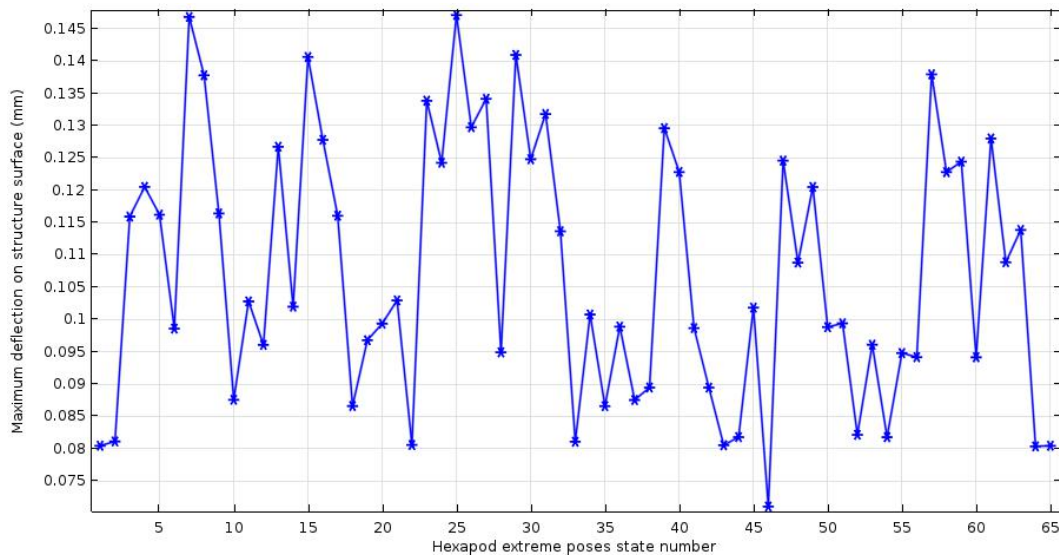

Figure 4-26: Variation of maximum deflections of outer structure surface during different hexapod extreme poses

As seen from the plot, the deflection of the outer structure is very small. An weak part of the outer structure is the reinforce beam elements within the back frame of the structure to support the projector. This could be further optimized by replacing the beam element with a bigger size. However, seen from the stationary analysis so far, the structure is performing well to support the payloads at any hexapod pose.

Transient dynamic test of base frame design

Now the structure will be tested in dynamic conditions, and the simulation will be conducted with transient analysis to check the structure response when actuating the outer structure to the required maximum non-simultaneous acceleration in each degree of freedom within
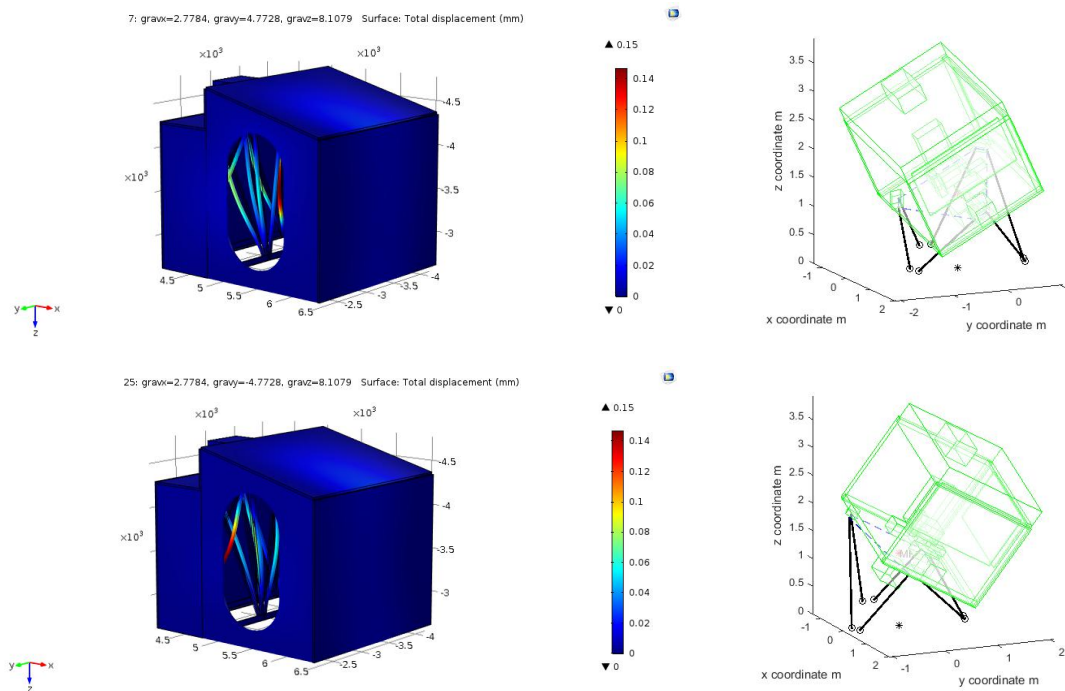
Figure 4-27: Outer structure performance under worst stationary load cases

0.1s at its neutral pose. In COMSOL, the actuating loads added to the bottom mounting surface can be realized by adding a rigid connector with applied force and applied moment to the bottom mounting surface. Then the structure response can be collected within 0.1s. By running the simulation, surface stress within 0.1s and surface displacement within 0.01s is shown in Figure 4-28.

As seen from the results, when applying the loads within 0.1s, the stress among the surface are under 30 MPa, which is under the material yielding stress level.

Eigen-mode analysis

In dynamic cases, the first elastic eigenmodes of the outer structure with loaded masses starts from 44 Hz as shown in Figure 4-29. The reinforce beams within the back frame of the outer structure start to oscillate with certain modes first. This has indicated the critical point of the reinforce beam again, however, this natural frequency is still within the safe region of the defined 10 Hz operating frequency.

4-5-6 Assembly of outer structure and with base frame

The frame will further be stiffened by sandwich panels attached with it. However, connection between the panels and outer frame is constrained to non permanent method like bolts, since the panels need to be removed when switching experiment setups and inside supporting items. Thus the panels for the outer structure need to be verified with bolt connection (shear joint)
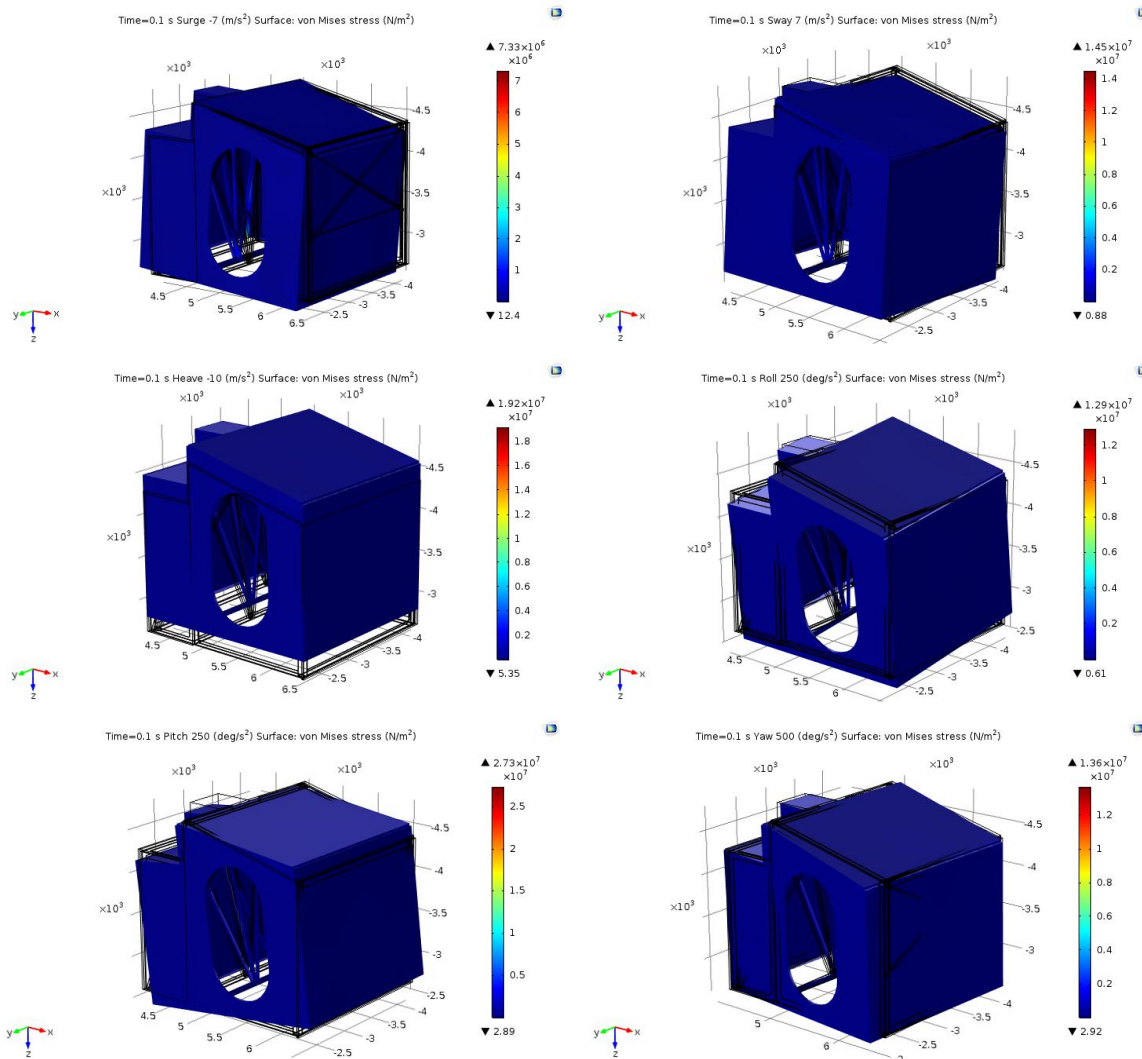
Figure 4-28: Transient FEM analysis with outer structure surface stress under worst dynamic load cases at hexapod's neutral pose (each row denotes the maximum non-simultaneous acceleration in surge, sway, heave, roll, pitch and yaw degree of freedom)

especially with sandwich structures under dynamic conditions.

As stated in the manufacture section, the outer structure frame is manufactured as five individual part, the back frame, front frame, two side frames and the top beam. All these individual parts are welded as an entity, and they can be easily bolted together on the flange of the L profile. The advantage of using L profile is that it is easy to drill holes and apply bolts. After, honeycomb panels are bolted to the corresponded frame of the outer surface. The assembly procedure is to bolt the back frame panels first, then the top frame panels, after the front frame panels and in the end the front side frame panels. The assembly procedure is illustrated in Figure 4-30.
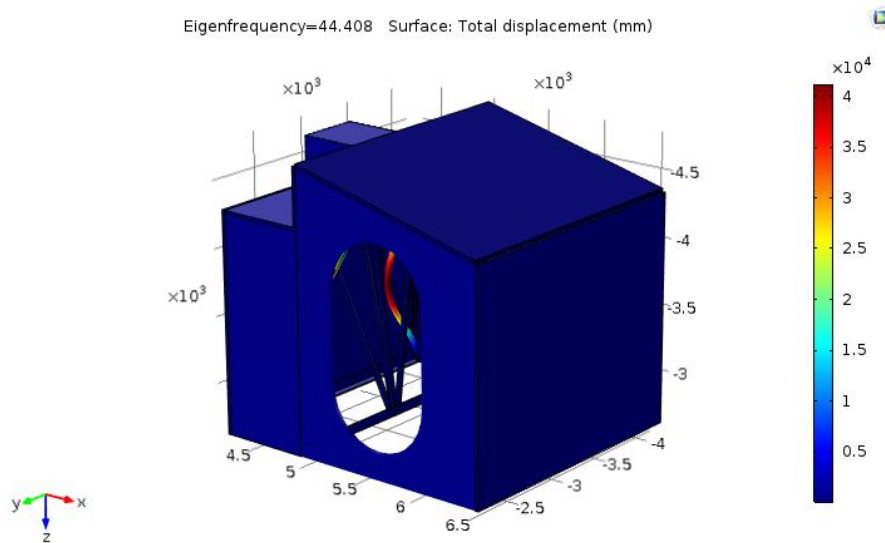
Eigenfrequency=44.408   Surface: Total displacement (mm)

Figure 4-29: Modal analysis of the outer structure under loaded masses
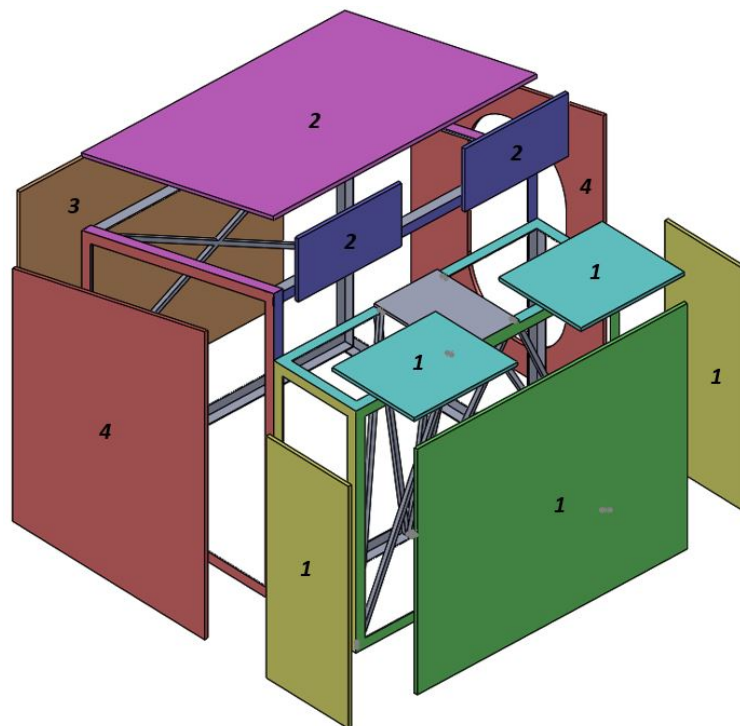
Figure 4-30: Assembly of outer structure with frame individual elements

The assembly between outer structure and base frame also use bolt joints. By drilling holes on the connecting flange of L profile and mounting nodes on the base frame, the bolts can be applied to connect the two structure with each other.

Joining between the honeycomb panels with outer structure frame can be optional, for example

inserts connection and out-plane strip connection. (refer Figure 2-7) As stated in the literature study with bolting of honeycomb, either joining method has its advantages and disadvantages. In this design project, the production costs is limited to 20 keuro, thus choosing inserts for bolting can be very time-consuming and costly. Thus, using metal strip attached to the edge of honeycomb on the mounting region and bolted with bolts and washer is a good solution for connection between honeycomb panels and the frame.

4-5-7   Production cost estimation

For the outer structure, the productions cost are mainly from the L profile frame's material cost and welding cost, the honeycomb's material cost. For the honeycomb plate, the total cost for the material will be around 2 keuro. The L aluminum profile with around 40m long in total will be around 500 euro. The manufacturing of welding each individual frame will cost more. However, the total cost of the outer frame will be within 5 keuro.

4-6   Cabin structure assembly overview

An overview of the whole cabin structure can be seen in Figure 4-31. An evaluation of the final design will be elaborated in the last chapter.
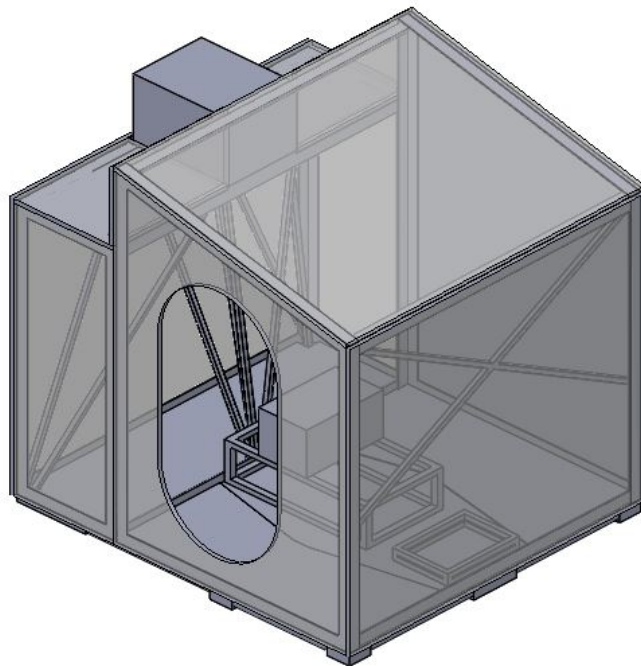

Figure 4-31: Cabin assembly top-level design overview

<div style="text-align: right">

Chapter 5

</div>

Validation of cabin structure design

From the previous chapter, a detailed design process was conducted with the design of cabin structure. Aspects regarding to the material, manufacture method, structure element, joining method, estimated cost and structural response with respect to multiple load cases are analyzed and evaluated throughly. However, how the structure performs in reality is always complicated. Thus assumptions have to be made during the design process, and validations have to be conducted to verify the credibility of the assumptions.

Thus, in this chapter, the design project is finalized with first an through-all evaluation of the complete design result as well as the whole design process. Meanwhile, several critical assumptions with the stiffness of bolt joints are also pointed out. This is verified with a test of the assumed connection. In the end, the dynamic capabilities of the hexapod motion simulator is verified with the a group of compared experiments.

5-1 Cabin design evaluation

As shown in the end of last chapter a top-level complete cabin design in Figure 4-31, its properties and boundaries will be evaluated with respect to the environment constraints and user wishes in the following subsection. The method been applied during the design process will be evaluated with its effectiveness and efficiency as well.

5-1-1 Final cabin structure design evaluation

As summarized before from the problem definition, main aspects leading the design are the dimensional constraint, mass properties limited by the hexapod, production costs limited by the user as well as the modularity and stiffness requirement. Now, each aspect will be evaluated individually according to the defined boundaries.

Modularity evaluation of designed cabin structure

The modularity of the designed cabin are stated as follows. The whole cabin structure is detachable with a welded base frame, back frame, two side frames and a front frame. The filling-in panels are all bolted with the frame. This has provided with enough modularity for disassemble the shell when experimental setups needs to be exchanged fast. Moreover, the bolted joints make it very convenient and fast to reassemble. Fixed hole positions eliminated the necessity to calibrate. In summary, the designed cabin structure has met the required modularity properties.

Dimensional evaluation of designed cabin structure

The designed cabin assembly has its total dimension of 2.05m width, 2.275m depth and 1.8m height on the front while 2.08m height (including the projector) on the back. From the motion reference point to the front is 1.35m depth while 0.925m depth to the back. The cabin profile is verified by importing the 3D drawing to the motion envelope model. By the first test, the designed cabin are matching the room's boundaries with interferences of around 30mm with the side walls. On the back, the motion envelope is matching the room size. In order to eliminate this potential collisions, the honeycomb front panels around the front corner can be cut to avoid the risks. A modified cabin front corner can be seen in Figure 5-1.
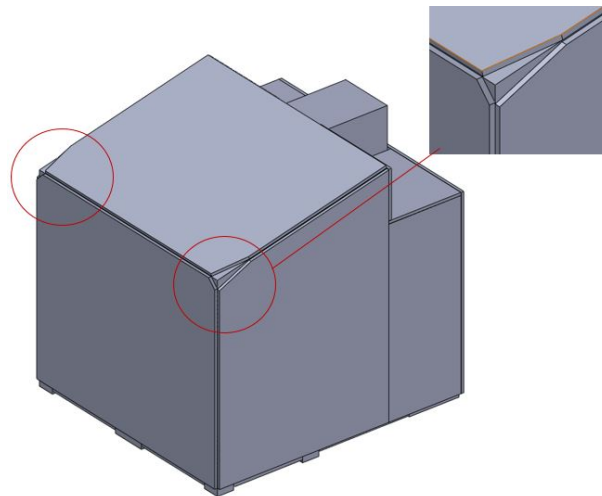

Figure 5-1: Modification of cabin front corner to avoid potential collision with side walls

By doing this modification, motion envelope model test can be conducted again and results can be seen in Figure 5-2.

The safety margin left on the backside is 11mm while on the left side and right side are 1mm and 33mm. On the left side is very critical with only 1mm left. This can be easily improved further by reducing the width of the cabin. However, by further narrowing down the width of cabin will influence the optimal positioning of the components, for example the screen and the pedals of control devices. Due to the fact that the model itself is a very conservative model, so is the motion lab mapping model, thus as long as the cabin structure will not interference

Figure 5-2: Modification of cabin front corner to avoid potential collision with side walls

the wall in the motion lab room model, it is safe to be operated within the room.

The inner volume left for importing the components is around 2m (1976mm), which gives sufficient space for projecting the image with a size of 1.8m*1m (w*h). The height of inner volume on the front is 1.7m (1690mm) which gives sufficient height to place the screen. The depth on the front is 1.5m (1547mm) which also gives sufficient length for mounting control device setups. Thus, the inner volume can satisfy the optimal positioning of the components.

Stiffness evaluation of designed cabin structure

During the detailed design process in last chapter, the stiffness was evaluated with respect to the base frame and outer structure respectively. Each individual part has sufficient stiffness as a self-support structure. By assembly of both substructure parallel, the total stiffness will be increased. This conclusion is under assumption of the mounting of the parts will not reduced its stiffness during dynamic situations. A validation of the mounting stiffness will be discussed in the next section. With this assumption, a model can be built in Figure 5-3.
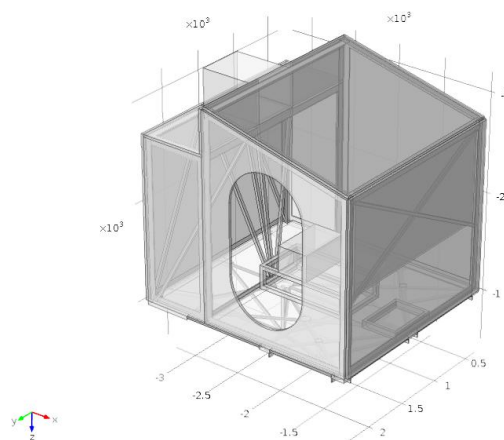

Figure 5-3: Cabin model for running simulation in COMSOL

The maximum deflection through the whole structure surface in each of the 64 extreme hexapod poses are shown in Figure 5-4. The highest value generates at pose number 15 and 29 with about 0.55mm. This has meet the required maximum 1mm deflection. For translational and rotational respectively, the maximum deflection is 0.45mm and 0.0014 rad (0.08 deg).
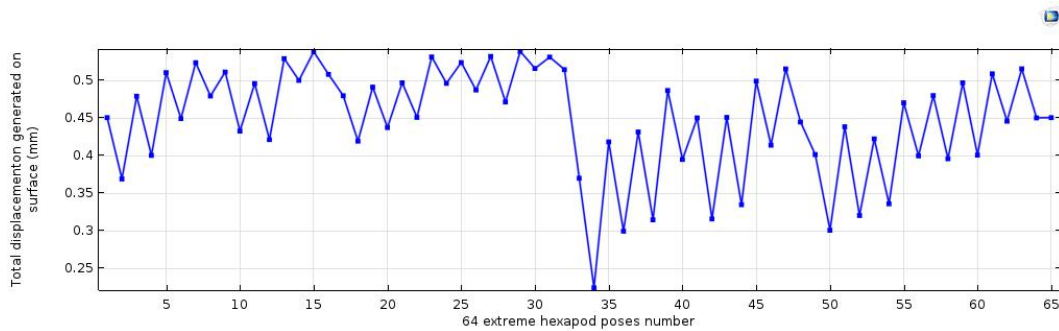

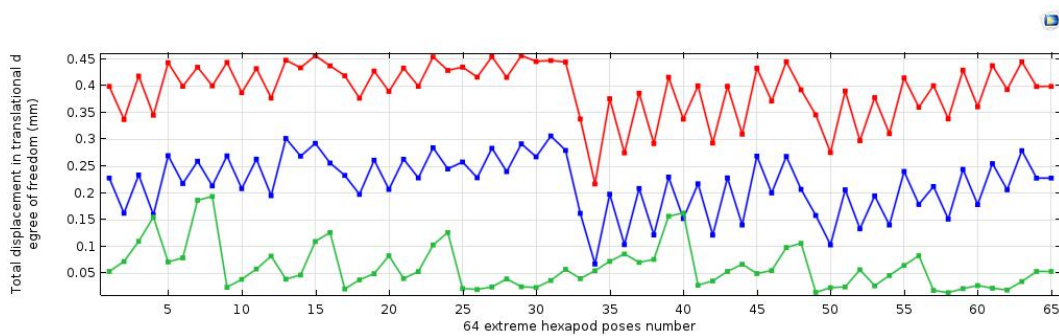**Figure 5-4:** Total deflection generated by gravity with all 64 extreme poses

Figure 5-5: Deflection in each translational degree of freedom generated by gravity with all 64 extreme pose (blue-deflection field X component; green-deflection field Y component; red-deflection filed Z component)
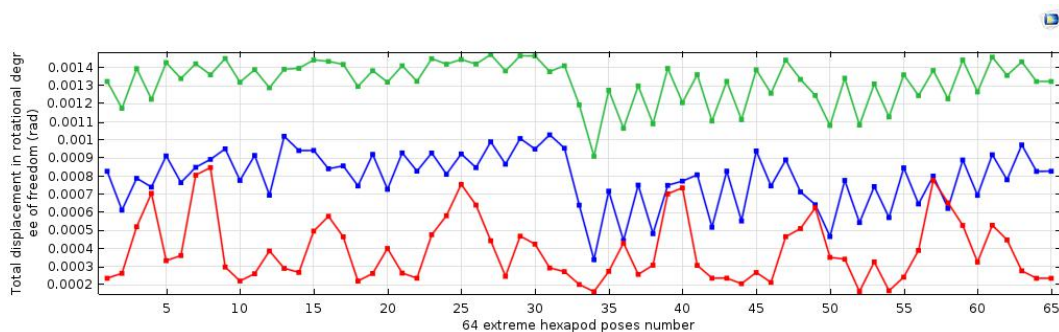

Figure 5-6: Deflection in each rotational degree of freedom generated by gravity with all 64 extreme pose (blue-curl of deflection X component; green-curl of deflection Y component; red-curl of deflection Z component)

The stress along the surface also has its values under 90 MPa. The stationary load case with 64 extreme poses is illustrated in Figure 4-12.
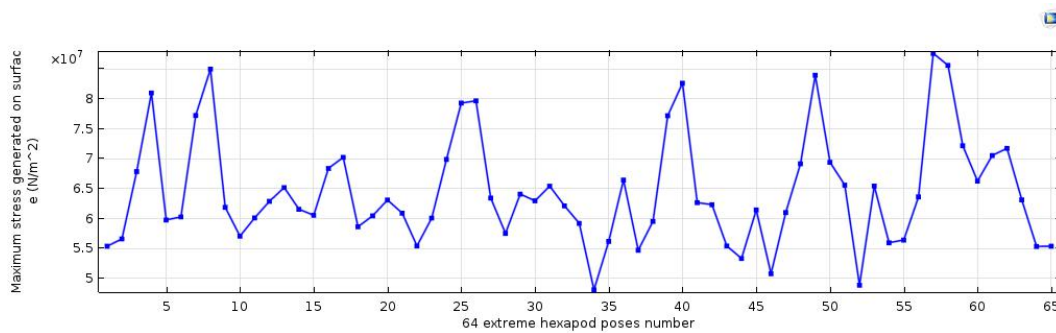
Figure 5-7: Maximum stress generated on cabin structure surface by gravity with all 64 extreme poses

Natural frequency evaluation of designed structure

The total structure including the mounted components weighs 1140 kg. Its modal shape can be evaluated as well in FEM software COMSOL around 44.3 Hz, when the reinforce beams inside the back frame of outer structure starts to oscillate first. Thus the natural frequency can be further improved with a better design to substitute the reinforce beams inside the back frame. However, for this design case, with an operating frequency lower than 10 Hz, it is good enough.
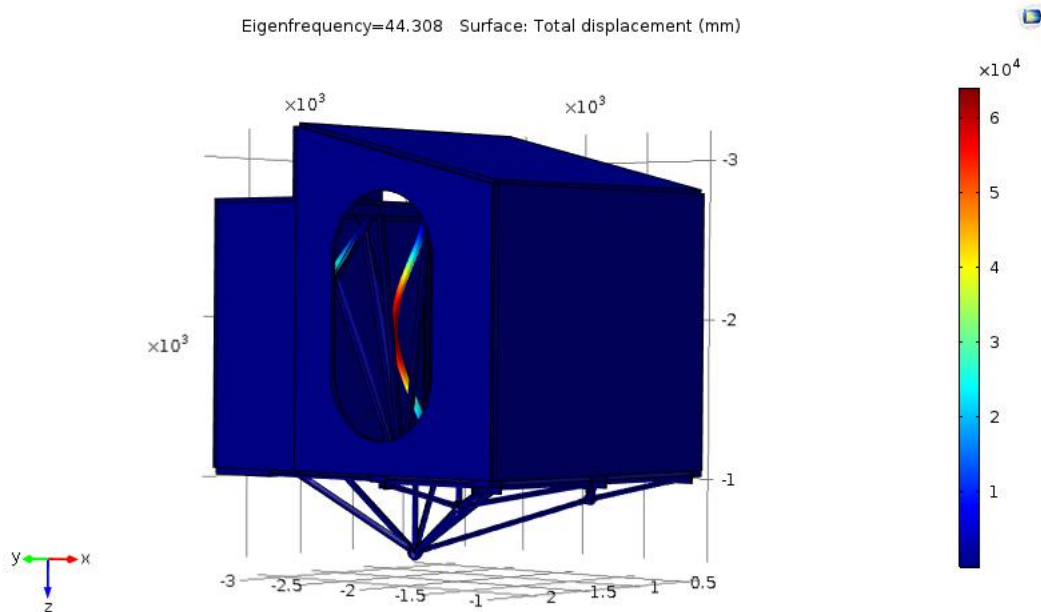

Figure 5-8: First elastic eigenmode of the cabin assembly

Mass properties evaluation of designed cabin structure

The designed cabin assembly has its mass properties with mass, center of mass and moment of inertia measured directly from the 3D drawing software SolidWorks. See a summary in Table 5-1. The total weight of the cabin structure will weigh around 745 kg, which is within the boundary of 930 kg (refer Table 3-4). It has left 700 kg for importing devices and occupants. The center of gravity lies 0.5m above the MRP, which is much lower than the required 1m (refer Table 3-4). The moment of inertia with respect to the MRP is also under the boundary of (1300, 1200, 1600) kgm^2 (refer Table 3-4).
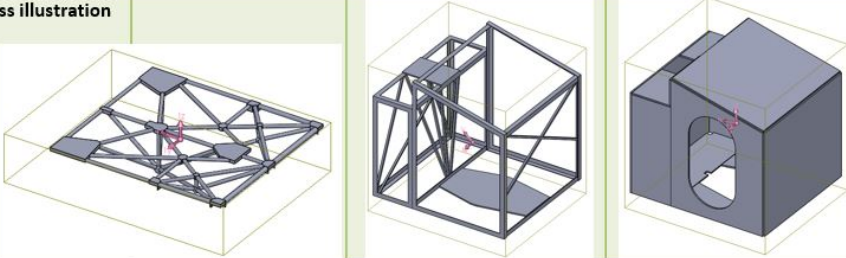
	Base frame	Outer structure frame + Base metal plate	Honeycomb filling panels	Total assembly
Material density	Steel: 7.85 kg/m³	Aluminum: 2.7 kg/m³	Aluminum: 0.292 kg/m³	
Mass	375 kg	210 kg	160 kg	**745 kg**
Center of gravity *in MRP coordinate system*	*(X, Y, Z) =* (0.13, 0, -0.12) m	*(X, Y, Z) =* (0.14, 0, -0.91) m	*(X, Y, Z) =* (0.19, -0.05, -1.18) m	*(X, Y, Z) =* **(0.15, -0.05, -0.57) m**
Moment of inertia *taken at the MRP coordinate system*	*(Ixx, Iyy, Izz) =* (167, 203, 348) kgm²	*(Ixx, Iyy, Izz) =* (360, 406, 201) kgm²	*(Ixx, Iyy, Izz) =* (393, 415, 208) kgm²	*(Ixx, Iyy, Izz) =* **(920, 1024, 757) kgm²**
Center of mass illustration				**Boundary condition** **Mass < 930 kg** **Z-axis < 1m** **Ixx, Iyy, Izz = (1200, 1300, 1600) kgm2**

Table 5-1: Cabin structure mass properties evaluation

Production costs evaluation of designed cabin structure

The production costs can be summarized regarding to the base and outer structure respectively. The difficulty of manufacturing the base is the welding of the base frame. However, this is highly dependent on the workshop quote. Here 10 keuro is given to have the base frame manufactured, and it should be a conservative estimation of the cost. For the outer structure, the cost will focus on the honeycomb panels, an estimation of 2 keuro is made for purchasing the honeycomb panels. And the rest part will included within 1 keuro. Thus in total, the manufacture cost should be under the promoted 20 keuro.

5-2   Honeycomb bolted joints connection validation

In the resulted design, the outer structure is mainly stiffened by the aluminum honeycomb panels, thus the stiffness of the connection between the frame and panels are important relating the total stiffness of the cabin assembly. As stated in the previous section, the honeycomb panels are very good at bearing distributed loads, which means it has its weakness of the core when carrying point or line loads. Thus normal bolts will not be a safe option for connecting

the honeycomb with the frame. But still, many special joining method is developed regarding to the honeycomb mounting.

As stated in the literature study, in-plane joints with the inserts is a very stiff joining solution. The general process to make honeycomb inserts is illustrated in Figure 5-9. First step is to drill holes with the size of the insert on the honeycomb panel, then the holes and inserts need to be cleaned. After, tapes have to be attached around the holes to keep them clear for bolts. By attaching a tab to the top of insert, the glue can be injected through the small hole on one side of the tab, until it came out from the other side, the region destroyed has fully filled with glue. Now the insert is well installed inside the honeycomb panel.
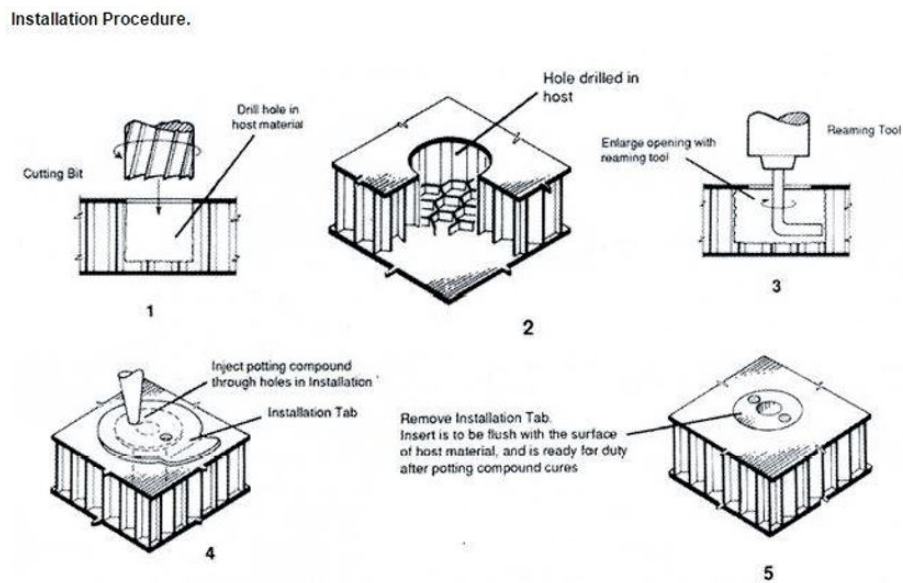

Figure 5-9: Honeycomb inserts installation general procedures[12]

A self-made honeycomb inserts panel can be seen in Figure 5-10. It cost around 1 hour to finish the whole process.
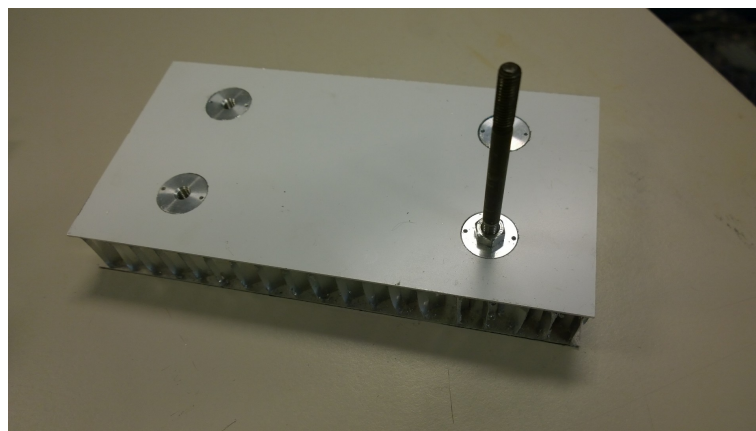

Figure 5-10: A self-made honeycomb inserts

This is a very good way to stiffen bolts within the honeycomb core structure. Since the destroyed part of core structure is well reinforced with glue, and the stiffness of the connection is then totally depended on the strength of the glue and the bolt being used. Usually with a good glue, the strength will be much higher than a normal M6 bolt, then with highly applied loads, the bolt will be first to break than the honeycomb inserts.

A force-tensile test bench is use to test the strength of the insert joints. The setup can be seen in Figure 5-11.
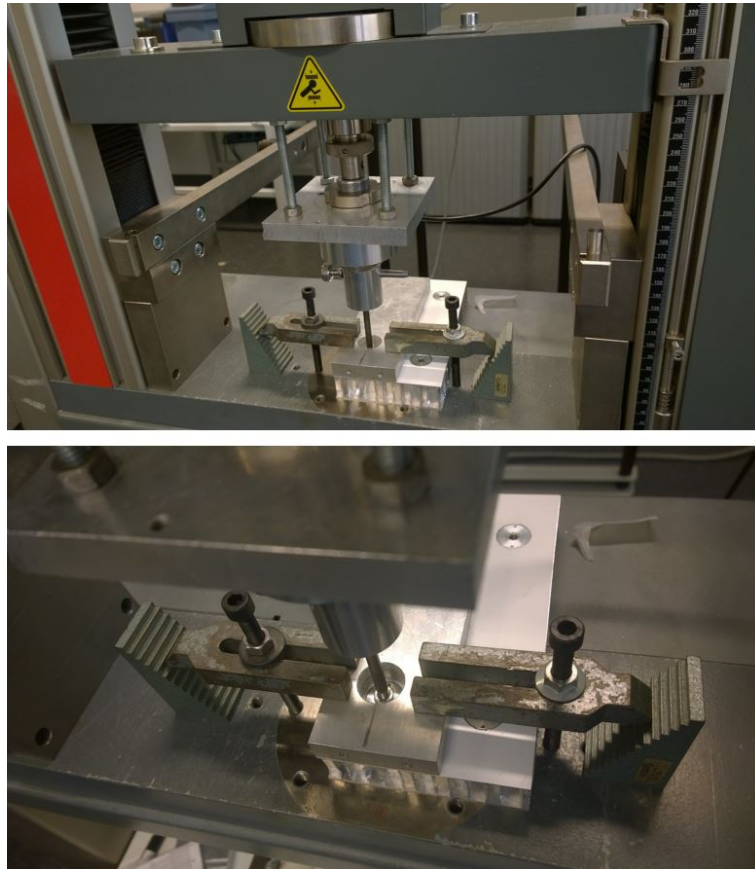

Figure 5-11: A force-tensile test bench setup for testing pulling stiffness of honeycomb inserts

With a static force up to 1kN applied on the insert, a travel of 0.15mm can be seen in the measurement as plotted in Figure 5-12. Thus the stiffness with the insert connection is about $6(10^6)N/m$. This is within the required stiffness of the hexapod motion simulator.

However, in the resulted design, each honeycomb panels has relatively large size, which will requires about 15-20 bolts on each edge of the panel, thus in total about 500 bolts will be required for bolting all the honeycomb panels. This requires relatively large work labor for manufacturing. However, an alternative way to solve this problem is use out-plane joining methods. By using a metal strip as the joint between bolts (together with washer if necessary) and honeycomb panel surface, the force applied to the honeycomb panel can be well spread, then the stiffness will be depended on the area of the metal strip. With the wider the strip,
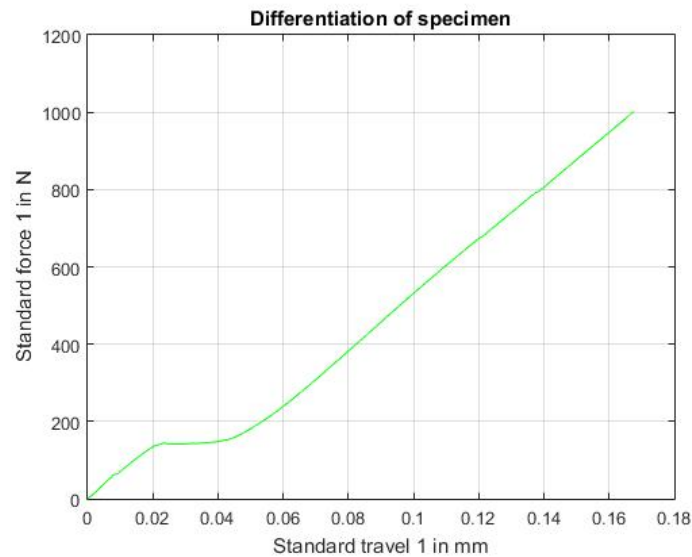
Figure 5-12: A force-tensile test bench setup for testing pulling stiffness of honeycomb inserts

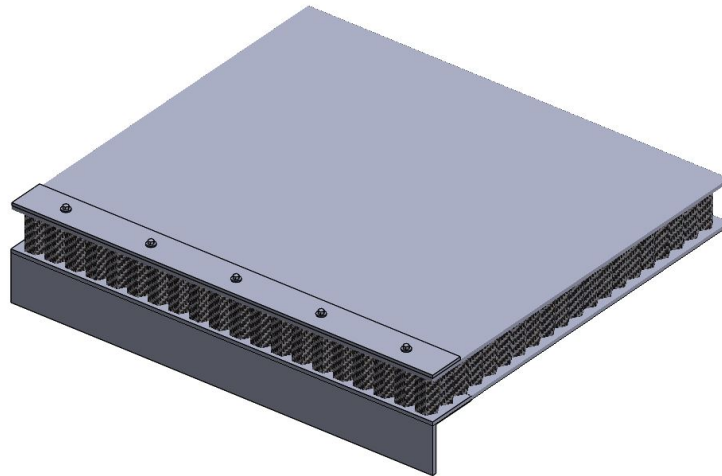the less stress created within the honeycomb panel. An example can be seen in Figure 5-13.

Figure 5-13: An alternative out-plane bolted joining method of honeycomb panel plate

Both bolted joining method can provide required stiffness and is feasible to be applied in the manufacture of the cabin structure. Inserts joint can save the weight and has a good outlook, however it take more labor to manufacture and is more costly. Metal strip out-plane bolt is very cheap and easy to drill holes and assembly, however, it adds more weight to the total cabin structure. Both method will have added magnitudes to the factors regarding weight and production costs, however these are within allowed boundaries.

5-3   Hexapod motion simulator dynamic capabilities verification

Due to the limited time of this project, the designed cabin structure could not be manu-
factured to conduct the dynamic test when integrated with the hexapod motion simulator.
However, the dynamic capability of the hexapod motion simulator can be validated with an
alternative cabin sample which has equivalent weight. See the alternative cabin sample in
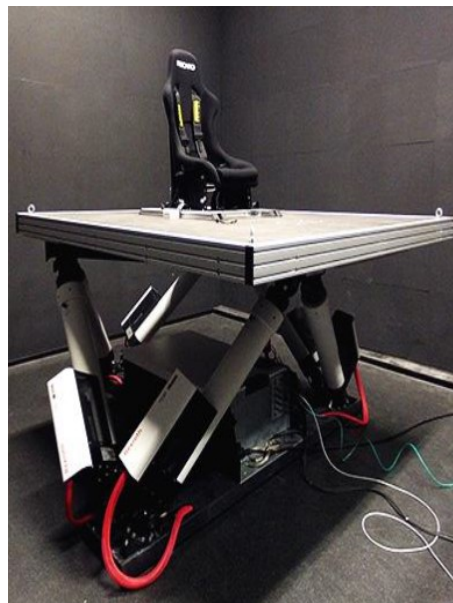Figure 5-14. It has a weight of around 1175 kg and a center of mass lies 0.27m above the MRP.

Figure 5-14: An alternative cabin sample used for conducting dynamic test with hexapod motion
simulator

Three experiment groups are test for comparison of the results. The first one is tested with no
payload on the top of the hexapod platform (refer Figure 5-15 on the left), its gross moving
load is only the weight of the hexapod motion simulator itself. The second comparison exper-
iment setup is with a Bosch Rexroth made cabin (refer Figure 5-15 in the middle). The total
weight measured by the hexapod system is around 1102 kg. A third comparison experiment
setup is with a MPI made cabin weighs 1175 kg, which is a huge wooden floor mounted upon
the hexapod motion simulator (refer Figure 5-15 on the right).

For conducting the dynamic identification of the hexapod motion simulator, frequency re-
sponse analyzer, a control software that is provided by Bosch Rexroth, is used. By input a
sine wave movement at several frequencies (sweep) and in each degree of freedom (surge, sway,
heave, roll, pitch and yaw), and by measuring the motion response of the motion system, a
frequency response was obtained that can be visualized in Bode plots. The input signal for
test within each degree of freedom is shown in Figure 5-16 with the amplitude of the frequency
sweep signal used with different gross moving loads respectively for each degree of freedom
(surge, sway, heave, roll, pitch and yaw).

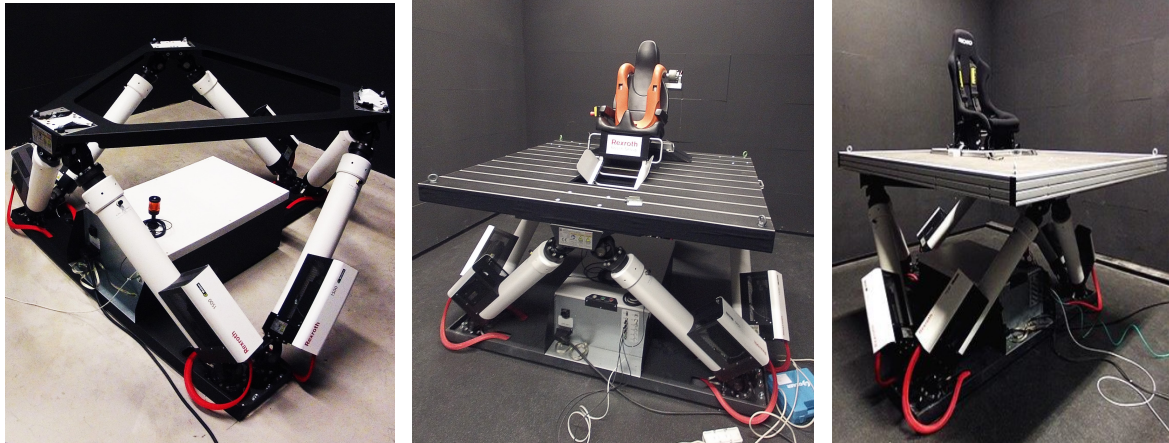| Cases	No cabin	Bosch cabin	MPI cabin
Payload	0	1102kg	1175kg
Gross Moving Load	253kg	1355kg	1428kg

Figure 5-15: Three sample groups used for conducting dynamic test with hexapod motion simulator
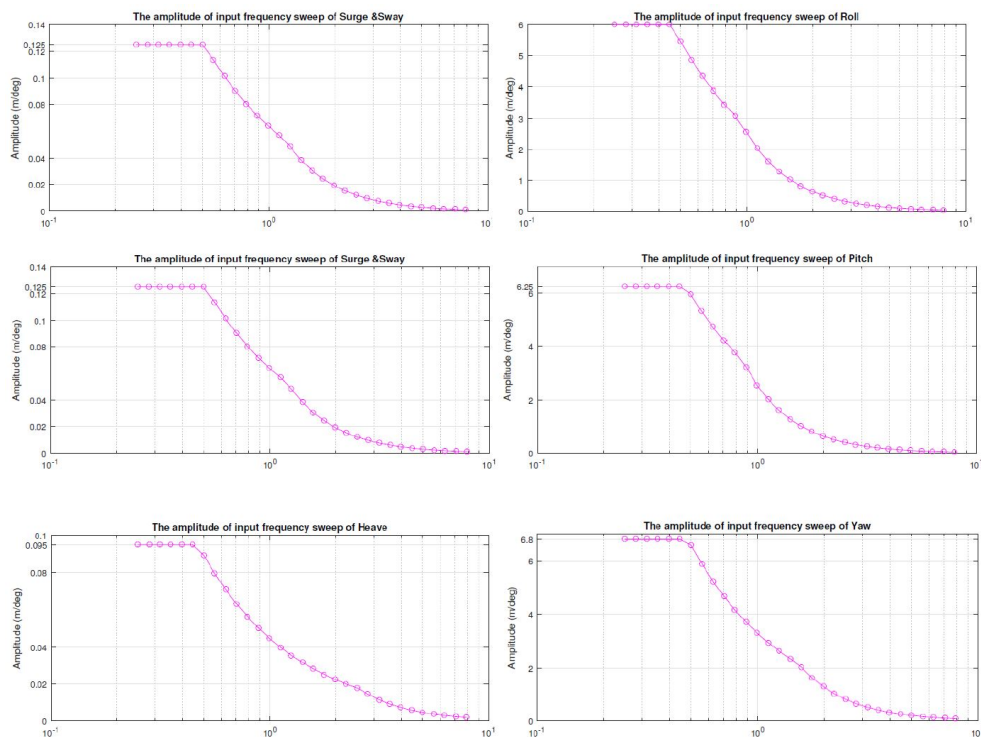

Figure 5-16: Plot of input signal amplitude in in each degree of freedom of hexapod motion simulator

The sweep data starts at 0.25 Hz and stops at 8 Hz, and the amplitude of the input decreases at high frequency area to protect the hexapod system. In Figure 5-16 the translation DOFs are on the left side including surge, sway and heave from top to bottom, the rotation DOFs are on the right side including roll, pitch and yaw from top to bottom.

In Figure5-17 showing the bode plots represent all the three payload cases in different color (no cabin case is denoted by blue line; Bosch cabin case is denoted by red line; MPI cabin case is denoted by green line). As seen that hexapod performs well within 8 Hz, which means the increasing weight of payload will not affect the dynamic capabilities of the hexapod simulator.

One place might need attention is that the frequency response plots of Surge, Sway and Yaw showed small deviations in the no cabin case (blue line) starting from 4Hz to 7Hz (refer Figure 5-17). This is because that in the no cabin case there is no payload attached to the triangular frame of the hexapod, which leads to the collection of the actuator joints to be not rigid enough during the motion. In contrast, the Heave, Roll and Pitch doesn't show any obvious weak performance of the no cabin case. This has given further reason why the cabin should be a rigid system and should be connected stiffly.
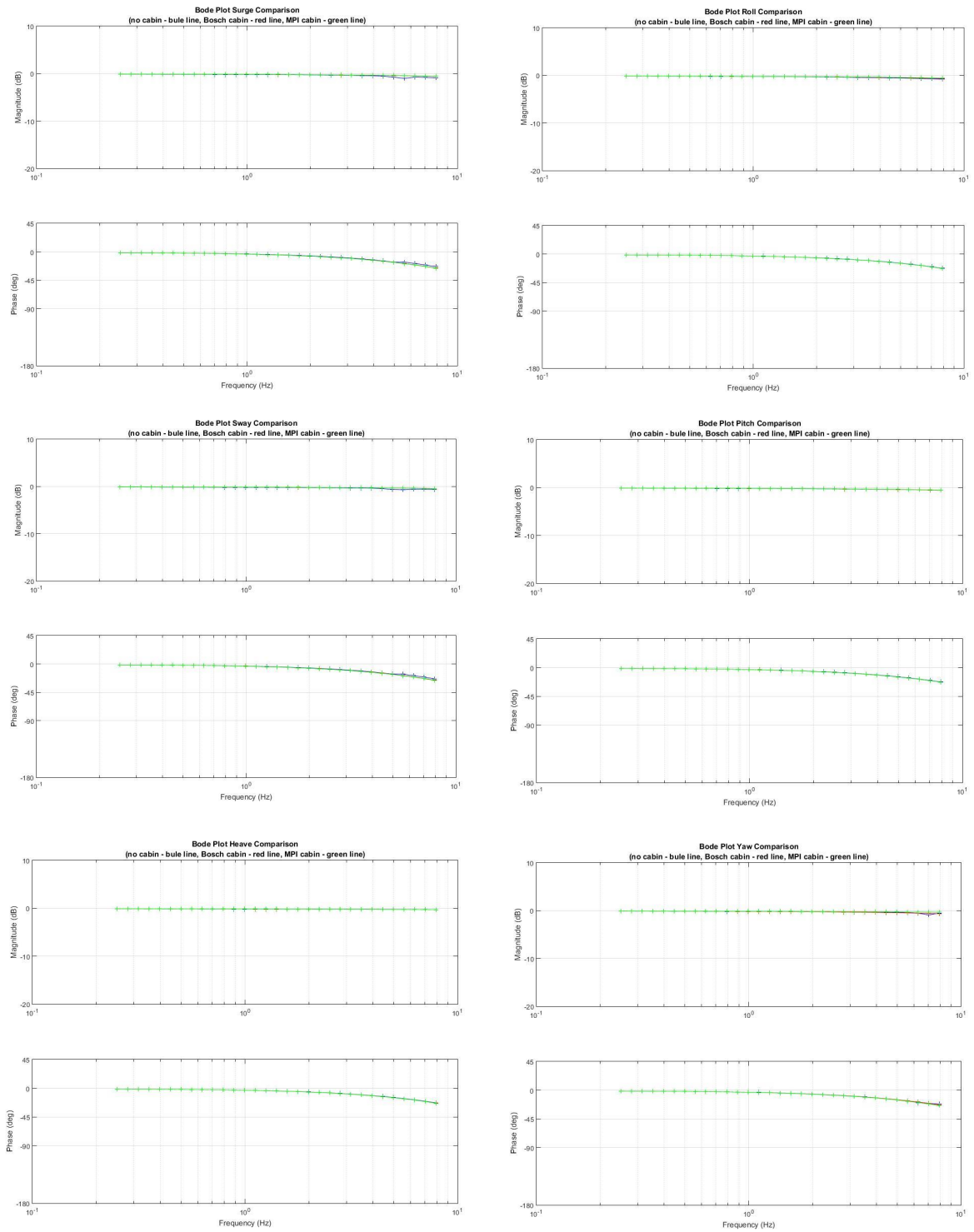
Figure 5-17: Frequency response in Bode Plots

Conclusion

The resulted design has a detachable structure system made of several frame and panel sub-structures. The base frame is a self-supported structure made of welded steel pipe. It has sufficient stiffness to support all the components under motion as an individual part. Its structure is optimized with respect to stiffness, production costs and the optimal positioning of required components. While the compromise is the relatively large weight which is not a critical factor in this design task. The outer structure frame is assembled with several aluminum boxes made of L profile elements. And the outer structure frame is stiffened by attaching aluminum honeycomb panels on the outside of each frame. This is out of the consideration of a light upper structure with acceptable moment of inertia to reduce the transmitted loads to the actuators. Stiff bolted joining method with honeycomb composite material is carefully selected to resist the risks of corrosion around the bolt in dynamic conditions. The whole design is able to access the limited motion lab entrance with disassembled parts and reassembled again easily inside the motion lab. Every time when changing experiment setups, the side panels can be removed fast by releasing the bolts to provide more space for exchanging setups inside the cabin. After the setups is mounted, the panels can be quickly repositioned in the same place.

The overall design of a multi-purpose research cabin has met the required functionality with high structural modularity.Its stiffness and natural frequency are also verified with FEM analysis both as individual part and as an assembly. The bolted connection between parts is verified with hand-calculations and simple tests especially for the bolting of honeycomb panels. And at last, the hexapod motion simulator is identified with its dynamic capabilities to verify the effects of different payload weight within boundary. A summary can be seen in Table 5-2. The design of a simple cabin structure concept which is detachable with high modularity while maintaining high stiffness has contributed to the desired functionality of the research motion simulator.

This research of a modular cabin structure design has promoted the development of multi-functional research motion simulators. This simple concept of a detachable cabin structure assembled with basic elements has not only improved the efficiency of exchanging components

	Modularity	Dimension			Stiffness			Mass properties		Costs (keuro)
		Access (m)	Work space (m) (w*d*h)	Inner volume (m) (w*d*h)	Axial	Rotational	Dynamical (Hz)	Weight (kg)	Moment of inertia (kgm²)	
Cabin structure assembly	detachable	detachable	2.1*2.25*2.1	1.8*2.2*2.05	defined by critical components: projector translational < 1mm, rotational < 0.003 rad; screen translational <1 mm, rotational < 0.005 rad		defined as natural frequencies	< 930	< 1.3*1.2*1.6 (10³)	< 20
Design	detachable	detachable	2.05*2.275*2.08	2*2.225*2.03			44	745	920*1024*757	15
Base frame	permanent	< 2*2.15	thickness < 0.05				> 10	< 450	COG -to- MRP distance < 1m	< 10
Design	permanent	0.56*2.05	thickness = 0.04				37	375		...
Outer structure frame	removable	< 2*2.15	thickness < 0.025		Total structure surface displacement max. 0.55mm: translational max. 0.45mm; rotational max. 0.0015 rad		> 10	< 100	COG -to- MRP distance 0.5m	< 4
Design	detachable	0.6*2					44	150		0.5
Panels	removable	< 2*2.15	thickness = 0.025				> 10	< 200		< 2
Design	removable	0.025*2					...	160		2

Table 5-2: Summary of designed cabin structure capabilities compare to requirements

for different function, to increase the simulator's functionality, but also provided sustainability of reusing the structure parts when the motion simulator is dismantled.

Appendix A

Cabin load case analysis

A calculation model is generated in MATLAB for the static and dynamic load case analysis of the hexapod motion simulator. An illustration of the model principle is shown in Figure A-1.
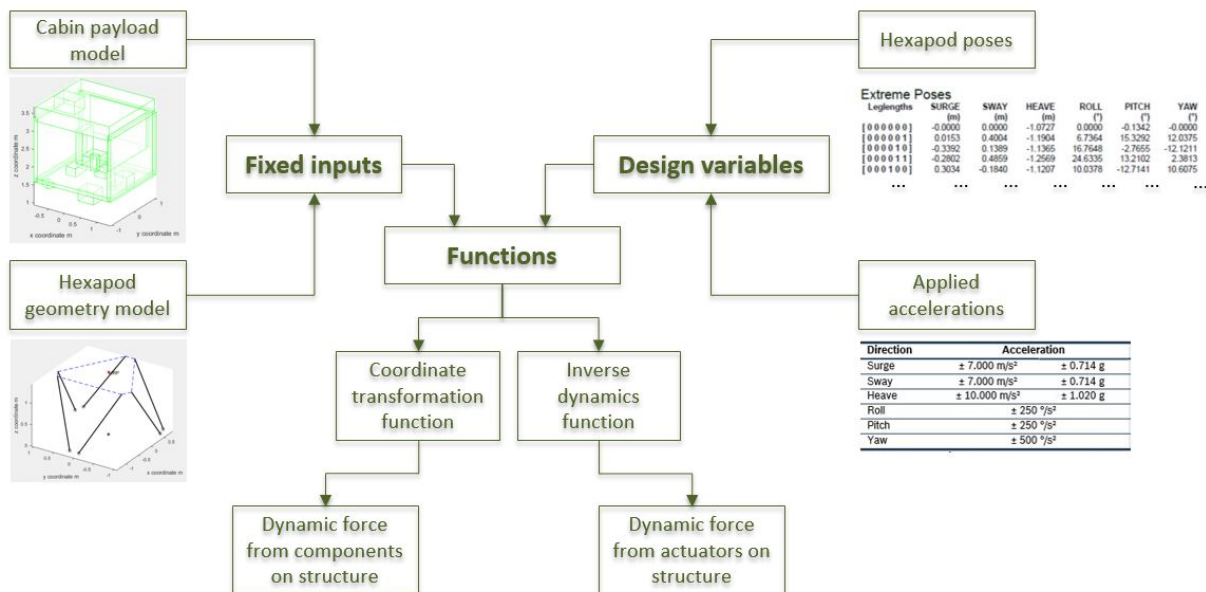

Figure A-1: Illustration of cabin load case analysis model

Fixed inputs includes 1) a cabin payload model which provided the defined payload mass positioning and bounding dimensions; 2) a hexapod geometry model which constrains the actuator orientation and its stroke.

Design variables includes 1) the transformation data from hexapod neutral pose to 64 extreme poses; 2) the maximum non-simultaneous accelerations of hexapod motion simulator (refer Table 2-1).

Functions includes the transformation function from generalized coordinate system to moving platform coordinate system; 2) the inverse dynamics calculation function of the required actuator force to accelerating each components.

The aim of this model is to analyze the load case both exerted from actuators and from the payloads acting on the cabin structure in both static and dynamic conditions.

A-1   Fixed inputs

A geometry model of hexapod can be built first with the coordinates of rotational center point of each joint (12 in total) from both hexapod base and platform measured from the 3D model in SolidWorks. This is because the relative position of joint center points will not change with respect to each other during the motion, so that it can define the geometry of the hexapod. Then the main components of cabin denoted as bounding box payloads can be modeled with respect to the hexapod MRP.

A-1-1   Hexapod geometry model and accuracy analysis

A reference point as the origin of the generalized coordinate is create by projecting the motion reference point of the platform in Z-direction (heave) on the floor surface in its settled pose (when all the actuators retracted). (Where motion reference point denotes the reference point of hexapod for maximum excursions, velocities and accelerations). The generalized coordinate system axis is defined by the movements in each degree of freedom as seen in Figure 2-9. Surge denoted the translation in longitudinal x direction; Sway denotes the translation in lateral y direction; Heave denotes the translation in vertical z direction; Roll denotes the rotation about x axis; Pitch denotes the rotation about y axis; Yaw denotes the rotation about z axis.[2].

The hexapod will be simplified in Matlab with three parts: the lower joint plane denoted by the 6 rotation points of the lower joints, the upper joint plane denoted by the 6 rotation points of upper joints and 6 actuator legs denoted by lines from upper joints to their corresponding lower joints.

The lower joint plane is fixed to the floor, which makes it a fixed input parameter that measured in the SolidWorks model. The motion reference point (MRP), defined as $148mm$ towards x-direction with respect to the geometric origin of the upper joint plane, is fixed to the moving platform as well as the upper joint plane, which makes them variable inputs given by the displacement in 6 degree of freedom with respect to the general coordinate system on the floor. Then, the simplified hexapod model can be well defined in Matlab, see an example of settled pose in FigureA-2.

As a remark, the rotation transformation of upper joint plane with respect to the general coordinate system is finished by applying the Yaw angle about the Z-axis first, then the Pitch
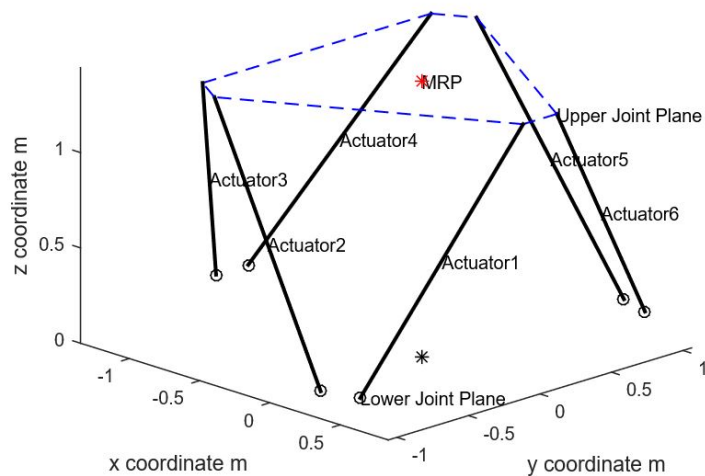
Figure A-2: Hexapod simplified model in settled pose in Matlab

angle about the **new** Y-axis and then the Roll angle about the **new** X-axis, since the angles are all Euler angles as stated in the hexapod manual. Then, the translation of the upper joint plane can be added to the previous transformation.

To calibrate this model, an error analysis was conducted using a data sheet contains the displacements of MRP in each degree of freedom of all the 64 extreme poses of hexapod (when all its actuators either extended or retracted). By inserting the data to the hexapod model, the deflection between the actuator length calculated in this model and the theoretical values can be obtained. As measured in the 3D model in SolidWorks, the extended actuator length is $1.9589m$ and the retracted actuator length is $1.3039m$ (includes the stroke within the cushioning zones). And for all the 64 poses tested, the maximum error of this model is 0.5926%. This error is assumed allowable and the model is assumed to be accurate for further calculation.

A-1-2   Cabin payload model

The total cabin payloads involved for load calculation are defined by taking into account all the possible components and giving the conservatively estimated value of weight to each component.

File simulator.modelinput.m

```
% File simulator_model_input.m

% Fixed input parameters of simulator (cabin payload) model
% Dimensions are measured from the simulator model in SolidWorks
```

```
%*DEFINITIONS*******************************************************
% MRP : Motion Reference Point, the reference point for maximum excursions,
%       velocities and accelerations.
% LJP : Lower Joint Plane, the plane through the rotation points of the
%       universal joints of the base frame of hexapod.
% UJP : Upper Joint Plane, the plane through the rotation points of the
%       universal joints of the moving platform.
% RP  : Reference Point, the projection by MRP in z-direction on the floor
%       at hexapod's settled pose.

% RP coordinate system : generalized coordinate system fixed to ground.
% MRP coordinate system: moving coordinate system fixed to the moving
%                        platform of the motion system.
%*******************************************************************

%******************
% SI-Units: m
%******************

%% Hexapod model
% Lower Joint_Rotation Points_Coordinates_in RP coordinate system
% Matrix 6*3 (actuator nr.*coordinate in 3 axis(x- y- z-))
  P_l = [ 0.57677 0.99532 -0.14385
          0.36132  1.06015 -0.14385
         -1.34758  0.11250 -0.14385
         -1.34758 -0.11250 -0.14385
          0.36132 -1.06015 -0.14385
          0.57677 -0.99532 -0.14385];

% Upper Joint_Rotation Points_Coordinates_in MRP coordinate system
% Matrix 6*3 (actuator nr.*coordinate in 3 axis(x- y- z-))
  P_uo = [ 0.84235 0.11750 0
          -0.54124 0.91631 0
          -0.74475 0.79881 0
          -0.74475 -0.79881 0
          -0.54124 -0.91631 0
           0.84235 -0.11750 0];

%% Cabin model
% Cabin model contains
% 1)Seat+Occupant2)Projector3)Monitors4)PlatformNodes5)PowerSupply6)Computers
% 7)BaseFloor8)SideWalls9)ControlDevices

% Assume each payload is a bounding box with mass evenly distributed
% Parameters
% D_c: the dimensions of each bounding box [depth(x) width(y) height(z)]
% m_c: the mass of each payload
% P_c: coordinates of the centroid of each payload
% T_c: transformation matrix of the relative coordinate system
% I_c: moment of inertia of each payload with respect to its centroid

% CABIN = struct();

  CABIN.D_co = [];
  CABIN.m_co = [];
  CABIN.P_co = []; %coordinates of centroid with respect to MRP
```

```
  CABIN.I_co = []; %moment of inertia with respect to MRP

% Seat+Occupant(backrest)_Nr.1
  CABIN = addComponent(CABIN,[0.1964 0.4982 0.9204], 60, [-0.0982 0 -1.0198], eye(3));
% Seat+Occupant(base)_Nr.2
  CABIN = addComponent(CABIN,[0.4320 0.4982 0.2680], 200, [0.2160 0 -0.6936], eye(3));
% Projector_Nr.3
  CABIN = addComponent(CABIN,[0.6286 0.4604 0.3620], 50, [-0.5802 -0.0238 -2.0563], eye(3));
% Monitor/Screen_Nr.4
  CABIN = addComponent(CABIN,[0.0200 1.7900 1.0000], 30, [1.2101 0 -1.4020], eye(3));
% Monitor/Screen_Nr.5
  CABIN = addComponent(CABIN,[1.7900 0.0200 1.0000], 30, [0.3101 1 -1.4020], eye(3));
% Monitor/Screen_Nr.6
  CABIN = addComponent(CABIN,[1.7900 0.0200 1.0000], 30, [0.3101 -1 -1.4020], eye(3));
% MountingBlockF_Nr.7
  CABIN = addComponent(CABIN,[0.1990 0.3240 0.1140], 10, [0.8466 0 -0.0962], eye(3));
% MountingBlockL_Nr.8
  CABIN = addComponent(CABIN,[0.1990 0.3240 0.1140], 10, [-0.6450 0.8611 -0.0962], [-1/2
      -sqrt(3)/2 0; sqrt(3)/2 -1/2 0; 0 0 1]);
% MountingBlockR_Nr.9
  CABIN = addComponent(CABIN,[0.1990 0.3240 0.1140], 10, [-0.6450 -0.8611 -0.0962], [-1/2
      sqrt(3)/2 0; -sqrt(3)/2 -1/2 0; 0 0 1]);
% PowerSupply_Nr.10
  CABIN = addComponent(CABIN,[0.2850 0.5200 0.2250], 20, [-0.3425 0 -0.2905], eye(3));
% Computers_Nr.11
  CABIN = addComponent(CABIN,[0.47 0.42 0.348], 20, [0.087 0 0.326], eye(3));
% BaseFrame_Nr.12
  CABIN = addComponent(CABIN,[2.25 2.1 0.1], 500, [0.225 0 -0.203], eye(3));
% SideFrameF_Nr.13
  CABIN = addComponent(CABIN,[0.1 2.1 1.75], 40, [1.35 0 -1.025], eye(3));
% SideFrameL_Nr.14
  CABIN = addComponent(CABIN,[2.25 0.1 1.80], 40, [0.225 1 -1.05], eye(3));
% SideFrameR_Nr.15
  CABIN = addComponent(CABIN,[2.25 0.1 1.80], 40, [0.225 -1 -1.05], eye(3));
% SideFrameB_Nr.16
  CABIN = addComponent(CABIN,[0.1 2.1 1.80], 40, [-0.9 0 -1.05], eye(3));
% SideFrameU_Nr.17
  CABIN = addComponent(CABIN,[2.25 2.1 0.4], 40, [0.225 0 -2.0563], eye(3));
% ControlDevices_HelicopterCollectiveStick_Nr.18
  CABIN = addComponent(CABIN,[0.1500 0.3360 0.1200], 12, [0.1971 -0.4330 -0.4250], eye(3));
% ControlDevices_HelicopterCyclicStick_Nr.19
  CABIN = addComponent(CABIN,[0.3326 0.4401 0.1780], 20, [0.4284 -0.1500 -0.3270], eye(3));
% ControlDevices_HelicopterSideStick_Nr.20
  CABIN = addComponent(CABIN,[0.2130 0.1200 0.4388], 10, [0.4556 0.3550 -0.7793], eye(3));
% ControlDevices_Helicopter_Pedal_Nr.21
  CABIN = addComponent(CABIN,[0.3524 0.3500 0.3566], 16, [1.1340 0 -0.3194], eye(3));
% ControlDevices_CarSetup_Nr.22
  CABIN = addComponent(CABIN,[0.6506 0.5010 0.7254], 25, [0.9630 0 -0.5559], eye(3));

%% Gravity (m/s^2)
  g = 9.81;

%% Mounting-block
% Distance between actuating point and center of mass
  t_MD = 0.0626;

%end of hexapod_cabin_input_model.m
```

File addComponent.m

```matlab
% Function addComponent.m

function [CABIN] = addComponent(CABIN,D_c,m_c,P_c,T_c)

    NoC = size(CABIN.D_co,1);
    NoCI = size(CABIN.I_co,3);

    CABIN.D_co(NoC+1,:)   = D_c;
    CABIN.m_co(NoC+1,:)   = m_c;
    CABIN.P_co(NoC+1,:)   = P_c;

    [I_c] = moi(D_c,m_c,P_c,T_c);

    CABIN.I_co(:,:,NoCI+1)  = I_c;
    CABIN.T_co(:,:,NoCI+1)  = T_c;

end
```

File drawPayloadC.m

```matlab
% Function drawPayloadC.m
% A function to draw each payload bounding box

function drawPayloadC(P_c,D_o,R,T_o)

x=([0 1 1 0 0 0;
    1 1 0 0 1 1;
    1 1 0 0 1 1;
    0 1 1 0 0 0]-repmat(0.5,4,6)).*D_o(1);
y=([0 0 1 1 0 0;
    0 1 1 0 0 0;
    0 1 1 0 1 1;
    0 0 1 1 1 1]-repmat(0.5,4,6)).*D_o(2);
z=([0 0 0 0 0 1;
    0 0 0 0 0 1;
    1 1 1 1 0 1;
    1 1 1 1 0 1]-repmat(0.5,4,6)).*D_o(3);

for u = 1:6
    for w = 1:4
        B = [x(w,u) y(w,u) z(w,u)]*T_o'*R + [P_c(1) P_c(2) P_c(3)];
        x(w,u) = B(1);
        y(w,u) = B(2);
        z(w,u) = B(3);
    end
end
for n=1:6
    h=patch(x(:,n),-y(:,n),-z(:,n),'w','FaceAlpha',.3);
    set(h,'edgecolor','g')
end
```

A-2   Input variables

The coordinates of extreme poses of hexapod is imported to determine the moving platform states. The maximum acceleration and deceleration is imported to calculate the force generated at each actuator to drive the platform.

A-2-1   Hexpaod maximum acceleration and velocity applied with payloads

The accelerations are defined relative to the motion reference point with the motion system in its neutral position. With the designed gross moving load, the system can provide the non-simultaneous accelerations and acceleration onsets as shown in Figure A-3.

Direction	Velocity		Acceleration		Acceleration onset
Surge	± 0.79 m/s	± 31.1 in/s	± 7.000 m/s²	± 0.714 g	± 10.0 g/s
Sway	± 0.81 m/s	± 31.8 in/s	± 7.000 m/s²	± 0.714 g	± 10.0 g/s
Heave	± 0.55 m/s	± 21.6 in/s	± 10.000 m/s²	± 1.020 g	± 10.0 g/s
Roll	± 34.3 °/s		± 250 °/s²		± 600.0 °/s²/s
Pitch	± 37.4 °/s		± 250 °/s²		± 600.0 °/s²/s
Yaw	± 41.3 °/s		± 500 °/s²		± 600.0 °/s²/s

Figure A-3: Non-simultaneous velocities and accelerations defined by the hexapod

A-2-2   Extreme pose coordinate values

The extreme poses are defined with the values in each degree of freedom needed to transform the moving platform coordinate system.

Rexroth
Bosch Group

2   Technical information

2.1   Data

Design: Motion Designer
Date: 19-Feb-15.

Extreme Poses

Leglengths	SURGE (m)	SWAY (m)	HEAVE (m)	ROLL (°)	PITCH (°)	YAW (°)
[0 0 0 0 0 0]	-0.0000	0.0000	-1.0727	0.0000	-0.1342	-0.0000
[0 0 0 0 0 1]	0.0153	0.4004	-1.1904	6.7364	15.3292	12.0375
[0 0 0 0 1 0]	-0.3392	0.1389	-1.1365	16.7648	-2.7655	-12.1211
[0 0 0 0 1 1]	-0.2802	0.4859	-1.2569	24.6335	13.2102	2.3813
[0 0 0 1 0 0]	0.3034	-0.1840	-1.1207	10.0378	-12.7141	10.6075
[0 0 0 1 0 1]	0.3501	0.2005	-1.2849	10.4359	2.4361	23.3005
[0 0 0 1 1 0]	-0.0021	0.0046	-1.3011	30.4837	-16.4524	-4.5370
[0 0 0 1 1 1]	0.0792	0.3291	-1.4407	30.3997	-1.9905	11.2474
[0 0 1 0 0 0]	0.3034	0.1840	-1.1207	-10.0378	-12.7141	-10.6075
[0 0 1 0 0 1]	0.3585	0.6254	-1.1779	-6.4406	4.9491	-0.9234
[0 0 1 0 1 0]	-0.0737	0.3351	-1.2413	3.6548	-10.1873	-24.0098
[0 0 1 0 1 1]	0.0044	0.7330	-1.2957	11.4194	7.7775	-11.4705
[0 0 1 1 0 0]	0.5387	0.0000	-1.1648	-0.0000	-27.0720	0.0000
[0 0 1 1 0 1]	0.6485	0.4153	-1.2566	-0.5446	-12.3307	11.0606
[0 0 1 1 1 0]	0.1984	0.1904	-1.3820	18.3730	-24.6104	-16.4220
[0 0 1 1 1 1]	0.3327	0.5746	-1.4521	19.6168	-10.2247	-2.3907
[0 1 0 0 0 0]	-0.3392	-0.1389	-1.1365	-16.7648	-2.7655	12.1211
[0 1 0 0 0 1]	-0.3232	0.2959	-1.2908	-7.0613	7.4574	22.4886
[0 1 0 0 1 0]	-0.7267	-0.0000	-1.1243	-0.0000	-9.8382	0.0000
[0 1 0 0 1 1]	-0.6653	0.4022	-1.2878	11.9176	4.9796	11.5508
[0 1 0 1 0 0]	-0.0737	-0.3351	-1.2413	-3.6548	-10.1873	24.0098
[0 1 0 1 0 1]	-0.0331	0.0814	-1.4172	-0.0150	-0.2035	35.9253
[0 1 0 1 1 0]	-0.4174	-0.1506	-1.3624	16.6524	-19.9349	9.1124
[0 1 0 1 1 1]	-0.3352	0.2174	-1.5288	19.4500	-6.7387	22.4813
[0 1 1 0 0 0]	-0.0021	-0.0046	-1.3011	-30.4837	-16.4524	4.5370
[0 1 1 0 0 1]	0.0425	0.4682	-1.4128	-24.2399	-3.8916	12.1781
[0 1 1 0 1 0]	-0.4174	0.1506	-1.3624	-16.6524	-19.9349	-9.1124
[0 1 1 0 1 1]	-0.3565	0.6172	-1.4615	-5.1094	-3.2396	-0.4885
[0 1 1 1 0 0]	0.1984	-0.1904	-1.3820	-18.3730	-24.6104	16.4220
[0 1 1 1 0 1]	0.2804	0.2548	-1.5194	-15.3391	-13.1759	25.3534
[0 1 1 1 1 0]	-0.1974	-0.0000	-1.5323	0.0000	-30.2711	0.0000
[0 1 1 1 1 1]	-0.0737	0.4301	-1.6550	4.7896	-16.0000	10.4171
[1 0 0 0 0 0]	0.0153	-0.4004	-1.1904	-6.7364	15.3292	-12.0375
[1 0 0 0 0 1]	-0.0394	0.0000	-1.4246	-0.0000	33.8259	0.0000
[1 0 0 0 1 0]	-0.3232	-0.2959	-1.2908	7.0613	7.4574	-22.4886
[1 0 0 0 1 1]	-0.3198	0.0589	-1.5073	14.4169	26.5454	-8.7600
[1 0 0 1 0 0]	0.3585	-0.6254	-1.1779	6.4405	4.9491	0.9234
[1 0 0 1 0 1]	0.3342	-0.2299	-1.4810	8.9082	23.4925	13.9859
[1 0 0 1 1 0]	0.0425	-0.4682	-1.4128	24.2399	-3.8916	-12.1781
[1 0 0 1 1 1]	0.0786	-0.1422	-1.6492	26.0560	14.2727	3.4891
[1 0 1 0 0 0]	0.3501	-0.2005	-1.2849	-10.4359	2.4361	-23.3005
[1 0 1 0 0 1]	0.3342	0.2299	-1.4810	-8.9082	23.4925	-13.9859
[1 0 1 0 1 0]	-0.0331	-0.0814	-1.4172	0.0150	-0.2035	-35.9253
[1 0 1 0 1 1]	-0.0027	0.3062	-1.5962	4.5329	19.8743	-23.4303

DOC.   : GENERIC-02-32-0000-ENV-0001
REV.   : 00
DATE   : 17-02-15
PROJECT : GENERIC

Rexroth
Bosch Group

[1 0 1 1 0 0]	0.6485	-0.4153	-1.2566	0.5446	-12.3307	-11.0606
[1 0 1 1 0 1]	0.7099	0.0000	-1.4976	-0.0000	6.7693	0.0000
[1 0 1 1 1 0]	0.2804	-0.2548	-1.5194	15.3391	-13.1759	-25.3534
[1 0 1 1 1 1]	0.3782	0.1190	-1.7097	16.2223	4.2954	-11.0686
[1 1 0 0 0 0]	-0.2802	-0.4859	-1.2569	-24.6335	13.2102	-2.3813
[1 1 0 0 0 1]	-0.3198	-0.0589	-1.5073	-14.4169	26.5454	8.7600
[1 1 0 0 1 0]	-0.6653	-0.4022	-1.2878	-11.9176	4.9796	-11.5507
[1 1 0 0 1 1]	-0.6759	-0.0000	-1.5263	-0.0000	21.1904	-0.0000
[1 1 0 1 0 0]	0.0044	-0.7330	-1.2957	-11.4194	7.7775	11.4705
[1 1 0 1 0 1]	-0.0027	-0.3062	-1.5962	-4.5329	19.8743	23.4303
[1 1 0 1 1 0]	-0.3565	-0.6172	-1.4615	5.1094	-3.2396	0.4885
[1 1 0 1 1 1]	-0.3247	-0.2278	-1.7223	11.6063	11.4540	12.9563
[1 1 1 0 0 0]	0.0792	-0.3291	-1.4407	-30.3997	-1.9905	-11.2474
[1 1 1 0 0 1]	0.0786	0.1422	-1.6492	-26.0560	14.2727	-3.4891
[1 1 1 0 1 0]	-0.3352	-0.2174	-1.5288	-19.4500	-6.7387	-22.4813
[1 1 1 0 1 1]	-0.3247	0.2278	-1.7223	-11.6063	11.4540	-12.9563
[1 1 1 1 0 0]	0.3327	-0.5746	-1.4521	-19.6168	-10.2247	2.3907
[1 1 1 1 0 1]	0.3782	-0.1190	-1.7097	-16.2223	4.2954	11.0686
[1 1 1 1 1 0]	-0.0737	-0.4301	-1.6550	-4.7896	-16.0000	-10.4171
[1 1 1 1 1 1]	0.0000	0.0000	-1.8758	0.0000	-0.0710	0.0000

The "leg-lengths" show which actuator is extended and which actuator is retracted. For example [1 0 1 0 0 0] is a system position with actuator 1 and 3 completely extended (1) and the other four actuators completely retracted (0).

2.2   Instructions

To generate the motion envelope of a particular payload, the payload has to be available in 3D drawing software. It is convenient to attach a coordinate system to the payload that has its origin in the MRP with the X-axis pointing forward, the Y-axis pointing to the right and the Z-axis pointing downward (refer to figure 1-3). Note that the XY plane of this coordinate system lies 153.7 mm below the mounting surface of the payload (refer to figure 1-2). To position the payload in space for a certain system position, start with the MRP on the floor (refer to figure 1-2). Use the values X, Y and Z from the table to move the MRP (note that a negative value of Z moves the payload up). Use the Yaw from the table to rotate the payload (including the coordinate system) about the Z-axis. Use the Pitch from the table to rotate the payload (including the coordinate system) about the new Y-axis. Finally, use the Roll from the table to rotate the payload (including the coordinate system) about the new X-axis. Save this position of the payload and repeat the procedure for all 64 system positions. Overlay all results to determine the complete envelope.

A-3 Function

A transformation function of the coordinate system from generalized coordinate system to the moving platform coordinate system is built. A inverse dynamics calculation function of actuator force required to accelerating all the components is built.

A-3-1 Cabin moving platform coordinate system transformation model

File function part1

```
%Function simulatorF.m
%Analysis model of force exerted by hexapod actuators

function [R,P_MRP,P_u,P_c,Act,L,f,F_vec,F, F_node, M_node] = simulatorF(delt_x,...
    delt_y,delt_z,thet_x,thet_y,thet_z,P_l,P_uo,CABIN,g,acc,vel,t_MD)

%****************************
% SI-Units: m, N, s, deg
%****************************
% INPUT PARAMETERS:
% Variables:
% delt_x : translation displacement of MRP in x-axis(surge) (m).
% delt_y : translation displacement of MRP in y-axis(sway) (m).
% delt_z : translation displacement of MRP in z-axis(heave) (m).
% thet_x : rotation displacement of MRP around x-axis(roll) (deg).
% thet_y : rotation displacement of MRP around y-axis(pitch) (deg).
% thet_z : rotation displacement of MRP around z-axis(yaw) (deg).

% Fixed input parameters:
% P_l : coordinates of the rotation points of the 6 lower joints with
%       respect to RP.(m)
% P_uo : coordinates of the rotation points of the 6 upper joints with
%       respect to MRP.(m)
% P_co : each sub-payload's centroid position with respect to the MRP (m).
% acc : accelerations applied at MRP. (m/s^2 or rad/s^2)

% OUTPUT PARAMETERES:
% R      : rotation matrix in terms of three Euler angles at MRP.
% P_MRP  : motion reference point position in fixed coordinate (m).
% P_u    : upper joint center point position in fixed coordinate (m).
% P_c    : subpayload's centroid position in fixed coordinate (m).
% Act    : actuators denoted by vectors from upper joint center to the
%          cooresponding lower joint center (m). (6*3 matrix)
% L      : length of each actuator (m). (6*1 matrix)

%% Coordinate transformation of MRP
% Rotation of coordinate system at MRP

  R_z = [cos(thet_z) sin(thet_z) 0
        -sin(thet_z) cos(thet_z) 0
         0           0           1]; % Rotation matrix at MRP with Yaw

  R_y = [cos(thet_y) 0 -sin(thet_y)
         0           1 0
```

```
         sin(thet_y) 0 cos(thet_y)]; % Rotation matrix at MRP with Pitch

  R_x = [1 0          0
         0  cos(thet_x) sin(thet_x)
         0 -sin(thet_x) cos(thet_x)]; % Rotation matrix at MRP with Roll

  R = R_x*R_y*R_z;

% Translation of coordinate system at MRP
  T = [delt_x delt_y delt_z];

%% Position of platform and cabin system in general coordinate
% MRP coordinate in general coordinate
  P_MRP = T;

% Rotation points of upper joints in the general coordinate
  P_u = bsxfun(@plus, P_uo * R, T);

% Centroid of each payload in general coordinate
  P_c = bsxfun(@plus, CABIN.P_co * R, T);

%% Actuator length and orientation
% Actuator vector described from its upper-joint to its lower-joint
  Act = P_l - P_u;

% Length of each actuator
  L = sqrt(sum(Act.^2,2));
```

A-3-2   Force required from actuators for accelerating all the components

Moment of inertia of payload with respect to MRP

Due to the fact that all the maximum accelerations are defined with respect to the MRP, thus the moment of inertia used for dynamic calculations has to be transformed from centroid coordinate system to the MRP moving platform coordinate system. As seen in Figure A-4
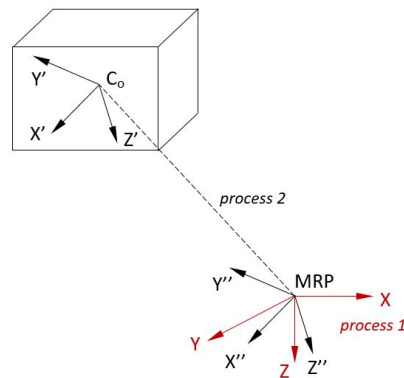
Figure A-4: Moment of inertia with respect to another coordinate system

First, it is assumed that all the motions are defined in a coordinate system fixed to the moving platform of the hexapod motion system. It has its origin at the MRP and XY plane lying in the upper joint plane. This means each components is also fixed to the moving platform coordinate system. With this assumption, the moment of inertia of each component will be calculated with respect to the moving platform coordinate system, which makes it invariable for different hexapod poses.

Since all the components are denoted by a bounding box (like a cube) with mass evenly distributed, the parallel axis theorem (and the rotation axis theorem) can be applied to make calculation a little easier. Suppose the component's bounding cube has dimensions d, w and h denoting its depth, width and height, the moment of inertia can be first calculated with respect to its centroid coordinate system C that the cube is symmetric with respect to the X, Y, Z axis and has its centroid at the origin:

$$\mathbf{I_C} = \begin{bmatrix} \frac{1}{12}(w^2 + h^2)m & 0 & 0 \\ 0 & \frac{1}{12}(d^2 + h^2)m & 0 \\ 0 & 0 & \frac{1}{12}(d^2 + w^2)m \end{bmatrix} \tag{A-1}$$

Suppose the centroid coordinate system C of the component is rotated by T with respect to the moving platform coordinate system O, where

$$\mathbf{R} = \begin{bmatrix} 1 & 0 & 0 \\ 0 & cos\theta_x & sin\theta_x \\ 0 & -sin\theta_x & cos\theta_x \end{bmatrix} \begin{bmatrix} cos\theta_y & 0 & -sin\theta_y \\ 0 & 1 & 0 \\ sin\theta_y & 0 & cos\theta_y \end{bmatrix} \begin{bmatrix} cos\theta_z & sin\theta_z & 0 \\ -sin\theta_z & cos\theta_z & 0 \\ 0 & 0 & 1 \end{bmatrix} \tag{A-2}$$

and translation $(x,\ y,\ z)$ with respect to the moving platform coordinate system, using the parallel axis theorem and rotation axis theorem, the moment of inertia with respect to the moving platform coordinate system O can be derived as:

$$\mathbf{I_O} = \mathbf{T} \cdot \mathbf{I_C} \cdot \mathbf{T^T} + \begin{bmatrix} m(y^2 + z^2) & 0 & 0 \\ 0 & m(x^2 + z^2) & 0 \\ 0 & 0 & (x^2 + y^2)m \end{bmatrix} \tag{A-3}$$

This calculation can be applied to all the components inside the cabin. When given an angular acceleration exerted at the MRP, the moment at each components with respect to the MRP can be achieved using Euler's equation

$$\Sigma\mathbf{M_C} = (\mathbf{I_{O1}} + \mathbf{I_{O2}} + \dots) \cdot \dot{\omega}_O + (\omega_O \times (\mathbf{I_{O1}} \cdot \omega_O) + \omega_O \times (\mathbf{I_{O2}} \cdot \omega_O) + \dots) \tag{A-4}$$

```
% Function moi.m
% Moment of inertia calculation of each payload with respect to MRP
  function [I_c] = moi(D_c,m_c,P_c,T_c)

  D = D_c(1);
  W = D_c(2);
  H = D_c(3);
  X = P_c(1);
```

```matlab
  Y = P_c(2);
  Z = P_c(3);

% moment of inertia with respect to its centroid coordinate system C
  I_c1 = [m_c*(H^2 + W^2)/12                 0                    0;
                            0  m_c*(D^2 + H^2)/12                 0;
                            0                 0  m_c*(D^2 + W^2)/12];

% suppose th centroid coordinate system C of the payload is rotated by T
% with respect to the moving platform coordinate system O
% rotaion axis theorem
  I_c2 = T_c*I_c1*T_c';

% translation with respect to the moving platform coordinate system
% parallel axis theorem
  I_c3 = [m_c*(Y^2+Z^2)      -m_c*X*Y       -m_c*X*Z;
              -m_c*X*Y  m_c*(X^2+Z^2)       -m_c*Y*Z;
              -m_c*X*Z       -m_c*Y*Z  m_c*(X^2+Y^2)];

% the moment of inertia with respect to the moving platform coordinate
% system O
  I_c = I_c2 + I_c3;

  end
```

Dynamic load cases exerted by the accelerating components

```matlab
%Function simulatorF.m
%Analysis model of force exerted by hexapod actuators

function [R,P_MRP,P_u,P_c,f] = baseframe(delt_x,delt_y,delt_z,...
    thet_x,thet_y,thet_z,P_uo,CABIN,g,acc,vel)

%****************************
% SI-Units: m, N, s, deg
%****************************

%% Coordinate transformation of MRP
% Rotation of coordinate system at MRP

  R_z = [cos(thet_z) sin(thet_z) 0
        -sin(thet_z) cos(thet_z) 0
         0           0           1]; % Rotation matrix at MRP with Yaw

  R_y = [cos(thet_y) 0 -sin(thet_y)
         0           1 0
         sin(thet_y) 0 cos(thet_y)]; % Rotation matrix at MRP with Pitch

  R_x = [1 0           0
         0  cos(thet_x) sin(thet_x)
         0 -sin(thet_x) cos(thet_x)]; % Rotation matrix at MRP with Roll

  R = R_x*R_y*R_z;

% Translation of coordinate system at MRP
```

```
  T = [delt_x delt_y delt_z];

%% Position of platform and cabin system in general coordinate
% MRP coordinate in general coordinate
  P_MRP = T;

% Rotation points of upper joints in the general coordinate
  P_u = bsxfun(@plus, P_uo * R, T);

% Centroid of each payload in general coordinate
  P_c = bsxfun(@plus, CABIN.P_co * R, T);

%% Weight effect of components
% Gravity acceleration
  grav = [0 0 g] / R;
  f = zeros(6,1);
  for e = [1:22]

      I = CABIN.I_co(:,:,e+1);
%       P = CABIN.P_co(e,:);
%       P = bsxfun(@minus,P_uo,P);
      M = CABIN.m_co(e);

      F = [(acc(1:3)'-grav')*M;
           I*acc(4:6)' + cross(vel',I*vel')];

      f = f + F;
  end
```

Dynamic load cases exerted by the actuators to accelerating the components

To calculate the forces generated at each actuator, free body diagram method can be used by cutting the joints and applying the Newton-Euler equations of motions to the individual rigid body. Then the joint forces exerted on the body can be derived.

The platform consists one rigid body and six hinges, apply the Newton-Euler equations of motion for the body

$$T_1 + T_2 + T_3 + T_4 + T_5 + T_6 = m_C \ddot{x} \tag{A-5}$$

$$H_1 + H_2 + H_3 + H_4 + H_5 + H_6 = m_C \ddot{y} \tag{A-6}$$

$$V_1 + V_2 + V_3 + V_4 + V_5 + V_6 + m_C g = m_C \ddot{z} \tag{A-7}$$

$$(V_1 l_{1y} + V_2 l_{2y} + \cdots + V_6 l_{6y}) - (H_1 l_{1z} + H_2 l_{2z} + \cdots + H_6 l_{6z}) = \mathbf{I_O} \dot{\omega_{Ox}} \tag{A-8}$$

$$(T_1 l_{1z} + T_2 l_{2z} + \cdots + T_6 l_{6z}) - (V_1 l_{1x} + V_2 l_{2x} + \cdots + V_6 l_{6x}) = \mathbf{I_O} \dot{\omega_{Oy}} \tag{A-9}$$
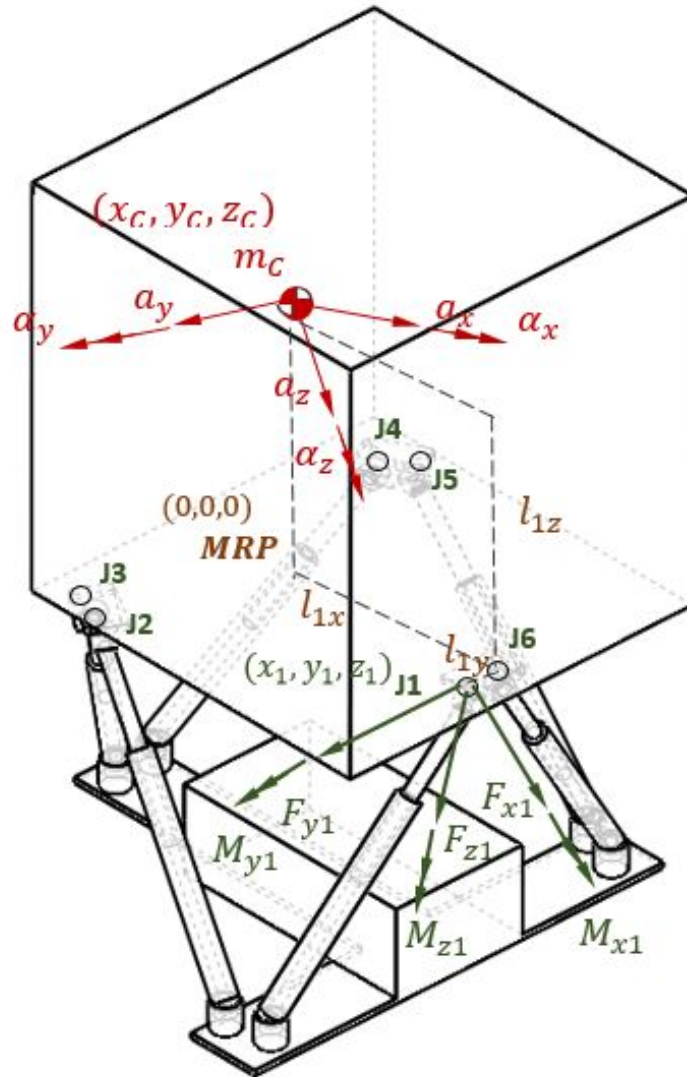
$$(H_1 l_{1x} + H_2 l_{2x} + \cdots + H_6 l_{6x}) - (T_1 l_{1y} + T_2 l_{2y} + \cdots + T_6 l_{6y}) = \mathbf{I_O}\dot{\omega}_{Oz} \qquad \text{(A-10)}$$

In these 6 equations of motion it has 24 unknown, the forces in the 6 joints and the 6 accelerations, the 18 more equations can be solved by defining a prescribed acceleration and a pose of hexapod that the direction of the total force assembled in each actuator is fixed.

Assume the acceleration defined is

$$\mathbf{q} = [\mathbf{a}; \dot{\omega}] = [a_x; a_y; a_z; \alpha_x; \alpha_y; \alpha_z]; \qquad \text{(A-11)}$$

Also assume the actuator direction and is denoted by

$$\vec{act}_i = (x_i, y_i, z_i); (i = 1, 2, 3, 4, 5, 6) \tag{A-12}$$

Thus the force exerted by each actuator, f_i, can be solved by

$$\Sigma\mathbf{F} = \begin{bmatrix} \frac{x_1}{\sqrt{x_1+y_1+z_1}} & \cdots & \frac{x_6}{\sqrt{x_6+y_6+z_6}} \\ \frac{y_1}{\sqrt{x_1+y_1+z_1}} & \cdots & \frac{y_6}{\sqrt{x_6+y_6+z_6}} \\ \frac{z_1}{\sqrt{x_1+y_1+z_1}} & \cdots & \frac{z_6}{\sqrt{x_6+y_6+z_6}} \end{bmatrix} \cdot \mathbf{f}; \tag{A-13}$$

$$\Sigma\mathbf{M_C} = \begin{bmatrix} \frac{z_1 l_{1y}-y_1 l_{1z}}{\sqrt{x_1+y_1+z_1}\sqrt{l_{1x}+l_{1y}+l_{1z}}} & \frac{z_2 l_{2y}-y_2 l_{2z}}{\sqrt{x_2+y_2+z_2}\sqrt{l_{2x}+l_{2y}+l_{2z}}} & \cdots \\ \frac{x_1 l_{1z}-z_1 l_{1x}}{\sqrt{x_1+y_1+z_1}\sqrt{l_{1x}+l_{1y}+l_{1z}}} & \frac{x_2 l_{2z}-z_2 l_{2x}}{\sqrt{x_2+y_2+z_2}\sqrt{l_{2x}+l_{2y}+l_{2z}}} & \cdots \\ \frac{y_1 l_{1x}-x_1 l_{1y}}{\sqrt{x_1+y_1+z_1}\sqrt{l_{1x}+l_{1y}+l_{1z}}} & \frac{y_2 l_{2x}-x_2 l_{2y}}{\sqrt{x_2+y_2+z_2}\sqrt{l_{2x}+l_{2y}+l_{2z}}} & \cdots \end{bmatrix} \cdot \mathbf{f}; \tag{A-14}$$

The force along each actuator can be further decomposed to $f_\perp$ which is normal to the platform plane (the shear force) and $f_\parallel$ which is coplanar to the platform (the stress force) for analysis of the internal force of the cabin base frame.

File function part2

```
%% Force calculation
% Ratio of the component in each direction to its total
  Act_o = Act / R;
  r_o = bsxfun(@rdivide,Act_o,L);
  f = zeros(6,1);

% Gravity acceleration
  grav = [0 0 g] / R;

  for e = 1:22

      I = CABIN.I_co(:,:,e+1);
      P = CABIN.P_co(e,:);
      P = bsxfun(@minus,P_uo,P);
      M = CABIN.m_co(e);

      F = [(acc(1:3)'-grav')*M;
          I*acc(4:6)' + cross(vel',I*vel')];
      E = [r_o';
          diag([P(:,2) -P(:,3)]*r_o(:,[3,2])')';
          diag([-P(:,1) P(:,3)]*r_o(:,[3,1])')';
          diag([P(:,1) -P(:,2)]*r_o(:,[2,1])')']; % Transformation matrix

      f = f + E \ F;
  end

% Force vector
```

```matlab
%   r = bsxfun(@rdivide,Act,L);
  F_vec = bsxfun(@times,r_o,f);


%% Loads transformed to the 3 mounting-block on platform
% Force transformed to the mounting-blocks
  F_node = [F_vec(1,:)+F_vec(6,:);
            F_vec(2,:)+F_vec(3,:);
            F_vec(4,:)+F_vec(5,:)];

% Moment transformed to the mounting-blocks (in general coordinate system)
  M_node = zeros(3,3);
  M_node(1,:) = [(F_vec(1,3)-F_vec(6,3))*t_MD, 0 , (F_vec(6,1)-F_vec(1,1))*t_MD];
  M_node(2,:) = [(F_vec(2,3)-F_vec(3,3))*t_MD/2, (F_vec(3,3)-F_vec(2,3))*t_MD*sqrt(3)/2,
      ((F_vec(3,1)-F_vec(2,1))*t_MD/2+(F_vec(2,2)-F_vec(3,2))*t_MD*sqrt(3)/2)];
  M_node(3,:) = [(F_vec(4,3)-F_vec(5,3))*t_MD/2, (F_vec(4,3)-F_vec(5,3))*t_MD*sqrt(3)/2,
      ((F_vec(5,1)-F_vec(4,1))*t_MD/2+(F_vec(5,2)-F_vec(4,2))*t_MD*sqrt(3)/2)];
```

A-4   Results

File force calculation.m

```matlab
%Program loadcase_calculation_model.m
%A model used for load calculation of cabin in Quasi-static
%situation, with any given inputs: simulator/ pose/ acceleration/ initial
%velocity/ cabin simplified model/...

%% initialization
clear all
clf
hold off

simulator_model_input;

%max.acceleration exerted at MRP
load('acc.mat');

%initial velocity at MRP
load('vel.mat');

%64 extreme poses of hexapod described in displacement of 6 degree of freedom
load('poses.mat');

delt_x = poses(:,1);
delt_y = poses(:,2);
delt_z = poses(:,3);
thet_x = poses(:,4).*pi./180;
thet_y = poses(:,5).*pi./180;
thet_z = poses(:,6).*pi./180;

%% Model calculation

%test
```

```matlab
i = 7;
j = 1;
k = 1;

F_tot = [];

% for i = 1:1:length(delt_x)
%     for j = 1:12
%         if j < 7
%             k = 1;
            [R,P_MRP,P_u,P_c,Act,L,f,F_vec] = simulatorF(delt_x(i),delt_y(i),...
                delt_z(i),thet_x(i),thet_y(i),thet_z(i),P_l,P_uo,CABIN,g,acc(j,:),vel(k,:));
%             F_tot(j,:,i) = f';
%         else
%             for k = 1:7
%                 [R,P_MRP,P_u,P_c,Act,L,f,F_vec] = simulatorF(delt_x(i),delt_y(i),...
%                 delt_z(i),thet_x(i),thet_y(i),thet_z(i),P_l,P_uo,CABIN,g,acc(j,:),vel(k,:));
%             F_tot(7*j+k-43,:,i) = f';
%             end
%         end
%     end
% end

%% For specific case analysis

% Force vector
F_end = (F_vec/10^4 + P_u);

% Plots of information
close all

figure
% subplot(131)
hold on
plot3(0,0,0,'k*') %reference point
plot3(P_MRP(1),-P_MRP(2),-P_MRP(3),'r*') %motion reference point
text(P_MRP(1),-P_MRP(2),-P_MRP(3),'MRP')
for l = 1:6
    plot3(P_l(l,1),-P_l(l,2),-P_l(l,3),'ko') %lower joint center
    plot3([P_u(l,1) P_l(l,1)],-[P_u(l,2) P_l(l,2)],-[P_u(l,3) P_l(l,3)],...
        'k-','linewidth',2) %actuator legs
    %plot3([F_end(l,1) P_u(l,1)], -[F_end(l,2) P_u(l,2)], -[F_end(l,3)
        P_u(l,3)],'r-','linewidth',2)
    %plot3(F_end(l,1), -F_end(l,2), -F_end(l,3), 'r.','MarkerSize',10)
end
for m = 1:5
    plot3([P_u(m,1) P_u(m+1,1)],-[P_u(m,2) P_u(m+1,2)],-[P_u(m,3) P_u(m+1,3)],...
        'b--','linewidth',1) %upper joint plane
end
%upper joint plane
plot3([P_u(6,1) P_u(1,1)],-[P_u(6,2) P_u(1,2)],-[P_u(6,3) P_u(1,3)],...
    'b--','linewidth',1)
%subsystems
for p = [1:4, 6:13, 15:21]
    D_o = CABIN.D_co(p,:);
    T_o = CABIN.T_co(:,:,p+1);
    drawPayloadC(P_c(p,:),D_o,R,T_o)
```

```
end
xlabel('x coordinate m')
ylabel('y coordinate m')
zlabel('z coordinate m')
hold off
view(3)
rotate3d
axis equal

subplot(222)
bar(1:6, [acc(j,:); 0 0 0 vel(k,:)]')
set(gca,'XTick',[1 2 3 4 5 6])
set(gca,'XTicklabel',{'surge','sway','heave','roll','pitch','yaw'})
xlabel('Degree of Freedom of MRP-coordinate')
ylabel('Acceleration &Velocity in each DoF')
title('Acceleration &initial velocity applied to the cabin')

subplot(223)
bar(1:6,lactu(i,:))
xlabel('Actuator from 1-6')
ylabel('Stroke state either 0(retracted) or 650mm(extended)')
title('Actuator states denoted by length')

subplot(224)
bar(1:6,f)
xlabel('Actuator 1-6')
ylabel('Force exerted in each actuator')
title('Force exerted in each actuator (-:extended,+:retracted)')
```

A-4-1 Worst dynamic loads exerted from components and actuator

Critical payloads	Loading modes	Worst dynamic loads
Center payloads	translation in x/y/z-axis	3/ 3/ -5 (kN)
	rotation around x/y/z-axis	740/ 800/ 160 (Nm)
Edge payloads	translation in x/y/z-axis	3/ 3/ -5 (kN)
	rotation around x/y/z-axis	3/ 3.2/ 3.3 (kNm)
Mid-front payload	translation in x/y/z-axis	3.4/ 3/ -5 (kN)
	rotation around x/y/z-axis	2.3/ 3/ 3 (kNm)
Each mounting block	translation in x/y/z-axis	1.5/ 1.4/ -2.3 (kN)
	rotation around x/y/z-axis	-260/ 300/ 85 (Nm)

Table A-1: Base frame elements worst dynamic load cases

A-4-2 Extreme poses load case verification

In order to verify the method for worst load case analysis, the calculation will be repeated three times at hexapod's neutral pose, at hexapod's half-extreme poses and at hexapod's extreme poses respectively. In the end, a comparison of the results will be conducted to see if the extreme poses gain the worst load cases. The maximum forces could exerted in each joint

at neutral pose are collected in TableA-2. And the maximum forces could exerted in each joint at hlaf-extreme poses are collected in TableA-3. The maximum forces could exerted in each joint at extreme poses are collected in TableA-4.

Maximum forces	Act1	Act2	Act3	Act4	Act5	Act6
Extended	2.81kN	1.59kN	1.96kN	2.01kN	1.66kN	2.83kN
Retracted	0.76kN	0.55kN	1.27kN	1.26kN	0.52kN	0.74kN

Table A-2: Maximum forces exerted in each joint for neutral pose

Maximum forces	Act1	Act2	Act3	Act4	Act5	Act6
Extended	3.06kN	2.07kN	2.24kN	2.29kN	2.11kN	3.08kN
Retracted	1.31kN	1.14kN	1.92kN	1.92kN	1.09kN	1.29kN

Table A-3: Maximum forces exerted in each joint for all the half-extreme poses

Maximum forces	Act1	Act2	Act3	Act4	Act5	Act6
Extended	3.93kN	2.85kN	2.73kN	2.77kN	2.96kN	3.94kN
Retracted	2.39kN	2.02kN	2.92kN	2.93kN	1.99kN	2.36kN

Table A-4: Maximum forces exerted in each joint for all the extreme poses

From the results, it is clear to see that the forces from actuators increased from the calculation at neutral pose, half-extreme pose and extreme pose. And within the error tolerance range, the results of model at hexapod's half-extreme poses is close to the mean value of the results of model at hexapod's neutral pose and model at hexapod's extreme poses. Thus, this analysis method can be trusted and will be a conservative value.

Base frame beam element calculation
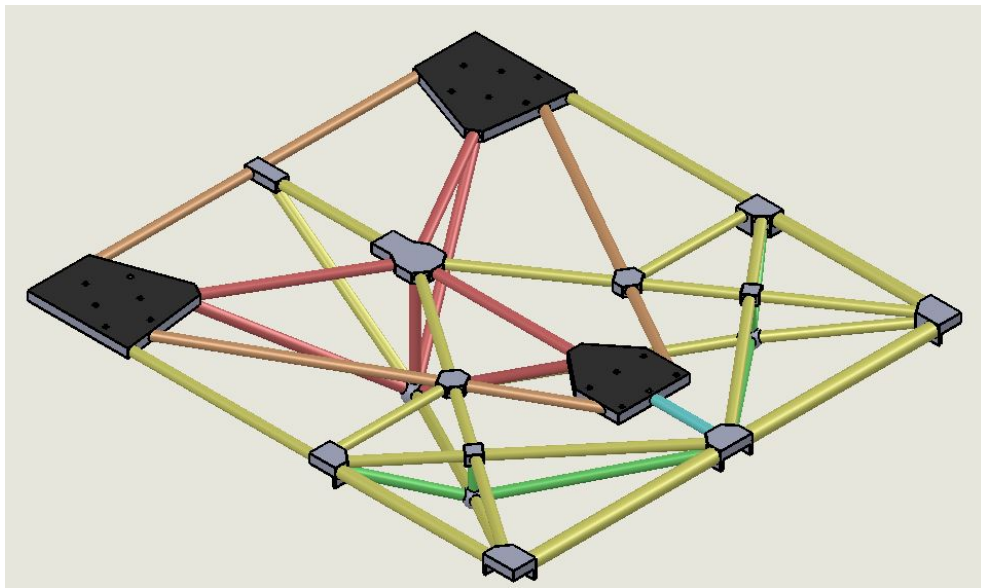
Payloads	Supporting Element	Loading modes	Worst dynamic loads
Center	Red beam element	translation in x/y/z-axis	3/ 3/ -5 (kN)
		rotation around x/y/z-axis	740/ 800/ 160 (Nm)
Edge	Yellow beam element	translation in x/y/z-axis	3/ 3/ -5 (kN)
		rotation around x/y/z-axis	3/ 3.2/ 3.3 (kNm)
Mid-front	Blue beam element	translation in x/y/z-axis	3.4/ 3/ -5 (kN)
		rotation around x/y/z-axis	2.3/ 3/ 3 (kNm)
Actuators	Orange beam element	translation in x/y/z-axis	1.5/ 1.4/ -2.3 (kN)
		rotation around x/y/z-axis	-260/ 300/ 85 (Nm)

Table B-1: Base frame payloads (as represented in the Figure) worst dynamic load cases

In Table B-1 showed the worst dynamic load cases that are created by the components and exert on the base frame structure, detailed derivation is shown in Appendix A-4. In Chapter 4-3-4 stated the determination of the outer diameter of beam profile as 40 mm. In the following sections, the thickness of the beam profile will be determined according to calculations with the required stiffness.

The required stiffness is defined by the maximum acceptable deflection due to the applied load. With the worst dynamic load cases summarized in Table B-1, the minimum thickness of the profile with sufficient stiffness can be derived using the maximum displacement.

The center payload supporting element (denoted by red) are parallel connected with the edge supporting elements (denoted by yellow and blue), thus their stiffness will add up. Within the edge supporting elements, the beams are series connected, and their deflection will add up. In this manner, the base frame is analyzed with center supporting element and edge supporting element respectively.

B-1 Center payload supporting element

Profile thickness determined with required translational stiffness

Firstly, the center supporting structure is analyzed with translational load modes. Here assume the element can be treated as truss structure as shown in Figure B-1. Suppose the cross-section area of each elements is A and the Young's modulus of the material is E. Suppose the worst vertical force of $5kN$ is applied to the truss at center joint D as the external force F, and a virtual joint force P is placed at the joint D where the displacement is to be determined. The reactions at the support point A, B and C are calculated and the results are shown in Figure B-1 on the right. Using the method of joints, the forces in each elements are also determined in Figure B-1 on the left.
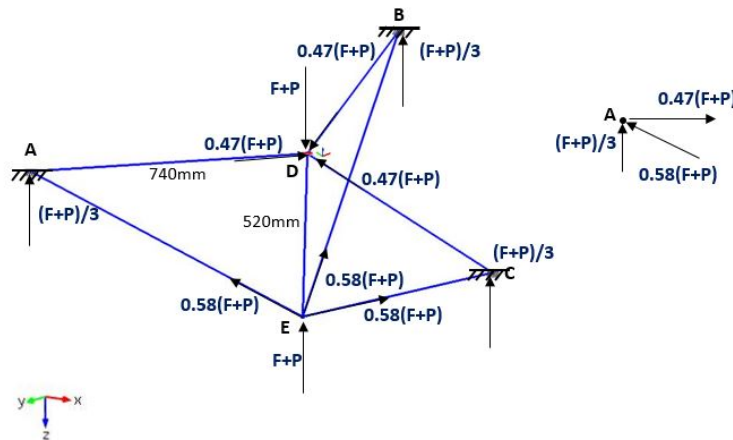
Figure B-1: Center payload support structure analysis for calculation of stiffness

Thus, the vertical displacement can be determined by listing the internal forces N and their partial derivatives $\partial N/\partial P$ in each element. By applying Castigliano's Second Theorem[13], the displacement can be derived as:

Member	N	$\partial N/\partial P$	$N(P=0)$	L	$N(\partial N/\partial P)L$
AD(CD/BD)	$0.47(F+P)$	0.47	$0.47F$	$0.74m$	818
AE(CE/BE)	$0.58(F+P)$	0.58	$0.58F$	$0.904m$	1521
DE	$F+P$	1	F	$0.52m$	2600

$$\Delta D_v = \Sigma N(\frac{\partial N}{\partial P})\frac{L}{AE} = \frac{9617N \cdot m}{AE} \tag{B-1}$$

From the required stiffness as defined in Table 3-4 in Chapter 3-7, the maximum acceptable displacement reacted to the worst vertical load are

$$D_v = 1mm \tag{B-2}$$

Substituting the numerical values for $E_{st} = 200GPa$, the required cross-section area of each element are

$$A_{st} = \frac{9617N \cdot m}{1mm200GPa} = 48.1mm^2 \tag{B-3}$$

With a safety factor of 2, the required cross-section area is 96.17 mm^2. Thus the required minimum thickness is

$$t = r_o - \sqrt{r_o{}^2 - \frac{A}{\pi}} = 1mm \tag{B-4}$$

From this calculation, a pipe profile with 1mm thickness is already sufficient for supporting the worst load cases in vertical direction.

Profile stiffness determined with required rotational stiffness

In rotational acceleration situations, the worst load case occur when applying a bending moment around y axis. Using beam deflection equations[13]:

$$v = \frac{-Mx^2}{8EI} \tag{B-5}$$

With the maximum acceptable displacement of 1mm, the minimum moment of inertia I can be derived as

$$I = \frac{-Mx^2}{8Ev} = 0.1105(10^6)mm^4 \tag{B-6}$$

Since the outer diameter of the profile is already determined as $d_o = 40mm$, the required inner diameter d_i can be calculated as

$$I = \frac{\pi}{4}(r_o{}^4 - r_i{}^4) \tag{B-7}$$

$$r_i = 11.78mm \tag{B-8}$$

Thus, 10mm is taken as the thickness of the profile with an outer-diameter of $40mm$.

Stiffness verification in COMSOL

An FEM analysis of the element can be quickly conducted to verify the stiffness. The center star structure is checked with the worst dynamic load cases in all degrees of freedom non-simultaneously as shown in Table B-2.

Worst dynamic load case	max. stress on surface	max. total deflection
Fx: 3 kN	4 MPa	0.01 mm
Fy: 3 kN	4 MPa	0.01 mm
Fz: -5 kN	9 MPa	0.06 mm
Mx: 740 Nm	71 MPa	0.25 mm
My: 800 Nm	78.5 MPa	0.4 mm
Mz: 160 Nm	11.5 MPa	0.06 mm

Table B-2: Base center star structure response for worst dynamic loads non-simultaneously
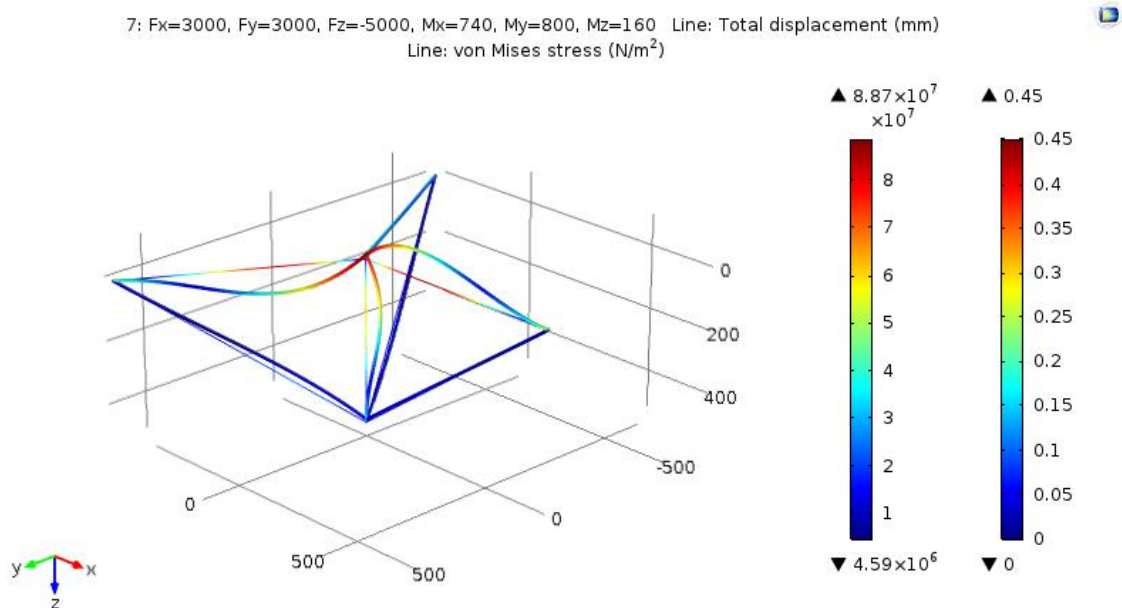
Figure B-2: Stiffness of center support element verified with simultaneous worst dynamic cases

The condition when the dynamic loads in all degrees of freedom are acting simultaneously is hard to predict since it is dependent on the simulation input. Here, a simultaneous dynamic load case is checked with worst loads in each degree of freedom, which is over engineered. The result can be seen in Figure B-2. The maximum deflection of the center payload support structure is still within $1mm$. Thus, it can be concluded that if the structure can survive this load case, then it can survive all the load cases.

B-2   Edge payloads supporting elements

For the edges of the base frame, critical load modes are the shear at the front edge which is generated by the heave of the screen or a person jumping at the corner, and the bending load when the screen and projector on the back side start to rotate. For the worst dynamic loads can be referred in Table B-1. Since the edges supporting structure are symmetric about the center line (x-axis), thus calculation can be conducted for half of the elements.

The method used in the previous subsection can also be applied for this calculation, however it is too time-consuming to calculate with this complex supporting structure. Generally with a supporting construction like a frame or trusses, when the deflection contributed from each part to the total compliance is not obvious, two principal ways can be applied to calculate the established stiffness at the force application point.[14]. As summarized, with beam i which has its stiffness as EA_i/l_i, for stiffness elements operating in parallel (refer Figure B-3 on the left), the total stiffness can be written as:
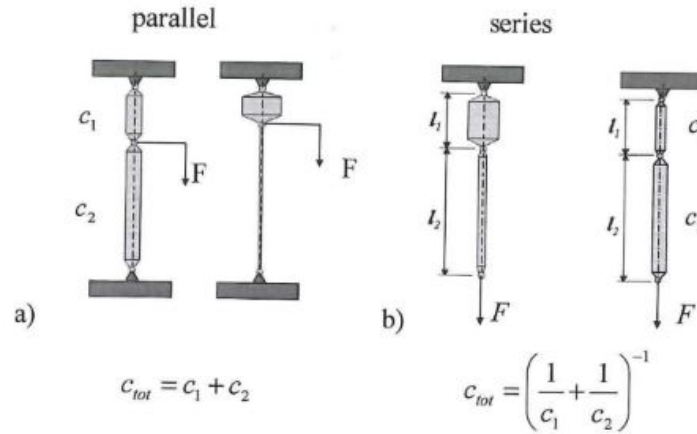
Figure B-3: Optimizing parallel and series members for maximum stiffness/volume ratio[14]

$$\frac{c_{total}}{E} = \Sigma \frac{A_i}{l_i i^2} \tag{B-9}$$

Thus, the maximum stiffness can be achieved by maximizing any A_i/l_i if the material volume is assumed being constant.

For series operation (refer Figure B-3 on the right), the total stiffness can be written as:

$$\frac{c_{total}}{E} = (\Sigma \frac{l_i i_i^2}{A_i})^{-1} \tag{B-10}$$

In this case, the maximum stiffness can be achieved if both elements are equally stiff.

To apply the stated principle in this design case, first the relationship between each element should be made clear. In Figure B-4 showed the involved beam elements denoted by numbers at the left side of half the edge supporting structure. A B C and D denote the fixed constraints. Except beam 10, the rest beams are all in one plane. Beam 10 extending in a plane that is vertical to the rests. The parallel or series connection relations are summarized in Figure B-3)
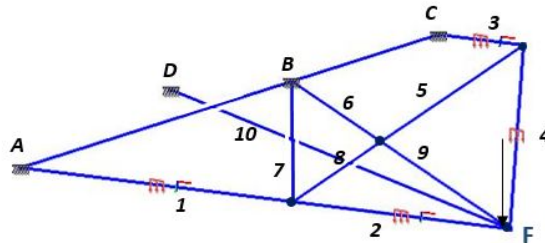
Figure B-4: Front corner support structure analysis for calculation of stiffness
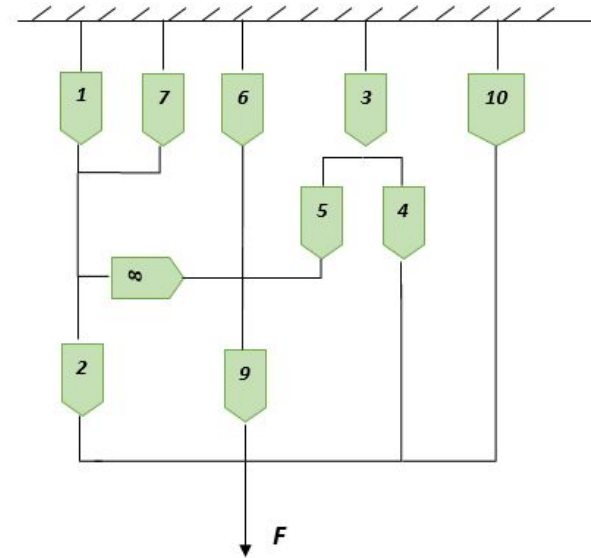
Figure B-5: Stiffness calculation using beam parallel connection or series connection theory

In order to simplify the problem, assume there is only 1,2 (series) and 6,9 (series) and 3,4

(series) and they all parallel connected with 10. The total stiffness at front corner is

$$c_{total} = \frac{1}{\frac{1}{c_1} + \frac{1}{c_2}} + \frac{1}{\frac{1}{c_6} + \frac{1}{c_9}} + \frac{1}{\frac{1}{c_3} + \frac{1}{c_4}} + c_{10} \tag{B-11}$$

Substitute the stiffness of each beam with EA_i/l_i, then the total stiffness can be written as

$$c_{total} = EA(\frac{1}{l_1 + l_2} + \frac{1}{l_6 + l_9} + \frac{1}{l_3 + l_4} + \frac{1}{l_{10}}) = 2.7EA \tag{B-12}$$

With the worst dynamic load case (jumping person at the corner), a transient force of around 3300 kN can be created, with a maximum allowable deflection of 1mm, the required stiffness from user is

$$c_{required} = \frac{F}{d} = 3.3(10^6)N/m \tag{B-13}$$

To save the manufacturing cost, the same beam profile is preferred to be used for the whole base frame. Thus, with an assumed beam element profile $40mm * 10mm$, the $c_{total} = 5(10^8)N/m$ which is sufficient for the required stiffness, then pipe profile with $40mm * 10mm$ is selected as the edge supporting elements. For the front edge, without the contact with the original triangular structure of the hexapod platform (refer Figure 2-8), it can be extended to the area below the mounting surface, thus profile $60mm * 5mm$ is selected for the front part to achieve a more efficient cross-section properties.(see the discussion in Chapter 4-3-4)

Stiffness verification in COMSOL

The deflection under worst dynamic load cases in each degree of freedom is evaluated with FEM and is summarized in Table B-3. Two worst dynamic load cases are shown in Figure B-6 with verification in COMSOL.

Worst dynamic load case	max. stress on surface	max. total deflection
Fx: 1.5 kN	6 MPa	0.08 mm
Fy: 1.5 kN	8 MPa	0.07 mm
Fz: -3.3 kN	37 MPa	0.85 mm
Mx: 1.5 kNm	62 MPa	0.93 mm
My: 1.5 kNm	53 MPa	0.63 mm
Mz: 1.65 kNm	4 MPa	0.03 mm

Table B-3: Base edge support structure response for worst dynamic loads non-simultaneously

B-3 Supporting elements between each mounting blocks

The supporting elements between each two mounting blocks are denoted with orange color in Table B-1. By stiffly interconnecting every two mounting blocks, the force exerted from actuators can be transferred to the cabin rigidly. Thus, the elements between the mounting
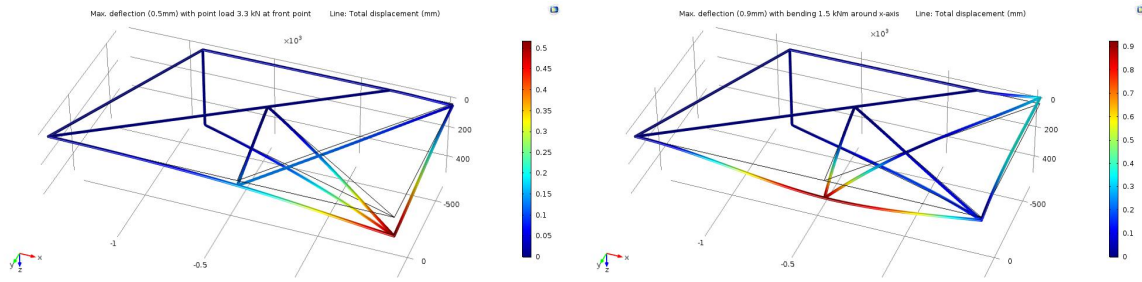
Figure B-6: Stiffness of edges supporting elements verified under worst dynamic load cases

Load modes	Beam deflection equations
Axial load case	$\delta = \dfrac{PL}{AE}$ $\qquad$ (B-14)
Shear load case	$v_{max} = \dfrac{PL^3}{12EI}$ $\qquad$ (B-15)
Bending load case	$v_{max} = \dfrac{M_0 L^2}{\sqrt{243}EI}$ $\qquad$ (B-16)
Torsion load case	$\phi = \dfrac{TL}{JG}$ $\qquad$ (B-17)

Table B-4: Beam deflection equations under different load modes

blocks have to be stiff enough under the worst dynamic load cases summarized in Table B-1. For calculating the beam deflection, equations been used are summarized in Table B-4.

For the triangular support structure, each beam element has length of around L=1.7 m and dimensional size of profile are constrained by the height of the base floor with 40 mm (see explanation in Chapter 4-3-4). Thus the thickness of beam profile can be determined with calculations according to the required stiffness. First calculation is conducted about axial loads, with maximum acceptable $1mm$ deflection, the required section area is

$$A = \frac{PL}{\delta E} = \frac{8(10^3)1.7}{1(10^{-3}200(10^9))} = 70mm^2 \qquad (B-18)$$

For shear, with maximum acceptable $1mm$ deflection, the required section moment of inertia is

$$Ix = \frac{PL^3}{12Ev_{max}} = \frac{12(10^3)1.7^3}{200(10^9)12(10^{-3})} = 24.5(10^6)mm^4 \tag{B-19}$$

$$Iy = \frac{PL^3}{12Ev_{max}} = \frac{7(10^3)1.7^3}{200(10^9)12(10^{-3})} = 14(10^6)mm^4 \tag{B-20}$$

For bending loads, with maximum acceptable $1mm$ deflection as well, the desired section moment of inertia is

$$Ix/y = \frac{M_0L^2}{\sqrt{243}Ev_{max}} = \frac{440 \cdot 1.7^2}{200(10^9)\sqrt{243}(10^{-3})} = 0.42(10^6)mm^4 \tag{B-21}$$

At last, for the torsion load, with maximum acceptable $0.003rad$ deflection, the required section properties can be derived as the followed methods. With pipe profile, the mean area is $A_m = \pi r_m{}^2$. Thus

$$\tau_{avg} = \frac{T}{2tA_m} = \frac{T}{2\pi t r_m{}^2} \tag{B-22}$$

The angle of twist can be derived as

$$\phi = \frac{TL}{4A_m{}^2G} \oint \frac{ds}{t} = \frac{TL}{4(\pi r_m{}^2)^2 Gt} \oint ds \tag{B-23}$$

The integral represents the length around the centerline boundary, which is $2\pi r_m$. Thus

$$\phi = \frac{TL}{2\pi r_m{}^3 Gt} \tag{B-24}$$

With the steel material are selected and substituting with numerical values, the final desired section properties $r_m{}^3t$ are $2.6e-7$.

From the calculation, the shear force acted on the triangular elements are very high that with limit height of $40mm$ as base frame, it is hard to achieve the required stiffness. While, the axial load and torsion can be satisfied easily but the transient shear and bending are not satisfied. However, it is hard to judge the result by now. Because as the base frame integrated as a single entity, the stiffness are added up due to the parallel connection. Furthermore, in a later stage, as the base frame covered by the panel floor, the stiffness will be further increased. With these two main reasons, here the $40mm*10mm$ hollow tube is selected at the moment, and the stiffness between each mounting blocks under the worst dynamic cases will be verified after the total base frame is completed.

B-4   Vertical stiffener reinforce elements

In the end, reinforce beams are added in purpose of adding stiffness to the whole structure. The profile is selected with pipe as well to simplify the manufacture process. The size of the profile is preliminarily chosen with $40mm*10mm$, and it can be adjusted later during the verification in FEM software analysis in Chapter 4-3-5.

Appendix C

Bolt joint calculation

When using the bolt joint clamping connection to assembly substructures, the clamp forces and preloads needs to be determined with the static and dynamic load cases that the assembly is expected to have. As referred in [15],the bolted joint design must be conducted with the analyzed external working load cases with respect to both axial (both concentric and eccentric) and side shear loads first. Then with the specified load cases, the bolt preload can be determined. Moreover, the safety factors against embedment and thread strip must be checked to insure the yielding in bearing area will not exceed the required amount for preload.

The calculation and design for the bolted joint with respect to each part of the assembly will be conducted in the following sections.

C-1   Bolt joint between hexapod and base frame

For the connection between base frame mounting surface and the hexapod mounting surface, the load conditions are mainly from the actuation of the mounting blocks. The external loading is derived as maximum axial load of 17.3 kN and maximum shear load of 15.7 kN.

The basic equation, $T = KDF$ can then be applied to the linear elastic clamping zone tightening calculation. Here, T denotes the applied torque, K denoted the friction coefficient, D denotes the bolt pitch diameter and F denotes the preload been applied. For steel to steel contact, the coefficient of friction can vary according to the environment conditions. At static dry condition, the factor is 0.5 to 0.6, while at dynamic dry condition, the factor is 0.4 to 0.6. However, under lubricated condition, the factor is 0.15.[16] Here, the contact surface is assumed to be lubricated. With a maximum shear load of 15.7 kN, the preload is determined as

$$F = V/\mu = 105kN \tag{C-1}$$

Thus, for the bolts connecting hexapod and base frame, preload will be required as 105 kN, while the torsion is 252 Nm. Since the hexapod provided the holes for mounting is 18mm with its diameter. Thus bolt M16 with specifics of maximum proof load of130 kN and maximum tensile stress of 1040 MPa is selected as the joint[1].

The tensile load is also check with the maximum axial load of 17.3 kN:

$$\sigma = P/A = 86 MPa < 1040 MPa \tag{C-2}$$

Furthermore, since each block has 6 bolts to bear the loads together, thus it has given a safety factor of more than 2 to secure the safety. And the preload for the mounting block surface from the base frame is also checked with its material yielding stress properties.

For worst compressive loads:

$$\sigma = (F_{preload} + P)/A_{nut} = 270 MPa < 550 MPa \tag{C-3}$$

$$\tau = (V_{actuting})/A_{nut} = 40 MPa < 412 MPa (550 MPa * 0.75) \tag{C-4}$$

Thus the selected connection is also validated with the base frame mounting surface.

C-2   Bolt joint between base frame and outer structure frame

The connection between base frame and outer structure transfers the load to actuate upper payloads. The maximum load condition for the contact surface is 3 kN in the axial load while 5 kN in shear loads. In the similar manner, with aluminum to steel contact, the friction coefficient in clean and dry surface condition is referred as 0.61 [2]. Thus, with a required shear load of 5 kN, the repload is determined with

$$F = V/\mu = 8.2 kN \tag{C-5}$$

By checking the bolt fastener manual[3], bolt M6 will a tolerance of proof load of 16.7 kN is selected as the joint. Then the applied torque can be calculated as

$$T = KDF = 30 Nm \tag{C-6}$$

For the mounting surface of aluminum, the stress and shear is check as well. As referred in the engineering book[11], the maximum allowable stress is 245 MPa and shear is 160 MPa with a poisson ratio of 0.33. The derived contact internal stress are

$$\sigma = (F_{preload} + P)/A_{nut} = 132 MPa < 245 MPa \tag{C-7}$$

$$\tau = V/A_{nut} = 60 MPa < 160 MPa (245 MPa * 0.6) \tag{C-8}$$

---

[1] http://www.rocksideltd.co.uk/technical_details/24-GRADE%2010.9%20BOLT%20&%20NUT%20(ISO).pdf
[2] http://www.engineeringtoolbox.com/friction-coefficients-d_778.html
[3] http://www.rocksideltd.co.uk/technical_details/24-GRADE%2010.9%20BOLT%20&%20NUT%20(ISO).pdf

Appendix D

Motion envelope analysis

D-1 Dynamical model validation in SolidWorks

First, to make a valid hexapod model that can behave similar to the real system, SolidWorks was chosen for certain reasons:

- it's more intuitive and suitable for a structural analysis and helps understand the configuration better

- it costs less time to build up the model and very convenient to check a more detailed design by simply replace the envisioned cabin

- it is easy and intuitive to check any collision with the lab room by simply adding a room model to the envelope

Second, in order to realise a dynamic model that is more flexible and easier to operate, an equivalent replacement of the universal joints was made. Each universal joint has 3 DOFs (considering the rotation between the rod and shell), thus ball joints also with 3 DOFs can be considered an alternative to replace the universal joints in the model. See a comparison of the two joints in FigureD-1. The necessity of this replacement is due to the fact that, the geometry of the motion base frame is not a equilateral triangle but an isosceles triangle that was optimized for a better dynamic performance of the hexapod, which makes it hard to operate the model using universal joints in SolidWorks.

After this modification of the original hexapod model provided by Bosch Rexroth, the two extreme positions of the actuator extended at 630mm and retracted at -20mm were realized in the SolidWorks model by adding a 'Distance Mate' from -20mm (with the inwards cushion zone) to 630mm (with the 15mm outwards cushion zone) between the rod part and shell part of the actuator model. Thus, the dynamic motion poses of the hexapod can be mimicked by manipulating the length of the actuators. For example in FigureD-2, left side shows the case with number 1,3,5 actuators extended and the rest retracted, while the right side shows the case with all actuators extended.
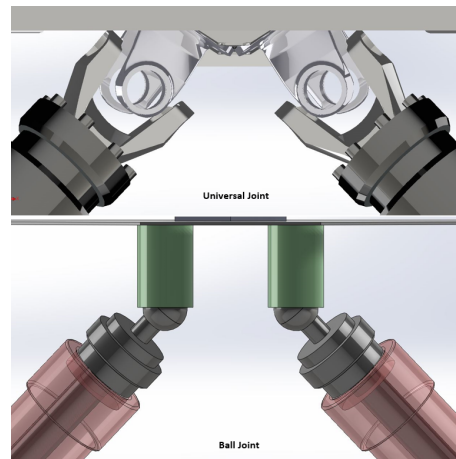
Figure D-1: Comparison of universal joint and ball joint
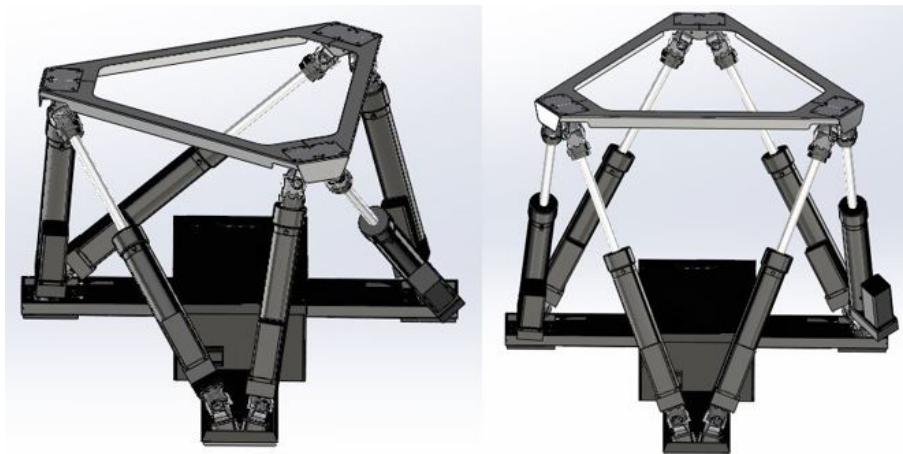
Figure D-2: Two pose examples of dynamical hexapod model in SolidWorks

D-1-1   Room model of Motion Lab

The mapping and surveying of the room was conducted using a digital laser range finder (Bosch PLR 25). During the measurement, each dimension was measured three times in three different positions (two edges and the middle). From the results, the three measurements for one dimension are different (but all within $1cm$), which indicates the wall of room is not exactly straight. Since it is hard to obtain the real shape of the room, the minimum or the most conservative measurement of each dimension was chosen as the one for building up the model. Meanwhile, the positioning of the base frame of hexapod with respect to the walls is also measured in this way. A resulted model can be seen in FigureD-3.

Potential collision obstacles are the side walls, the wall on the back, the fence on the front and the crane on the ceiling. For the walls and fence, the interferences can only be avoided by properly dimensioning the cabin size. However, to prevent interference between cabin and the lowest part of the crane from the ceiling, in addition to reducing the cabin's height, a testing
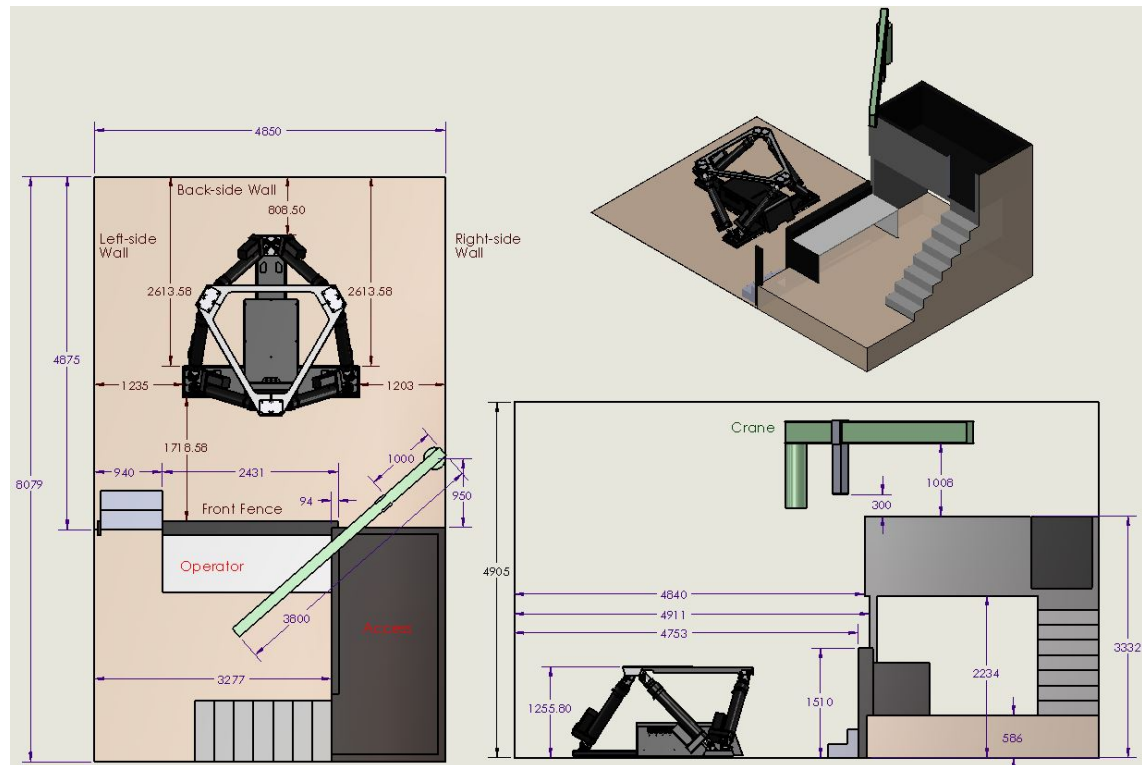
Figure D-3: Room model with available motion space measurements from side and top view

system can be installed to detect if the crane is in a safe position (away from the hexapod motion area) before any operation.

A simple calculation shows that at a maximum height of the cabin of 1574mm, collisions with the crane are avoided for any position of the cabin and any position of the crane. This height, however, is not ideal for accessing the cabin. Thus, in view of the crane, the installation of testing system is preferred.

D-1-2   Motion envelope model

Approach

The motion envelope depends on the shape and the location of the payload on the platform. The motion envelope is calculated by using the 64 extreme system positions, consisting of all combinations of the 6 actuators in either extended or retracted position. With a dynamical hexapod model in SolidWorks, the 64 extreme system positions can be obtained by manipulating the state of the actuator through the use of the property of the assembly to be 'Rigid' or 'Flexible'.

Motion envelope model with an envisioned cabin

An envisioned cabin with a standard dimensions of $2.2m * 2.0m * 1.8m (W * D * H)$ was used to test this motion envelope model, a result can be seen in the top two drawings in FigureD-4. A model to check the potential collisions inside the room can be seen in the bottom drawing in FigureD-4. It is clear to see if there exists potential interferences between payload and the room walls or any obstacles by measuring the parts which are marked by the red circles in the figure.
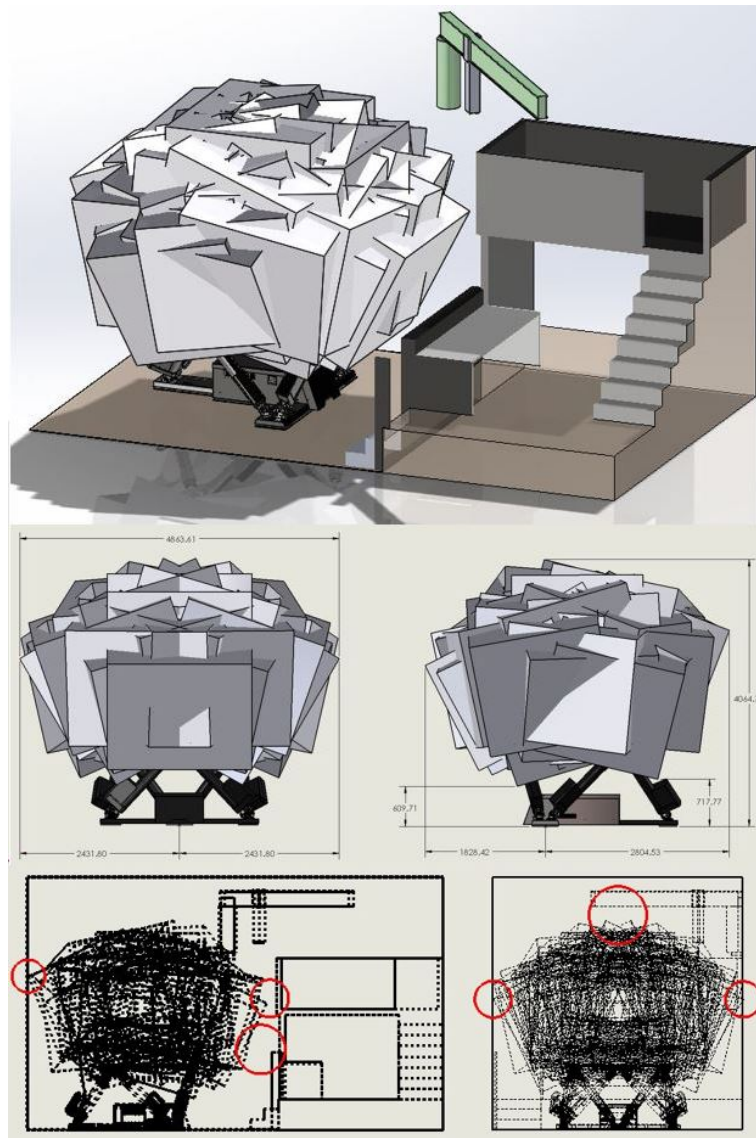
Figure D-4: Motion envelope model sample with an envisioned cabin and collision check with the room model

Bibliography

[1] S. K. Avani, *The Kinematic Design of Flight Simulator Motion-Bases*. Delft Univeristy Press, 1998.

[2] RvM, *eMotion-1500-6DOF-650-MK1 System Description*. Rexroth Bosch Group, the drive & control company, 12 2014.

[3] *NASA System Engineering Handbook*. National Aeronautics and Space Administration, 2007.

[4] T. A. S. Beukers, A. ;Van Baten, "Method of manufacturing a motion simulator, and a motion simulator," 1996.

[5] D. Stewart, "A platform with six degreed of fredom," *Proceedings of the Institute of Mechanical Engineers*, vol. 180, June 1965.

[6] T. Bitzer, *Honeycomb Technology, materials, desgin, manufacturing, applications and testing*. Tom Bitzer, 1997.

[7] H. H. Nieuwenhuizen, Frank M.; Bulthoff, "The mpi cybermotion simulator: A novel research platform to investigate human control behavior," *Journal of Computing Science and Engineering*, vol. 7, pp. 122–131, July 2013.

[8] G. R. G. Bianchi, G. S. Aglietti, "Optimization of bolted joints connecting honeycomb panels,"

[9] R. v. d. L. A.L.Schwab, "Multibody dynamics b," 1997.

[10] T. P. QUINN, "Process sensitivity of gmaw: Aluminum vs. steel," *The Welding Journal*, April 2002.

[11] M. F. Ashby, *Materials Selection in Mechanical Design*. Elsevier Ltd, 2011.

[12] J. Black, "Test verification of finite element analysis for honeycomb panel attachment inserts," 2015.

[13] R. C. Hibbeler, *Mechanics of Materials*. 2011.

[14] *Precision and Mechanism Design*.

[15] P. Ralph S. Shoberg, *Engineering Fundamentals of Threaded Fastener Design and Analysis*. RS Technologies, a Drivision of PCB Load & Torque, Inc.

[16] T. Irvine, "Damping properties of materials revision c," tech. rep., November 2004.

Glossary

List of Acronyms

MPI	Max Planck Institute for Biological Cybernetics
FEM	Finite Element Method
MRP	Motion Reference Point for maximum excursions, velocities and accelerations
UJP	Upper Joint Plane

List of Figures

List of Tables